STABILITY ANALYSIS OF SLIP ENERGY RECOVERY DRIVE

A DISSERTATION

submitted in partial fulfilment of the
requirements for the award of the degree

of
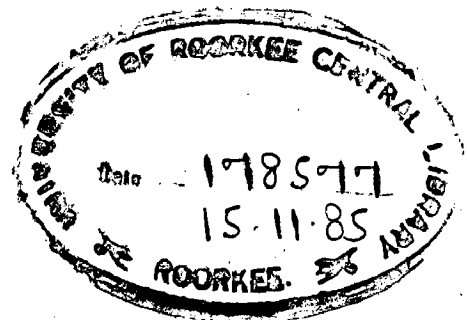
MASTER OF ENGINEERING

in

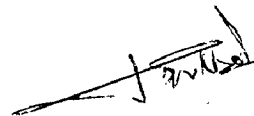ELECTRICAL ENGINEERING
(P.A.E.D.)

By

PANKAJ MITTAL

DEPARTMENT OF ELECTRICAL ENGINEERING
UNIVERSITY OF ROORKEE
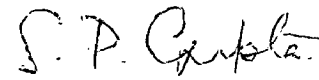ROORKEE, U.P. (INDIA)
May, 1985

CANDIDATE'S DECLARATION

I hereby certify that the work which is being presented in the thesis entitled 'STABILITY ANALYSIS OF SLIP ENERGY RECOVERY DRIVE' in fulfilment of the requirement for the award of the Degree of Master of Engineering, submitted in the Department of Electrical Engineering, University of Roorkee, is an authentic record of my own work carried out during a period from October 1984 to May 1985 under the supervision of Shri S.P. Gupta, Reader, Electrical Engineering Department, University of Roorkee, Roorkee.

The matter embodied in this thesis has not been submitted by me for the award of any other degree.

PANKAJ MITTAL

This is to certify that the above statement made by the candidate is correct to the best of my knowledge.

S.P. GUPTA
Reader
Elect. Engg. Deptt.
University of Roorkee
Roorkee — 247 667
India

PLACE: ROORKEE

DATED: MAY 27, 1985

ACKNOWLEDGEMENT

. ABSTRACT

Steady state and stability analysis of a constant power type slip energy recovery drive is presented in this work. The system equations are written in synchronously rotating reference frame. Complete performance under steady state is investigated. For stability study a set of non-linear differential equations describing the dynamics of the system is linearized about an operating point using small displacement theory. Using the characteristic equation of the linearized model and Routh Hurwitz criterion, instability regions in the torque slip plane have been established from the results of a digital computer study. Two subroutines for steady state analysis and stability analysis respectively have been developed. The latter directly gives the instability contour data to be plotted on CALCOMP plotter or to give a visual presentation on TEKTRONICS graphic terminal. Effects of various parameters of the system upon the instability region have been investigated and conclusions drawn.

TABLE OF CONTENTS

LIST OF SYMBOLS

V	$=$	instantaneous value of voltage
i	$=$	instantaneous value of current
V_{sm}	$=$	peak value of stator phase voltage
R_{ss}, R_{rr}	$=$	stator and rotor resistance, per phase
R_a	$=$	resistance of armature winding
R_F	$=$	resistance of smoothening inductor
R	$=$	$R_a + R_F$
L_F	$=$	inductances of smoothening inductor
L_a	$=$	self inductance of d.c. motor armature
L	$=$	$L_a + L_L$
L_{12}	$=$	mutual inductance between stator and rotor
L_M	$=$	$a\,L_{12}$
a	$=$	stator to rotor turns ratio
L_{ss}, X_{ss}	$=$	self inductance and reactance, respectively of stator
L_{rr}, X_{rr}	$=$	self inductances and reactance, respectively of rotor
s	$=$	per unit slip
p	$=$	differential operator, d/dt
P	$=$	number of poles on motor
w	$=$	electrical angular speed corresponding to fundamental component of the applied voltage, electrical rad/sec = 2π . Supply frequency in Hz.

w_r = electrical angular speed of the drive, electrical rad/sec. = $(1 - s)w$

T_e = electromagnetic torque

T_L = load torque

H   = inertia constant of drive in sec.

α = firing angle of the controlled rectifier

i_f = field current in amperes

Subscripts

a,b,c   = phase quantities

d   = direct axis quantities

q   = quadrature axis quantities

s   = stator quantities

r   = rotor quantities

R   = d.c. link quantities

Prefix

Δ = small deviation

CHAPTER I

INTRODUCTION

There is a growing demand for precise and reliable variable speed drive. The induction motor is a very attractive type of a.c. drive, because of its simple construction, ruggedness, low capital cost and absence of commutator problems. The speed control of induction motor may be accomplished by several methods, such as pole changing, pole amplitude modulation, stator voltage control, frequency control and rotor resistance control. All of these methods suffer from such disadvantages, as excessive power loss in control, complicated control circuitry, higher capital cost, lack of continuous variation in speed etc.

As a result of advances in solid state technology and with the availability of high power reliable and efficient thyristor converters, the use of schemes which employ stator voltage control, frequency changing, rotor resistance control and slip energy recovery are becoming more popular.

The slip energy recovery scheme utilizes the slip energy available at the slip rings instead of dissipating it in external rotor resistances. The recovered slip energy is either added to the main motor shaft itself or returned to the supply, thus resulting in

constant power and constant torque drives. In a constant
power drive the slip energy is supplied to an auxiliary
rotating machine which produces a reinforcing torque on
the induction motor shaft. The speed of the drive is
controlled by varying the excitation of the auxiliary
machine and varying the d.c. link current/(1-2). The power handling
capacity of the drive remains same at all speeds of operation.
In a constant torque drive the slip frequency of the rec-
overed energy is first converted to supply frequency and
then the recovered energy is returned to the supply. Speed
control is achieved by controlling the firing angle of the
line commutated inverter (3-5).

The concept of constant power slip energy recovery
drive is realised in the well known Kramer drive. It
consists of a wound rotor induction motor fed from three
phase balanced supply of fixed frequency and coupled on
the same shaft to a separately excited d.c. motor. Slip
ring voltage is fed to the armature of d.c. motor through
a three phase uncontrolled rectifier and filter circuit.
Speed of this drive is controlled in sub-synchronous region
by varying field current settings. The speed range is
limited on account of saturation of the d.c. motor magnetic
circuit.

Speed range of the drive may be increased further
by employing a controlled bridge rectifier instead of

uncontrolled one and controlling the firing angle of this rectifier. The efficiency of this system is good because most of the slip power is utilized by d.c. motor to provide additional torque to the shaft. However a good efficiency is achieved at the cost of power factor, which becomes poor under firing angle control. This drive can be used where large amount of power is to be handled and it is required to run the drive at very low speeds for short time intervals. The theoretical investigations of the steady state performance on the concept of equivalent circuit have been given by Hori (6). These studies deal with the various performance characteristics of a three phase bridge rectifier and the speed control system.

Gupta, and Verma (7) have discussed the steady state performance of a modified Kramer drive employing an electronic chopper in the rotor circuit. Speed is reduced further when field current control has been exhausted by varying the chopper duty cycle (8). It has been brought out that the presence of the rectifier bridge in the rotor circuit causes harmonic currents in the rotor and the stator, which produce harmonic torques. However, it is shown that rotor current harmonics do not significantly influence the overall performance. Experimental results are also tallied with theoretical results.

The development of static drives with controlled
thyristors in the circuit has led to the problem of system
instability, depending upon the parameters of the system.
Induction machines which are perfectly stable on an infinite
bus may become unstable with controlled thyristors in the
circuit.

The stability analysis of variable frequency static
drives have been carried out by many authors (9-16). They
have concluded that the system exhibits a large region of
instability at low supply frequencies even with normal
parameters. A static slip energy recovery drive having a
controlled rectifier in rotor circuit may exhibit instability
with certain combination of firing angle of the controlled
rectifier and the slip of the drive.

CONTRIBUTION BY THE AUTHOR

A rigorous mathematical model has been developed
for analyzing the steady state and dynamic behaviour of the
system. In order to derive the above, the system is
analyzed in a synchronously rotating reference frame.

Steady state equations for the system have been
derived. The performance characteristics under steady state
conditions have been computed and got plotted by CALCOMP
plotter. A subroutine for steady state analysis is developed
which gives directly the steady state performance of a

drive whose parameters are fed into it.

The perturbation equations are derived to investigate the stability of the drive. The characteristic equation has been obtained from the perturbation equations. These perturbation equations are simulated on a digital computer for which a program in FORTRAN language is developed which gives directly the points of stability contour for onward plotting by CALCOMP plotter. Unstable regions have been plotted in the torque firing angle plane. Effect of various system parameters upon the regions of instability has been studied and conclusions drawn.

CHAPTER II

DEVELOPMENT OF MATHEMATICAL MODEL

Generalised equations describing the behaviour of
slip-energy recovery drive employing controlled rectifier
are developed in this chapter, using the concept of direct
and quadrature axis components. The system has been analyzed
in a synchronously rotating reference frame. Basic equations
for the idealized induction motor are developed. Expressions
for the average value of controlled bridge rectifier are
established. The equations of the overall system are established
from the equations of induction machine, d.c. machine and from
the equations which predict the average values of the converter
variables. The equations have been so simplified that the
electrical characteristics can be represented by a set of four
simultaneous differential equations of the first order. An
equation of the electromagnetic torque completes the set of
system equations used in the study.

2.1 INTRODUCTION

Schematic diagram of slip energy recovery drive under
investigation is shown in fig. 2.1. This drive is a modified
form of Kramer drive. A Kramer drive consists of a wound
rotor induction motor fed from three phase balanced supply
of fixed frequency and coupled on the same shaft to a separa-
tely excited d.c. motor. The voltage across slip rings of
the induction motor is fed to the armature of d.c. motor
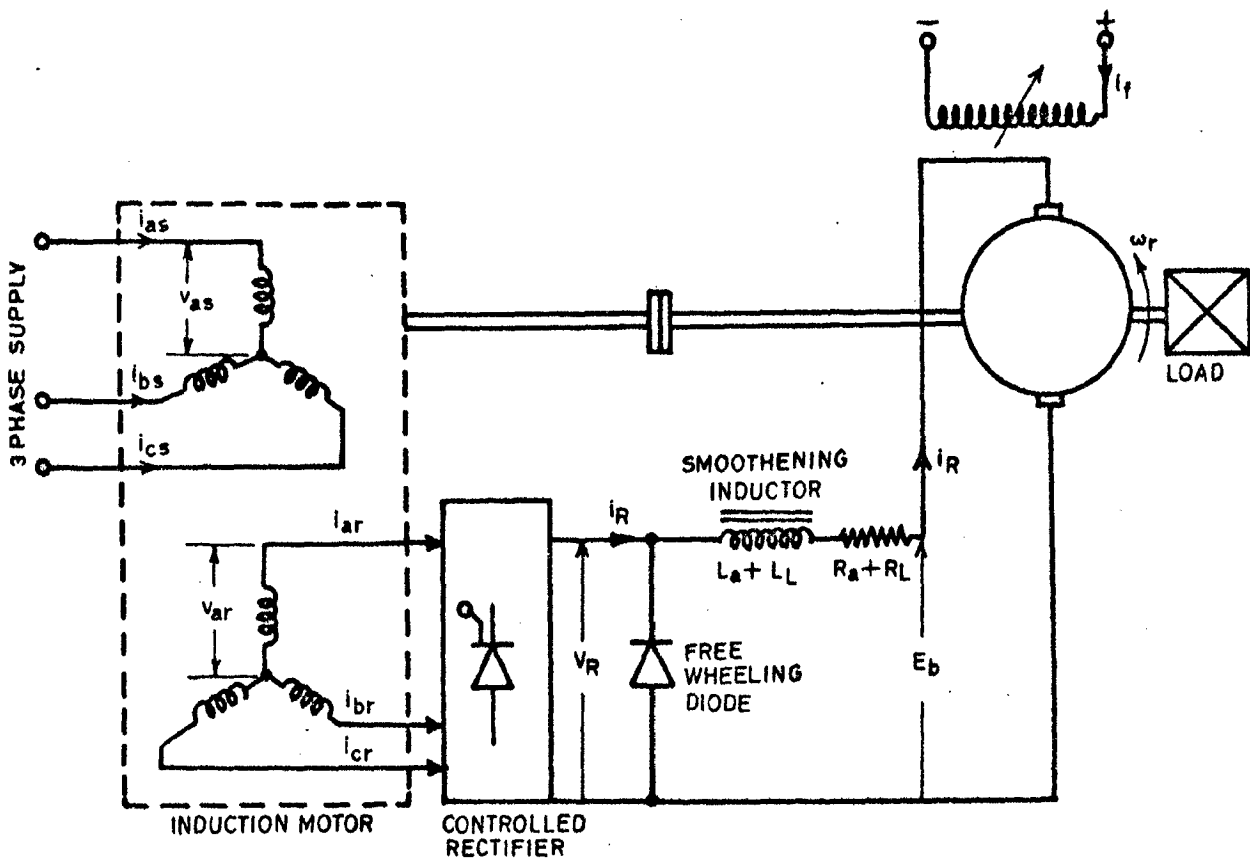
FIG. 2.1: SCHEMATIC OF SLIP ENERGY RECOVERY DRIVE

through a static three phase, uncontrolled bridge rectifier and a smoothening inductor. Speed is controlled in sub-synchronous region by controlling the field current of d.c. motor. The lowest speed is limited to about half the synchronous speed in a normally designed set in which rating of induction motor is equal to the rating of d.c. motor. This lowest speed is obtained on account of saturation of the d.c. motor magnetic circuit.

Speed range of the drive can be increased by employing controlled bridge rectifier instead of uncontrolled one and controlling the firing angle of/rectifier. Firing angle control is used after speed has been reduced to its lowest by field current control.

A mathematical model of the slip energy recovery drive is developed by the circuit equations derived in per unit in this chapter, neglecting saturation, hysteresis and eddy current effects in induction motor, voltage drops in rectifier and induction motor rotor current harmonics.

2.2 ESTABLISHMENT OF BASIC EQUATIONS FOR THE SYSTEM

2.2.1 EQUATIONS FOR INDUCTION MOTOR

The generalised equations describing the behaviour of induction motor under transient and steady state condition are established by considering it as an elementary two pole idealised machine. (17-18) The effect of number of poles is taken into account by multiplying the expression for torque by the number of pole pairs.

Schematic diagram of an ideal 3-phase induction motor is shown in fig. 2.2(a), wherein it is regarded as a group of linear coupled circuits. Distributed stator and rotor windings have been shown by concentrated coils. The connections and current conventions for the stator and rotor phases are shown in fig. 2.2(b).

Equations for induction motor are established from the concept of generalized theory of machines. For the analysis of electromechanical devices, it is necessary to establish equations for both electrical and mechanical systems. Thus a mathematical formulation will have

(i)   a set of voltage - current equations, relating the applied voltages to winding currents, using various circuit parameters.

(ii) an equation of motion.

Above two sets of equations are related by a third expression which gives electromagnetic torque developed in terms of winding currents and circuit parameters.

The induction motor voltage current equations expressed in synchronously rotating d-q reference frame are (17)

$$
\begin{bmatrix} V_{ds} \\ V_{qs} \\ V_{dr} \\ V_{qr} \end{bmatrix} = \begin{bmatrix} (R_{ss}+L_{ss}p) & -wL_{ss} & L_{12}p & -wL_{12} \\ wL_{ss} & (R_{ss}+L_{ss}p) & wL_{12} & L_{12}p \\ L_{12}p & -swL_{12} & (R_{rr}+L_{rr}p) & -swL_{rr} \\ swL_{12} & L_{12}p & swL_{rr} & (R_{rr}+L_{rr}p) \end{bmatrix} \begin{bmatrix} i_{ds} \\ i_{qs} \\ -i_{dr} \\ -i_{qr} \end{bmatrix}
$$

$$....(2.1)$$

AXIS OF
PHASE b_s

AXES OF
PHASE b_r

q-axis

b_s

b_r

a_s

a_r

c_r

c_s

AXIS OF MOTOR
PHASE-a_r

d-AXIS

AXIS OF STATOR
PHASE, a_s

AXIS OF PHASE c_r

AXIS OF PHASE
c_s

AXIS OF
PHASE b_r
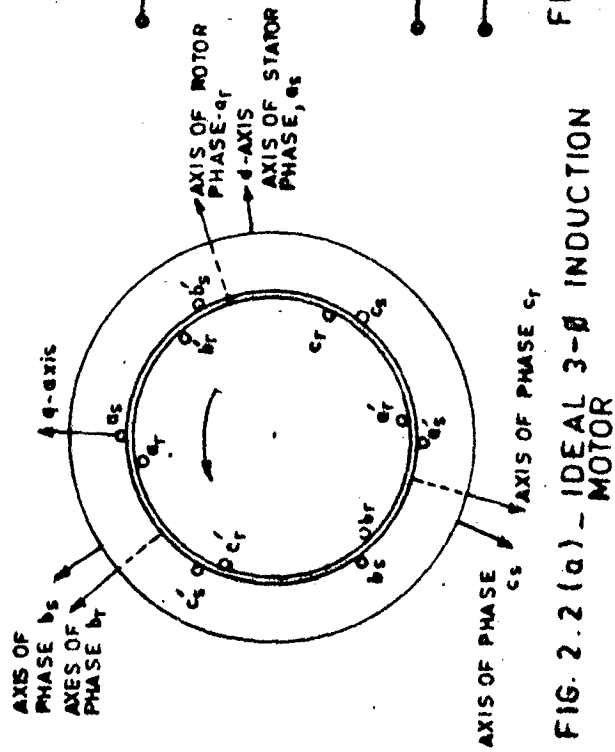
FIG. 2.2 (a) – IDEAL 3-∅ INDUCTION
MOTOR

a_s v_{as} i_{as}

v_{bs} b_s i_{bs}

v_{cs} c_s i_{cs}

a_r v_{ar} i_{ar}

v_{br} b_r i_{br}

v_{cr} c_r i_{cr}
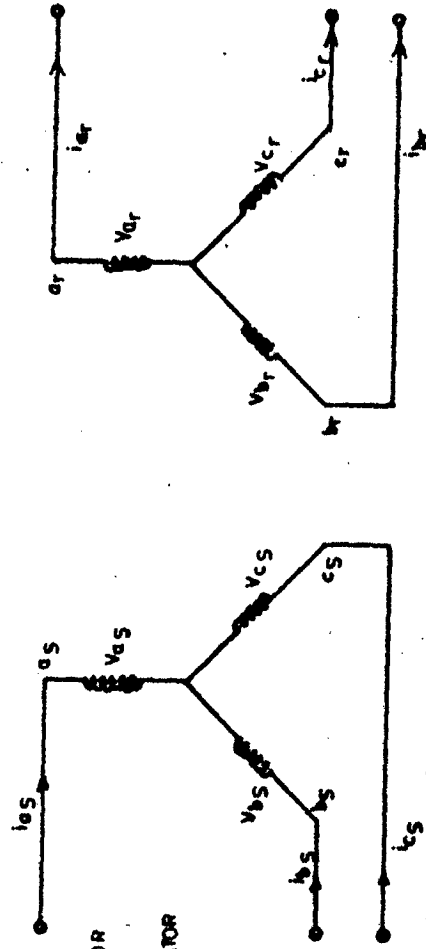
FIG. 2.2 (b) – CONNECTIONS AND CURRENT CONVENTIONS
FOR 3-∅ I MOTOR

The electromagnetic torque developed by the induction motor in N-m is given by

$$T_{e_{IM}} = \frac{3}{2} \frac{P}{2} L_{12} (i_{ds} i_{qr} - i_{qs} i_{dr}) \quad \ldots\ldots(2.2)$$

where P is the no.of poles of induction motor.

In writing above euations, conventional direction of power flow in the machine has been considered i.e. power flows into the motor at stator terminals and out of it at rotor terminals. Fig. 2.3 depicts the angular relationship of various axes of stator and rotor phases and those of synchronously rotating d-q reference frame, at any time t. Resolving phase voltages along d-q frame, the d-q voltage can be expressed as

Stator

$$V_{ds} = \frac{2}{3} \left[V_{as} \cos\theta + V_{bs} \cos(\theta - \frac{2\pi}{3}) + V_{cs} \cos(\theta + \frac{2\pi}{3}) \right] \quad \ldots(2.3)$$

$$V_{qs} = -\frac{2}{3} \left[V_{as} \sin\theta + V_{bs} \sin(\theta - \frac{2\pi}{3}) + V_{cs} \sin(\theta + \frac{2\pi}{3}) \right] \quad \ldots.(2.4)$$

Rotor

$$V_{dr} = \frac{2}{3} \left[V_{ar} \cos\beta + V_{br} \cos(\beta - \frac{2\pi}{3}) + V_{cr} \cos(\beta + \frac{2\pi}{3}) \right] \quad \ldots\ldots(2.5)$$

$$V_{qr} = -\frac{2}{3} \left[V_{ar} \sin\beta + V_{br} \sin(\beta - \frac{2\pi}{3}) + V_{cr} \sin(\beta + \frac{2\pi}{3}) \right] \quad \ldots(2.6)$$

where θ = wt, β = Angle of advancement of d-axis w.r.t. axis of phase a of rotor.

The choice of factor $\frac{3}{2}$ is arbitrary.

$$\dot{\theta} = \omega$$

$$\dot{\theta}_2 = \omega_\gamma$$
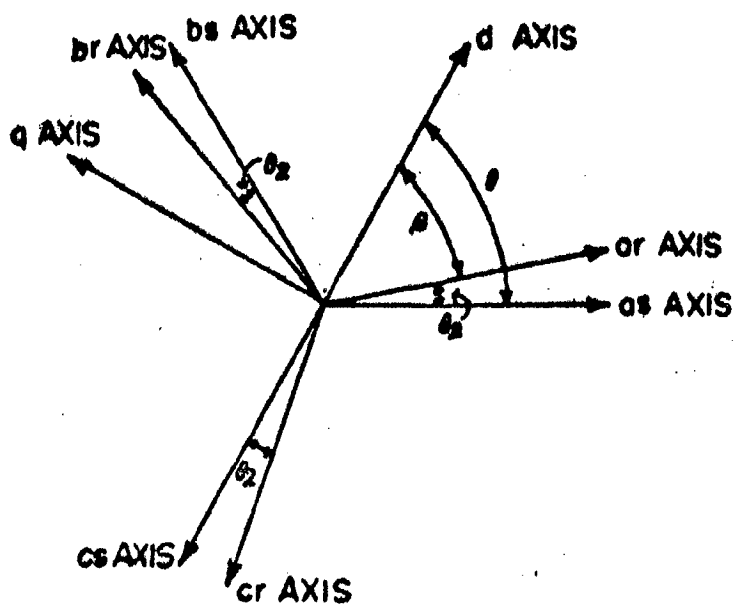
$$\beta = \theta - \theta_2$$

FIG. 2.3 Axes of 2 pole 3 phase symmetrical induction motor

If $t = 0$ instant be so chosen that at this instant $\theta = \beta = 0$, d-axis will be coinciding with axes as and ar, as is clear from equation (2.3) and equation (2.5) respectively.

Stator and rotor terminal voltages at any instant, may be expressed as

Stator

$$V_{as} = V_{sm} \cos\theta$$

$$V_{bs} = V_{sm} \cos(\theta - \tfrac{2\pi}{3})$$

$$V_{cs} = V_{sm} \cos(\theta + \tfrac{2\pi}{3}). \quad \dots\dots\dots(2.7)$$

Rotor

$$V_{ar} = V_{rm} \cos(\beta + \alpha_r)$$

$$V_{br} = V_{rm} \cos(\beta + \alpha_r - \tfrac{2\pi}{3})$$

$$V_{cr} = V_{rm} \cos(\beta + \alpha_r + \tfrac{2\pi}{3}) \quad \dots\dots(2.8)$$

where α_r is an arbitrary phase angle, which is equal to the phase difference between stator and rotor phase voltages of any phase at time zero.

Substituting from equations (2.7) and (2.8) in equation (2.3) to (2.6).

$$V_{ds} = \tfrac{2}{3} \left[V_{as} \cos\theta + V_{bs} \cos(\theta - \tfrac{2\pi}{3}) + V_{cs} \cos(\theta + \tfrac{2\pi}{3}) \right]$$

or,

$$V_{ds} = V_{sm} \quad \dots\dots\dots(2.9).$$

and

$$V_{qs} = 0 \quad \ldots\ldots\ldots (2.10)$$

$$V_{dr} = \frac{2}{3} \left[V_{ar} \cos\beta + V_{br} \cos(\beta - \frac{2\pi}{3}) + V_{cr} \cos(\beta + \frac{2\pi}{3}) \right]$$

$$= V_{rm} \cos\alpha_r \quad \ldots\ldots (2.11)$$

and

$$V_{qr} = V_{rm} \sin\alpha_r \quad \ldots\ldots (2.12)$$

2.2.2 EQUATIONS FOR CONTROLLED BRIDGE RECTIFIER

Assuming negligible ripple in the d.c. current at the rectifier output and neglecting voltage drop due to overlap, the average output voltage of a 3-phase, full wave, controlled rectifier bridge is given by (19-21)

$$V_R = \frac{3\sqrt{3}}{\pi} V_{rm} \cos\alpha \quad \ldots\ldots\ldots (2.13)$$

where V_{rm} is the peak value of fundamental phase voltage at rectifier input and α is firing angle.

Under the conditions, assumed above, the phase current at input to the rectifier is in the form of rectangular pulses of $\frac{2\pi}{3}$ duration, alternating at rotor frequency and having an amplitude of average d.c. current at the output i.e. i_R. The peak value of the fundamental component of phase current is therefore given by

$$i_{rm} = \frac{2\sqrt{3}}{\pi} i_R \quad \ldots\ldots\ldots (2.14).$$

Fundamental power input to the rectifier is

$$P_{in} = 3 \, V_{ph} \, i_{ph} \, Cos\phi$$

$$= 3 \, \frac{V_{rm}}{\sqrt{2}} \, \frac{i_{rm}}{\sqrt{2}} \, Cos\phi \quad \dots (2.15)$$

where ϕ is the phase angle between fundamental voltage and current of the rotor phase.

The power output from rectifier is given by

$$P_{out} = V_R \, i_R \quad \dots (2.16)$$

Substituting equation (2.13) and (2.14) in equation (2.16)

$$P_{out} = 3 \, \frac{V_{rm}}{\sqrt{2}} \, \frac{i_{rm}}{\sqrt{2}} \, Cos\alpha \quad \dots (2.17)$$

Since, the rectifier losses have been neglected, power input to the rectifier, should be equal to power output

or $\quad 3 \, \dfrac{V_{rm}}{\sqrt{2}} \, \dfrac{i_{rm}}{\sqrt{2}} \, Cos\phi = 3 \, \dfrac{V_{rm}}{\sqrt{2}} \, \dfrac{i_{rm}}{\sqrt{2}} \, Cos\alpha$

or $Cos\phi = Cos\alpha$

So, $\phi = \alpha. \quad \dots (2.18)$.

It shows that fundamental power factor angle is equal to the firing angle of bridge rectifier. It implies that fundamental component of rotor phase current lags the fundamental rotor phase voltage by an angle α°.

Therefore, the rotor phase currents can be expressed in accordance with the expression (2.8), as

$$i_{ar} = i_{rm} \, \text{Cos} \, (\beta + \alpha_r - \alpha)$$

$$i_{br} = i_{rm} \, \text{Cos} \, (\beta + \alpha_r - \alpha - \frac{2\pi}{3})$$

$$i_{cr} = i_{rm} \, \text{Cos} \, (\beta + \alpha_r - \alpha + \frac{2\pi}{3}) \, \ldots (2.19).$$

The transformation equation for rotor current may be written as

$$i_{dr} = \frac{2}{3} \left[i_{ar} \, \text{Cos}\beta + i_{br} \, \text{Cos}(\beta - \frac{2\pi}{3}) + i_{cr} \, \text{Cos}(\beta + \frac{2\pi}{3}) \right]$$

$$i_{qr} = -\frac{2}{3} \left[i_{ar} \, \text{Sin}\beta + i_{br} \, \text{Sin}(\beta - \frac{2\pi}{3}) + i_{cr} \, \text{Sin}(\beta + \frac{2\pi}{3}) \right]$$

$$\ldots (2.20)$$

Substituting expression (2.19) in expression (2.20),

$$i_{dr} = i_{rm} \, \text{Cos}(\alpha_r - \alpha)$$

$$i_{qr} = i_{rm} \, \text{Sin}(\alpha_r - \alpha) \, \ldots (2.21)$$

2.2.3 EQUATIONS FOR THE D.C. MOTOR

The voltage balance equation of the d.c. motor armature circuit is given by

$$V_R = (R + Lp)i_R + K_f \bullet i_f \, w_r \, \frac{2}{P} \, \ldots (2.22)$$

Since $w_r = (1 - s)w$ ....(2.23)

$V_R = (R + Lp) i_R + K_f i_f \frac{2}{P} w (1 - s)$ ......(2.24)

where R and L are total resistance and inductance of the armature circuit including smoothening inductor, K_f is rotational voltage coefficient (volts/rad/sec/field amp). The electromagnetic torque developed by the d.c. motor is given by

T_e DC $= K_f i_f i_R$ N-m .....(2.25)

Substituting for i_R from equation (2.14)

T_e DC $= \frac{\pi}{2/3} K_f i_f i_{rm}$ ......(2.26).

2.2.4 EQUATION OF THE DRIVE

Equations(2.1) can be rewritten now by directly substituting for V_{ds} and V_{qs} as V_{sm} and 0 respectively. Substitution for V_{dr} and V_{qr} is done in following manner.

Substituting equation (2.13) in equation (2.11)

$V_{dr} = \frac{\pi}{3/3} \frac{\cos \alpha_r}{\cos \alpha} V_R$ .....(2.27)

Combining equation (2.24), equation (2.14) and equation (2.27)

$V_{dr} = \frac{\pi}{3/3} \frac{\cos \alpha_r}{\cos \alpha} [(R+Lp)\frac{\pi}{2/3} i_{rm} + K_f i_f \frac{2}{P} w (1 - s)]$.

.....(2.28)

Substituting for i_{rm} from equation (2.21) in above equation

$$V_{dr} = \frac{\pi}{3\sqrt{3}} \frac{Cos\alpha_r}{Cos\alpha} \left[\frac{\pi}{2\sqrt{3}}(R + Lp) \frac{i_{dr}}{Cos(\alpha_r - \alpha)} + K_f \, i_f \, \frac{2}{P} w(1 - s) \right]$$

or

$$V_{dr} = \frac{\pi^2}{18} \frac{Cos\alpha_r}{Cos\alpha \, Cos(\alpha_r - r)} (R + Lp) \, i_{dr} + \frac{\pi}{3\sqrt{3}} \frac{Cos\alpha_r}{Cos\alpha} .$$

$$K_f \, i_f \, \frac{2}{P} w (1 - s) \qquad \ldots\ldots(2.29)$$

Similarly,

$$V_{qr} = \frac{\pi^2}{18} \frac{Sin\alpha_r}{Cos\alpha \, Sin(\alpha_r - \alpha)} (R + Lp) \, i_{qr} + \frac{\pi}{P\sqrt{3}} .$$

$$+ \frac{\pi}{3\sqrt{3}} . \frac{Sin\alpha_r}{Cos\alpha} \, K_f \, i_f \, \frac{2}{P}w (1 - s) \quad \ldots\ldots(2.30)$$

Substituting for V_{ds}, V_{qs}, $V_{\alpha r}$ and V_{qr} in equations (2.1) the final voltage current equations of the drive are obtained as

$$
\begin{bmatrix}
V_{sm} \\
0 \\
K_1(1-s)\dfrac{Cos\alpha_r}{Cos\alpha} \\
K_1(1-s)\dfrac{Sin\alpha_r}{Cos\alpha}
\end{bmatrix}
=
\begin{bmatrix}
(R_{ss}+L_{ss}p) & -wL_{ss} & L_{12}p & -wL_{12} \\
wL_{ss} & (R_{ss}+L_{ss}p) & wL_{12} & L_{12}p \\
L_{12}p & -swL_{12} & (R_{eq1}+L_{eq1}p) & -swL_{rr} \\
swL_{12} & L_{12}p & swL_{rr} & R_{eq2}+L_{eq2}p
\end{bmatrix}
\begin{bmatrix}
i_{ds} \\
i_{qs} \\
-i_{dr} \\
-i_{qr}
\end{bmatrix}
$$

$$\ldots\ldots(2.31)$$

where

$$K_1 = \frac{\pi}{3/3} \, K_f \, i_f \, \frac{2}{P} \, w$$

$$R_{eq1} = R_{rr} + \frac{\pi^2 R}{18} \frac{\cos \alpha r}{\cos \alpha \, \cos(\alpha r - r)}$$

$$L_{eq1} = L_{rr} + \frac{\pi^2 L}{18} \frac{\cos \alpha r}{\cos \alpha \, \cos(\alpha r - \alpha)}$$

$$R_{eq2} = R_{rr} + \frac{\pi^2 R}{18} \frac{\sin \alpha r}{\cos \alpha \, \sin(\alpha r - \alpha)}$$

$$L_{eq2} = L_{rr} + \frac{\pi^2 L}{18} \frac{\sin \alpha r}{\cos \alpha \, \sin(\alpha r - \alpha)}$$

The expression for electromagnetic torque developed by the system is obtained by adding the torque developed by the induction motor and that by the d.c. motor.

$$T_e = T_{e \, IM} + T_{e \, DC} \qquad \dots\dots(2.32)$$

Substituting from equation (2.2) and equation (2.26)

$$T_e = \frac{3}{2} \frac{P}{2} L_{12} (i_{ds} \, i_{qr} - i_{qs} \, i_{dr}) + \frac{\pi}{2/3} \, K_f \, i_f \, i_{rm} \qquad \dots\dots(2.33)$$

Equations (2.31) contain five unknown variables i.e. i_{ds}, i_{qs}, i_{dr}, i_{qr} and α_r. They can be reduced to four by expressing i_{dr} and i_{qr} in terms of i_{rm} and α_r from equations (2.21).

Generally the machine parameters are measured with respect to stator windings. Therefore it is more convenient

to refer all the quantities to the stator windings. Hence referring all quantities to the stator winding, the final equations of the system are,

$$
\begin{bmatrix}
V_{sm} \\
0 \\
aK_1(1\text{-}s)\dfrac{Cos\alpha_r}{Cos\alpha} \\
aK_1(1\text{-}s)\dfrac{Sin\alpha_r}{Cos\alpha}
\end{bmatrix}
\begin{bmatrix}
(R_{ss}+L_{ss}p) & -wL_{ss} & L_M p & -wL_M \\
wL_{ss} & (R_{ss}+L_{ss}p) & wL_M & L_M p \\
L_M p & -swL_M & (R_{eq1}' + L_{eq1}'p) & -swL_{rr}' \\
swL_M & L_M p & swL_{rr}' & (R_{eq2}' + L_{eq2}'p)
\end{bmatrix}
\begin{bmatrix}
i_{as} \\
i_{qs} \\
-i_{rm}'Cos\alpha_r \\
-i_{rm}'Sin\alpha_r
\end{bmatrix}
$$

where

$$L_M = aL_{12}$$

$$R_{eq1}' = a^2 R_{eq1}$$

$$L_{eq1}' = a^2 L_{eq1}$$

$$i_{rm}' = \dfrac{i_{rm}}{a} \qquad \dots\dots(2.34)$$

A prime is affixed to all referred quantities. Electromagnetic torque equation for the system may be expressed as

$$T_e = \frac{3}{2}\frac{P}{2} L_M (i_{ds}\, i_{qr}' - i_{qs}\, i_{dr}') + \frac{\pi}{2/3}\, a\, K_f\, i_f\, i_{rm}' \qquad \dots.(2.35).$$

2.3 EQUATIONS IN PER UNIT SYSTEM

Equations are presented in per unit form because it has numerous advantages -

(i)   A simple inspection of the per unit parameters immediately reveals much more about the basic nature of the machine than may be observed from the ordinary parameters.

(ii)   The numerical range of per unit parameters is small, therefore easy to solve on digital computer.

(iii)   Arbitrary numerical factors which may appear in the ordinary equations in d-q axes transformations are avoided.

The choice of the base values for various quantities are made so that computational effort is reduced. The base values chosen (Appendix-I) are as follows:

Unit Voltage = V_{base} = Peak value of rated phase voltage

in volts (V_{sm})

Unit Current = I_{base} = Peak value of rated phase current

in Amps (I_{sm})

Unit Impedance = Z_{base} = $\dfrac{V_{base}}{I_{base}}$, ohms

Unit Power = P_{base} = Rated apparent power = $\dfrac{3}{2} V_{sm} \cdot I_{sm}$,

Watts

Unit Frequency = F_{base} = Rated frequency in Hertz

Unit Mechanical Speed = $\acute{V}_{base}$ = $\frac{2}{P} w_b$, rad/sec.

Unit Torque = T_{base} = $\dfrac{P_{base}}{V_{base}}$, N-m

Equations (2.34) can be converted in per unit form by dividing each quantity with their base value. Prime affixed to all referred quantities may be withdrawn for simplification in handling the equations. First equation of equations (2.34) is given by

$$V_{sm} = (R_{ss} + L_{ss}p)\, i_{ds} - wL_{ss}\, i_{qs} - L_M p\, i_{dr} + wL_M\, i_{qr}$$

Dividing throughout by V_{base}

$$\frac{V_{sm}}{V_b} = \frac{(R_{ss}+L_{ss}p)i_{ds}}{V_b} - \frac{wL_{ss}\, i_{qs}}{V_b} - \frac{L_M p\, i_{dr}}{V_b} + \frac{wL_M}{V_b}\, i_{qr}$$

$$V_{sm(p.u.)} = \frac{(R_{ss}+\frac{w_b}{w_b} L_{ss}p)\, i_{ds}}{\frac{V_b}{i_b}\, i_b} - \frac{\frac{w}{w_b}\, w_b\, L_{ss}\, i_{qs}}{\frac{V_b}{i_b}\, i_b} -$$

$$\frac{\frac{w_b}{w_b} L_M p\, i_{dr}}{\frac{V_b}{i_b}\, i_b} + \frac{\frac{w}{w_b}\, w_b\, L_M\, i_{qr}}{\frac{V_b}{i_b}\, i_b}$$

$$V_{sm(p.u.)} = \frac{(R_{ss} + \frac{X_{ss}p}{w_b})}{Z_b} \frac{i_{ds}}{i_b} - F_R \frac{X_{ss}}{Z_b} \frac{i_{qs}}{i_b} -$$

$$\frac{X_M p}{w_b} \frac{i_{dr}}{Z_b} \frac{i_{dr}}{i_b} + F_R \frac{X_M}{Z_b} \frac{i_{qr}}{i_b}$$

or

$$V_{sm(p.u.)} = \left[R_{ss(p.u.)} + X_{ss(p.u.)} \frac{p}{w_b} \right] i_{ds(p.u.)} -$$

$$F_R \ X_{ss(p.u.)} \ i_{qs(p.u.)} - X_{M(p.u.)} \ \frac{1}{w_b} \ i_{dr(p.u.)}$$

$$+ \ F_R \ X_{M(p.u.)} \ i_{qr(p.u.)} \quad \ldots\ldots(2.36)$$

where $F_R = \frac{W}{w_b} = \frac{f}{f_b}$ is frequency ratio. It may also be interpreted as the applied frequency expressed in per unit. It simply predicts the behaviour of an induction motor at any operating frequency.

Remaining stator and rotor voltage equations can be converted to per-unit form in a similar way.

Final voltage current equation for the system can be expressed in matrix form as,

$$
\begin{bmatrix}
V_{sm} \\
0 \\
K_2 F_R(1-s) \dfrac{\cos\alpha_r}{\cos\alpha} \\
K_2 F_R(1-s) \dfrac{\sin\alpha_r}{\cos\alpha}
\end{bmatrix}
=
\begin{bmatrix}
(R_{ss}+X_{ss}\frac{p}{w_b}) & -F_R X_{ss} & X_M \frac{p}{w_b} & -F_R X_M \\
F_R X_{ss} & (R_{ss}+X_{ss}\frac{p}{w_b}) & F_R X_M & X_M \frac{p}{w_b} \\
X_M \frac{p}{w_b} & -s F_R X_M & (R_{eq1}+X_{eq1}\frac{p}{w_b}) & -s F_R X_{rr} \\
s F_R X_M & X_M \frac{p}{w_b} & s F_R X_{rr} & (R_{eq2}+X_{eq2}\frac{p}{w_b})
\end{bmatrix}
\begin{bmatrix}
i_{ds} \\
i_{qs} \\
-i_{rm}\cos(\alpha_r-\alpha) \\
-i_{rm}\sin(\alpha_r-\alpha)
\end{bmatrix}
$$

$$(2.37)$$

where

$$K_2 = K_1 \frac{a}{V_b}$$

Electromagnetic torque equation (2.35) for the system can also be converted to per unit form by dividing with T_{base}

$$\frac{T_e}{T_b} = \frac{\frac{3}{2}\frac{P}{2} L_M(i_{ds} i_{qr} - i_{qs} i_{dr})}{T_b} + \frac{a K_f i_f \frac{\pi}{2\sqrt{3}} i_{rm}}{T_b}$$

$$T_{e(p.u.)} = \frac{\frac{3}{2}\frac{P}{2} L_M (i_{ds} i_{qr} - i_{qs} i_{dr})}{\frac{3}{2}\frac{V_b i_b}{V_b}} + \frac{\frac{\pi}{2\sqrt{3}} a K_f I_f \dot{i}_{rm}}{\frac{3}{2}\frac{V_b i_b}{V_b}}$$

$$= \frac{\frac{P L_M}{2} \frac{2}{P} w_b}{Z_b} \left[\frac{i_{ds}}{i_b} \frac{i_{qr}}{i_b} - \frac{i_{qs}}{i_b} \frac{i_{dr}}{i_b} \right] +$$

$$\frac{\pi}{3\sqrt{3}} \frac{2}{P} w_b K_f i_f \frac{i_{rm}}{i_b} \frac{a}{V_b}$$

$$T_{e(p.u.)} = X_{M(pu)} i_{ds(pu)} i_{qr(pu)} - i_{qs(pu)} i_{dr(pu)}$$

$$+ K_2 i_{rm(pu)} \qquad \ldots\ldots\ldots (2.38)$$

Under dynamic condition, the developed electromagnetic torque is balanced by load torque and accelerating torque. The torque balance equation in p.u. form can be expressed as

$$T_e = T_L + T_a$$

or

$$T_e = T_L + J \frac{dw_r}{dt} \qquad \ldots\ldots(2.39)$$

where

T_a = Accelerating Torque

J = Rotational Moment of Inertia

w_r = Mechanical speed of rotor.

Moreover from equation (2.33)

$$w_r = w_s(1-s) = \gamma_b(1-s) \; F_R \qquad \ldots\ldots(2.40)$$

Now

Intertia Constt $H = \dfrac{\text{Kinetic Energy stored at synchronous speed}}{\text{Base Power}}$ (Base Mechanical Speed)

$$= \frac{\frac{1}{2} J \gamma_b^2}{P_b} \quad \text{Seconds} \qquad \text{Seconds}$$

$$\frac{\frac{1}{2} J \gamma_b}{T_b} \quad \text{Seconds}$$

or $J . \dfrac{2H \; T_b}{\gamma_b} \qquad \ldots\ldots(2.41)$

Combining equations no. (2.39), (2.40) and (2.41)

$$T_e = T_L + \frac{2H \; T_b}{\gamma_b} \quad \frac{d}{dt} \gamma_b (1-s) \; F_R$$

or $\dfrac{T_e}{T_b} = \dfrac{T_L}{T_b} + 2Hp(1 - s) \, F_R$

or $T_{e(pu)} = T_{L\,(pu)} + 2Hp(1 - s) \, F_R$

Equations (2.37) and (2.42) in per unit form, completely describe the behaviour of the drive.

2.4 CONCLUSION

The idealized model developed on the concept of coupled circuit approach is well suited for determining the dominant features of this system. The assumptions made in developing the model are quite justified for most of the practical purposes. The parameters involved in the model are such that they can be easily measured at the terminals of the machine. The model is extremely useful for carrying out steady state and stability studies of the slip energy recovery drive under investigation.

STEADY STATE ANALYSIS

3.1 INTRODUCTION

This chapter deals with the steady state analysis of the slip energy recovery drive presented in the previous chapter. Expressions of torque, supply current, power factor, efficiency, fundamental rotor phase current and d.c. link current are derived using the mathematical model developed earlier. Steady state performance has been investigated at different field current settings and different firing angle settings. Performance characteristics over a wide range of speed have been obtained.

3.2 SYSTEM EQUATIONS UNDER STEADY STATE

During steady state, the different phase voltages and phase currents attain a steady value and appear d.c. in nature, when referred to a synchronously rotating frame. Hence their time derivatives would fall to zero. Thus steady state equations of the system are obtained from the equations (2.37) by replacing all the terms associated with p by zeros. Hence final steady state equations can be expressed as

$$
\begin{bmatrix} V_{sm} \\ 0 \\ \dfrac{K_2 F_r(1-s)\cdot \cos\alpha_{ro}}{\cos\alpha} \\ \dfrac{K_2 F_R(1-s)\cdot \sin\alpha_{ro}}{\cos\alpha} \end{bmatrix} = \begin{bmatrix} R_{ss} & -F_R X_{ss} & 0 & -F_R X_M \\ F_R X_{ss} & R_{ss} & F_R X_M & 0 \\ 0 & -s_o F_R X_M & R_{eq1} & -s_o F_R X_{rr} \\ s_o F_R X_M & 0 & s_o F_R X_{rr} & R_{eq2} \end{bmatrix} \begin{bmatrix} i_{dso} \\ i_{qso} \\ -i_{rm_o}\cos(\alpha_{r_o}-\alpha) \\ -i_{rm}\sin(\alpha_{r_o}-\alpha) \end{bmatrix}
$$

$$\ldots\ldots(3.1)$$

where steady state quantities are identified by subscript o.

For given values of slip V_{sm}, i_f, α and F_R, above equation may be simultaneously solved to calculate the values i_{ds_0}, i_{qs_0}, i_{rm_0} and α_{r_0}. Substituting these values in equation(2.21), values of i_{dr_0} and i_{qr_0} can be obtained. Torque developed by the drive may be calculated using equation (2.38).

3.2.1 SOLUTION OF STEADY STATE EQUATIONS

Equation (3.1) can be solved by combining first two and last two equation together, as shown below:

$$V_{sm} + j0 = R_{ss}\, i_{ds_0} - F_R\, X_{ss}\, i_{qs_0} + F_R\, X_M\, i_{qr_0} \cdot Sin(\alpha_{r_0}-\alpha)$$

$$+ j[F_R\, X_{ss}\, i_{ds_0} + R_{ss}\, i_{qs_0} - F_R\, X_M\, i_{rm_0}\, Cos(\alpha_{r_0}-\alpha)]$$

$$V_{sm} \underline{/0^\circ} = R_{ss}(i_{ds_0} + j i_{qs_0}) + j\, F_R\, X_{ss}(i_{ds_0} + j i_{qs_0})$$

$$- j F_R\, X_M\, i_{rm_0} \cdot [Cos(\alpha_{r_0}-\alpha) + j\, Sin(\alpha_{r_0}-\alpha)]$$

$$V_{sm} \underline{/0^\circ} = (R_{ss} + j\, F_R\, X_{ss}) \hat{i}_{sm_0}$$

$$- j\, F_R\, X_M\, i_{rm_0} \underline{/\alpha_{r_0}-\alpha} \qquad \ldots\ldots(3.2)$$

where i_{sm_0} is the peak value of stator phase current under steady state.

Similarly, last two equations can be combined.

$$\frac{K_2 \, F_R (1-s_0) \, \cos\alpha_{r_0}}{\cos\alpha} + j \, \frac{K_2 \, F_R \, (1-s_0) \, \sin\alpha_0}{\cos\alpha} = - \, s_0 \, F_R \, X_M \, i_{qs_0}$$

$$- \, R_{eq_1} \, i_{rm_0} \, \cos(\alpha_{r_0} - \alpha) + s_0 \, F_R \, X_{rr} \, i_{rm_0} \, \sin(\alpha_{r_0} - \alpha) +$$

$$j[s_0 \, F_R \, X_M \, i_{ds_0} - s_0 \, F_R \, X_{rr} \, i_{rm_0} \, \cos(\alpha_{r_0} - \alpha) -$$

$$R_{eq_2} \, i_{rm_0} \, \sin(\alpha_{r_0} - \alpha)]$$

Substituting for R_{eq_1} and R_{eq_2} from equation (2.31)

in above equation and simplifying

$$\frac{K_2 \, F_R (1-s_0) \, /\alpha_{r_0}}{\cos\alpha} = j \, s_0 \, F_R \, X_M (i_{ds_0} + j \, i_{qs_0}) - R_{rr} \, i_{rm_0} \{\cos(\alpha_{r_0} - \alpha) + j \, \sin(\alpha_{r_0} - \alpha)\}$$

$$= \frac{\pi^2 R}{18 \, \cos\alpha} \, i_{rm_0} \{\cos\alpha_{r_0} - j \, \sin\alpha_{r_0}\} - j \, s_0 \, F_R \, X_{rr} \, i_{rm_0} \{\cos(\alpha_{r_0} - \alpha)$$

$$+ j \, \sin(\alpha_{r_0} - \alpha)\}$$

$$= j \, s_0 \, F_R \, X_M \, \hat{i}_{sm_0} - R_{rr} \, i_{rm_0} \, \underline{/\alpha_{r_0}} - \frac{\pi^2 R}{18 \, \cos\alpha} \, i_{rm_0} \, \underline{/\alpha_{r_0} - \alpha} -$$

$$j \, s_0 \, F_R \, X_{rr} \, i_{rm_0} \, \underline{/\alpha_{r_0} - \alpha}$$

$$\hat{i}_{sm_0} = \frac{\dfrac{K_2 \, F_R (1-s_0)}{\cos\alpha} + i_{rm_0} \left[\dfrac{\pi^2 R}{18 \, \cos\alpha} + R_{rr} + j(s_0 \, F_R \, X_{rr}) \, \underline{/-\alpha}\right]}{j \, s_0 \, F_R \, X_M} \, \underline{/\alpha_{r_0}}$$

$$\ldots\ldots(3.3)$$

Substituting equation (3.3) in equation (3.2) and

simplifying

$$V_{sm} \underline{/-\alpha_{r_0}} = \frac{(R_{ss} + j \, F_R \, X_{ss})}{j \, s_0 \, F_R \, X_M} \left[\begin{array}{c} \dfrac{K_2 F_R (1-s_0)}{\cos\alpha} + [R_{rr} \underline{/\alpha} + \dfrac{\pi^2 R}{18 \, \cos\alpha} \\ + j \, s_0 F_R \, X_{rr} \, \underline{/-\alpha}] \end{array}\right] i_{rm_0}$$

$$- j \, F_R \, X_M \, i_{rm_0} \, \underline{/-\alpha}$$

or,

$$\frac{V_{sm}\,s_o\,F_R\,X_M}{\sqrt{R_{ss}^2 + F_R^2\,X_{ss}^2}}\Big/\frac{\pi}{2} - \alpha_{r_o} - \tan^{-1}\frac{F_R\,X_{ss}}{R_{ss}} = \frac{K_2\,F_R(1-s_o)}{\cos\alpha}$$

$$+ i_{rm_o}\left[R_{rr}\cos\alpha + \frac{\pi^2 R}{18\cos\alpha} + s_o\,F_R\,X_{rr}\sin\alpha + \frac{s_o\,F_R^2\,X_M^2}{R_{ss}^2 + F_R^2\,X_{ss}^2}\right.$$

$$\left(R_{ss}\cos\alpha - F_R\,X_{ss}\sin\alpha)\right] - j\,i_{rm_o}\left[R_{rr}\sin\alpha - s_o\,F_R\,X_{rr}\cos\alpha +\right.$$

$$\frac{s_o\,F_R^2\,X_M^2}{R_{ss}^2 + F_R^2\,X_{ss}^2}\,(F_R\,X_{ss}\cos\alpha + R_{ss}\sin\alpha)]$$

or,

$$-Z_1\Big/\frac{\pi}{2} - \alpha_{r_o} - \tan^{-1}\frac{F_R\,X_{ss}}{R_{ss}} = Z_3 + i_{rm_o}\,Z_4 - j\,i_{rm_o}\,Z_5$$

$$\dots\dots(3.4)$$

where

$$Z_1 = \frac{V_{sm}\,s_o\,F_R\,X_M}{\sqrt{R_{ss}^2 + F_R^2\,X_{ss}^2}}$$

$$Z_2 = \frac{s_o\,F_R^2\,X_M^2}{R_{ss}^2 + F_R^2\,X_{ss}^2}$$

$$Z_3 = \frac{K_2\,F_R\,(1-s_o)}{\cos\alpha}$$

$$Z_4 = R_{rr}\cos\alpha + \frac{\pi^2 R}{18\cos\alpha} + s_o\,F_R\,X_{rr}\sin\alpha + Z_2(R_{ss}\cos\alpha -$$

$$F_R\,X_{ss}\sin\alpha)]$$

$$Z_5 = R_{rr}\sin\alpha - s_o\,F_R\,X_{rr}\cos\alpha + Z_2(F_R\,X_{ss}\cos\alpha + R_{ss}\sin\alpha)$$

Equating the magnitudes on both sides in equation (3.4)

$$|Z_1| = |Z_3 + i_{rm_0} Z_4 - j i_{rm_0} Z_5|$$

or $Z_1^2 = (Z_3 + i_{rm_0} Z_4)^2 + (Z_5 i_{rm_0})^2$

$$= Z_3^2 + i_{rm_0}^2 Z_4^2 + 2Z_3 Z_4 i_{rm_0} + Z_5^2 i_{rm_0}^2$$

or $i_{rm_0}^2 (Z_4^2 + Z_5^2) + 2Z_3 Z_4 i_{rm_0} + (Z_3^2 - Z_1^2) = 0$

or $Z_6 i_{rm_0}^2 + Z_7 i_{rm_0} + Z_8 = 0$ ......(3.5)

where

$$Z_6 = Z_4^2 + Z_5^2$$

$$Z_7 = 2Z_3 Z_4$$

$$Z_8 = Z_3^2 - Z_1^2$$

Equation (3.5) is a quadratic equation in i_{rm_0} which can be solved to obtain two values for i_{rm_0}. The positive value gives the magnitude of i_{rm_0}.

$$i_{rm_0} = \frac{-Z_7 + \sqrt{Z_7^2 - 4Z_6 Z_8}}{2Z_6}$$ .....(3.6)

Equating the angle of equation (3.4) α_r is obtained as

$$\alpha_r = \frac{\pi}{2} - \tan^{-1} \frac{F_\lambda X_{ss}}{R_{ss}} - \tan^{-1} \left(\frac{i_{rm_o} Z_5}{Z_3 + i_{rm_o} Z_4} \right) - \qquad \dots (3.7)$$

Having determined α_{r_o} and i_{rm_o}, phasor i_{sm_o} can be determined from equation (3.3), which in turn gives the values of i_{ds_o} and i_{qs_o}, as its real and imaginary part, respectively.

Thus equation (3.1) is solved for given value of slip, and values of i_{ds_o}, i_{qs_o}, i_{rm_o} and α_{r_o} are obtained. Varying the slip, entire operating range can be investigated.

3.2.2 EQUATION OF NO LOAD SLIP

Under ideal no load condition, the torque developed by the drive is zero. Ideal no load slip s_{nl} of the drive is calculated therefore by considering rotor currents to be zero.

Referring fig.(2.1)

$$\text{if } i_R = 0$$
$$V_R = E_b \qquad \dots \dots (3.8)$$

where $E_b = (1-s_o) \frac{2}{P} K_f i_f (F_R w_b)$ is the back emf in d.c. motor

Substituting V_R from equation (2.13) in equation (3.8)

$$\frac{3\sqrt{3}}{\pi} V_{rm} \cos\alpha = (1-s_o) F_R w_b \frac{2}{P} K_f i_f$$

or $\frac{3\sqrt{3}}{\pi} \left(\sqrt{2} \, s_{nl} \, E_2 \right) \cos\alpha = (1 - s_0) \, f_R \, w_b \, \frac{2}{P} \, K_f \, i_f$

where E_2 is induced emf in rotor phase under stand still condition (r.m.s. value).

or $\frac{3\sqrt{3}}{\pi} \left(\sqrt{2} \, s_{nl} \, \frac{E_1}{a} \right) \cos\alpha = (1 - s_{nl}) \, F_R \, w_b \, \frac{2}{P} \, K_f \, i_f$

or $\frac{3\sqrt{3}}{\pi} \left(s_{nl} \, \frac{V_{sm}}{a} \right) \cos\alpha = (1 - s_{nl}) \, F_R \, w_b \, \frac{2}{P} \, K_f \, i_f$

$$\ldots (3.9)$$

$$\text{as } \sqrt{2} \, E_1 \approx V_{sm}$$

Dividing equation (3.9) with V_{base} to convert it in per unit

$$\frac{\frac{3\sqrt{3}}{\pi} \left(s_{nl} \, \frac{V_{sm}}{a} \right) \cos\alpha}{V_b} = \frac{(1 - s_{nl}) \, w_b \, \frac{2}{P} \, K_f \, i_f}{V_b}$$

or
$$s_{nl} \, V_{sm} \cos\alpha = \frac{\pi}{3\sqrt{3}} \, \frac{a}{V_b} \, K_f \, i_f \, \frac{2}{P} \, F_R \, w_b \, (1 - s_0)$$

$$\ldots\ldots (3.10)$$

Substituting for K_2 from equation (2.37)

$$s_{nl} \, V_{sm} \cos\alpha = K_2 (1 - s_{nl}) \, F_R$$

or $s_{nl} = \dfrac{K_2 \, F_R}{K_2 \, F_R + V_{sm} \cos\alpha}$

$$\ldots\ldots (3.11)$$

3.2.3 EXPRESSIONS OF SUPPLY CURRENT AND POWER FACTOR

If phase currents are lagging the phase voltages by ϕ^0, then referring to equation (2.8), expressions for phase currents may be written as

$$i_{as_0} = i_{sm_0} \cos(\theta - \phi)$$

$$i_{bs_0} = i_{sm_0} \cos(\theta - \phi - \frac{2\pi}{3})$$

$$i_{cs_0} = i_{sm_0} \cos(\theta - \phi + \frac{2\pi}{3})$$

$$\dots (3.12)$$

Resolving these along d axis, i_{ds_0} may be expressed as

$$i_{ds_0} = \frac{2}{3} [i_{as} \cos\theta + i_{bs} \cos(\theta - \frac{2\pi}{3}) + i_{cs} \cos(\theta + \frac{2\pi}{3})]$$

$$\dots (3.13)$$

Substituting equation (3.12) in equation (3.13) and simplifying

$$i_{ds_0} = i_{sm_0} \cos\phi \qquad \dots (3.14)$$

Similarly

$$i_{qs_0} = i_{sm_0} \sin\phi \qquad \dots (3.15)$$

Combining equation (3.14) and equation (3.15)

$$i_{sm_0} = \sqrt{i_{ds_0}^2 + i_{qs_0}^2}$$

or

$$I_s = \frac{1}{\sqrt{2}} \sqrt{i_{ds_0}^2 + i_{qs_0}^2} \qquad \dots (3.16)$$

where I_s is the r.m.s. value of i_{sm_0}.

From equation (3.14), power factor is obtained as,

$$\cos\phi = \frac{i_{ds_0}}{i_{sm_0}} \qquad \dots (3.17)$$

3.2.4 EXPRESSION FOR D.C. LINK CURRENT

Combining equations (2.21)

$$i_{rm_0} = \sqrt{i_{dr_0}^2 + i_{qr_0}^2} \qquad \ldots\ldots(3.18)$$

Substituting equation (3.18) in equation (2.14)

$$i_R = \frac{\pi}{2\sqrt{3}} \sqrt{i_{dr_0}^2 + i_{qr_0}^2} \qquad p.u. \qquad \ldots(3.19)$$

3.2.5 EXPRESSIONS FOR POWER INPUT, POWER OUTPUT AND EFFICIENCY

$$P_i = \frac{3}{2} V_{sm} i_{sm} Cos\phi \ Watts$$

Dividing by P_b to convert it in per unit

$$P_{i_{(p.u.)}} = \frac{\frac{3}{2} V_{sm} i_{sm} Cos\phi}{P_b} = \frac{\frac{3}{2} V_{sm} i_{sm} Cos\phi}{\frac{3}{2} V_b i_b}$$

$$= V_{sm_{(p.u.)}} i_{sm_{(p.u.)}} Cos\phi$$

Substituting equation (3.14) in above equation

$$P_i = V_{sm} i_{ds} \ p.u. \qquad \ldots\ldots(3.20)$$

Power output, $P_0 = T_e (1-s_0) w_b F_R \frac{2}{P} \ Watts$

Dividing by P_b to convert it in per unit

$$P_{0_{(p.u.)}} = \frac{T_e (1-s_0) w_b F_R \frac{2}{P}}{P_b}$$

$$= \frac{T_e (1-s_0) w_b F_R \frac{2}{P}}{T_b \frac{2}{P} w_b}$$

or $P_{o(p.u.)} = T_{e(p.u.)} (1-s_o) F_R$

$$\dots\dots(3.21)$$

percentage Efficiency $= \dfrac{P_o}{P_i} \times 100$

$$\dots\dots(3.22)$$

3.2.6 EXPRESSION FOR LOSSES

In the ideal drive, mechanical losses such as friction and windage and iron losses i.e. hysteresis and eddy current losses are neglected. Only following copper losses are therefore present in the drive:

(i) Stator copper losses

(ii) Rotor copper losses

(iii) Armature copper losses in d.c. motor.

Stator copper losses $P_{cu-st} = 3 I_s^2 R_{ss}$ Watts

$$P_{cu-st(pu)} = \dfrac{\frac{3}{2} (i_{ds_o}^2 + i_{qs_o}^2) R_{ss}}{\frac{3}{2} i_b^2 Z_b}$$

$$P_{cu-st (p.u.)} = (i_{ds_o(p.u.)}^2 + i_{qs_o(p.u.)}^2) R_{ss(p.u.)}$$

$$\dots(3.23)$$

Similarly

Rotor copper losses $P_{cu-rt} = (i_{dr_o}^2 + i_{qr_o}^2) R_{rr}$

$$\dots(3.24)$$

Armature losses $= i_{R_o}^2 R = (\dfrac{\pi}{2/3} i_{rm_o})^2 R$

$$P_{cu-Arm_{(p.u.)}} = \frac{\frac{\pi^2}{12} i_{rm}^2 R}{\frac{3}{2} i_b^2 Z_b}$$

$$= \frac{\pi^2}{18} i_{rm_0 (p.u.)}^2 R_{(p.u.)} \quad \text{or}$$

$$= \frac{\pi^2}{18} [i_{dr_0 (p.u.)}^2 + i_{qr_0(p.u.)}^2] R_{(p.u.)}$$

$$\ldots\ldots(3.25)$$

3.3 ANALYTICAL RESULTS AND DISCUSSION

Performance of the system has been computed by simulating the steady state equations on a digital computer. Flow chart and listing of the program developed in FORTRAN language is presented in Appendix 3. Various performances characteristics viz, Torque-Slip, Supply Current-Slip, Fundamental rotor phase current-slip, Armature current slip, Power factor slip and Efficiency slip are obtained using CALCOMP Plotter.

Various measured parameters in p.u. of the drive are given in Appendix 2.

In this drive speed is lowered first by field current control and then by firing angle control of controlled bridge rectifier. This is done to achieve optimum system efficiency, as shown later in this chapter.

3.3.1 VARIATION OF IDEAL NO LOAD SLIP

Ideal no load slip is computed by equation (2.13). Variation of no load slip by field current control and by firing angle control is shown in fig.(3.1). It clearly indicates that the speed of the drive can be lowered only to about 50 % by field current control. By controlling firing angle, speed can be reduced further upto about 15% . Thus the system gives a wide speed range in subsynchronous region.

3.3.2 SUPPLY CURRENT-SLIP CHARACTERISTICS

Supply current drawn by the system has been computed using equation (2.5). Fig. 3.2 (a) and Fig. 3.2(b) show the supply current vs slip characteristics at different field current settings and different firing angle settings respectively. Both the curves show that supply current is same at no load slip. It is nothing but magnetizing current. Both the curves show that supply current increases on increasing the load. Fig. 3.2(a) shows that current under standstill is constant under field current control. Fig. 3.2(b) depicts roughly parallel characteristics on changing the firing angle settings. Starting current decreases on increasing the firing angle. This indicates that the drive may be started by setting field current at maximum and firing angle decreased from 90° till the drive develops sufficient starting torque.

In Fig. 3.2(a) and Fig. 3.2(b), the points marked as full load points are the points when supply current reaches
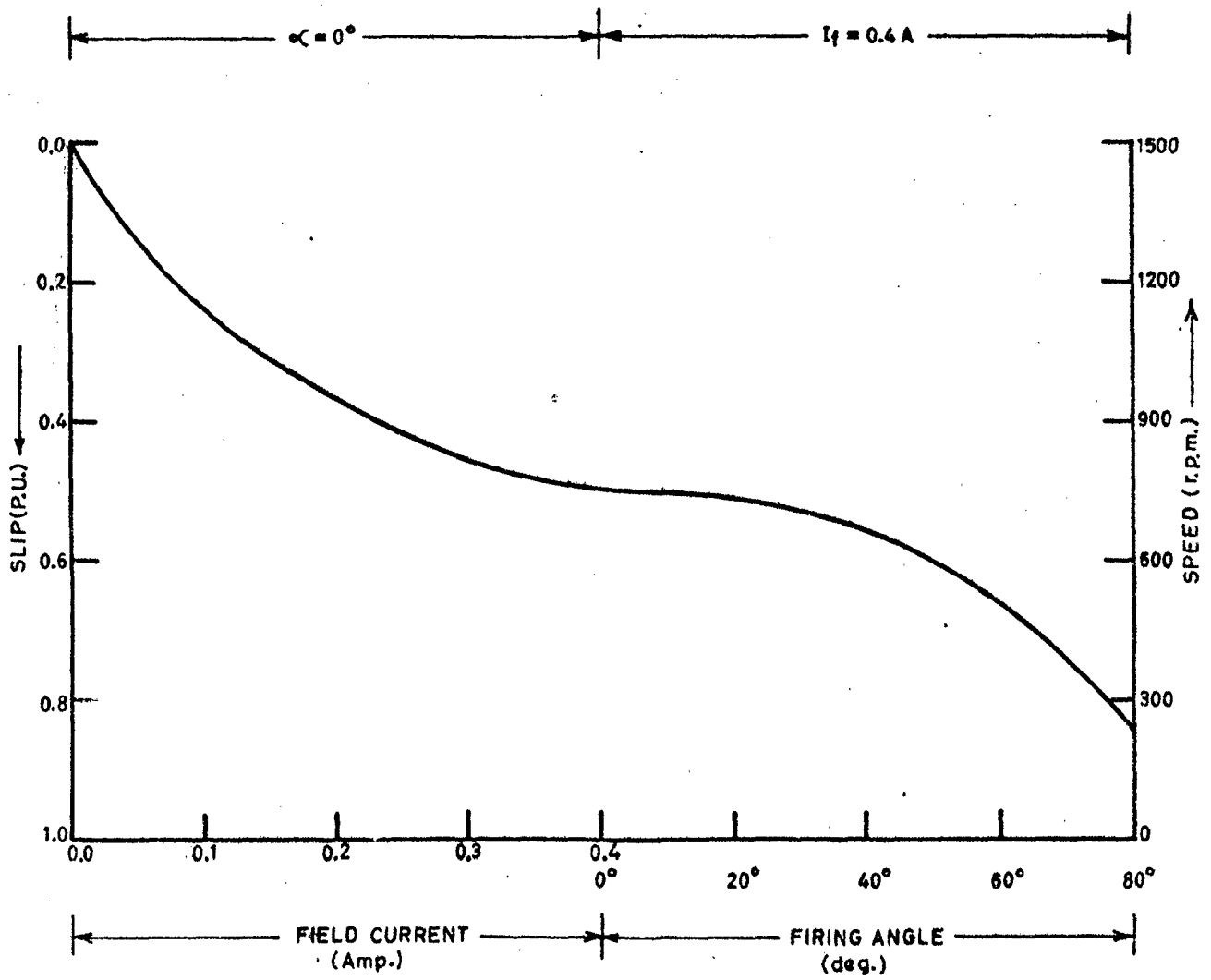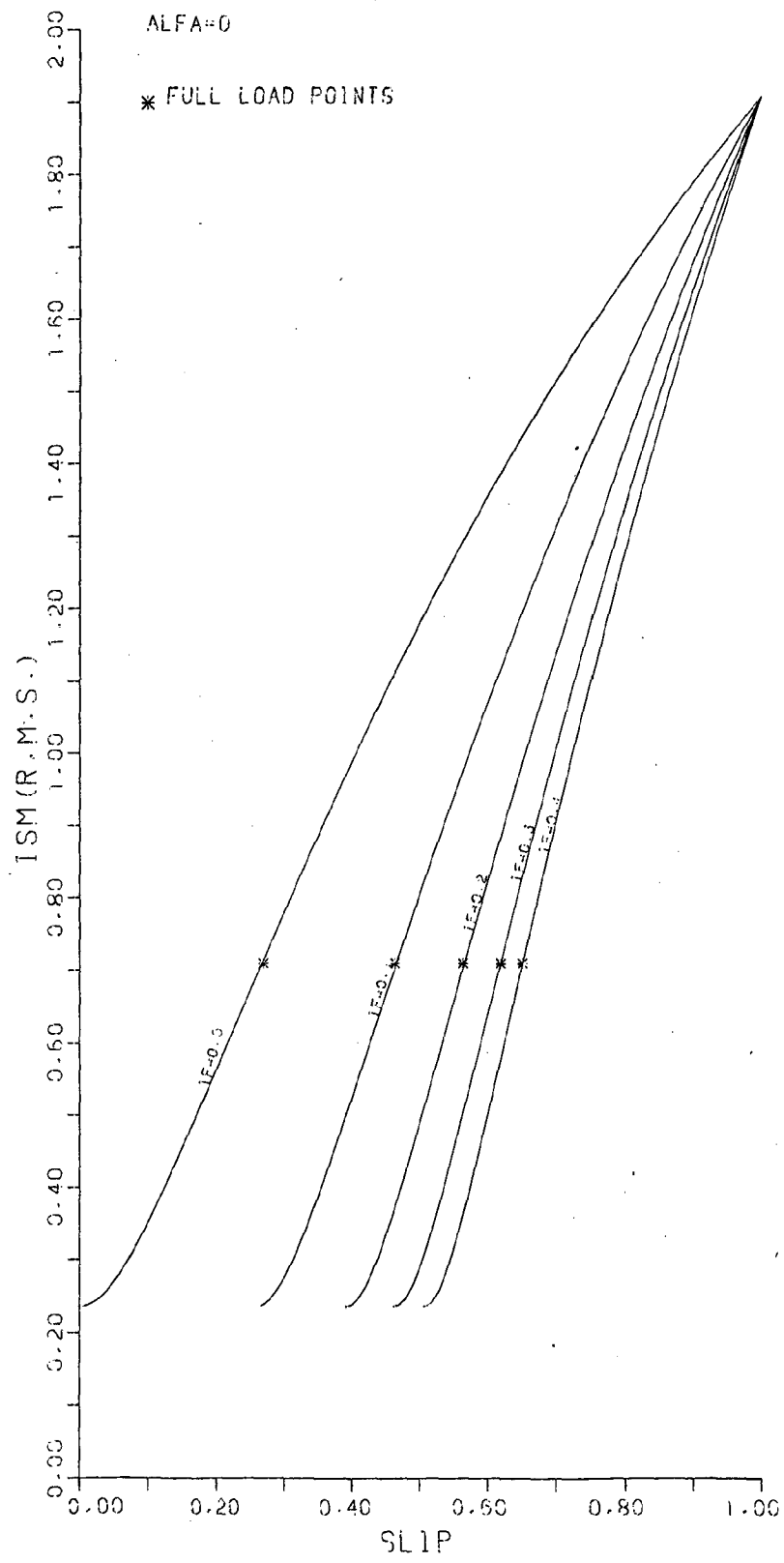
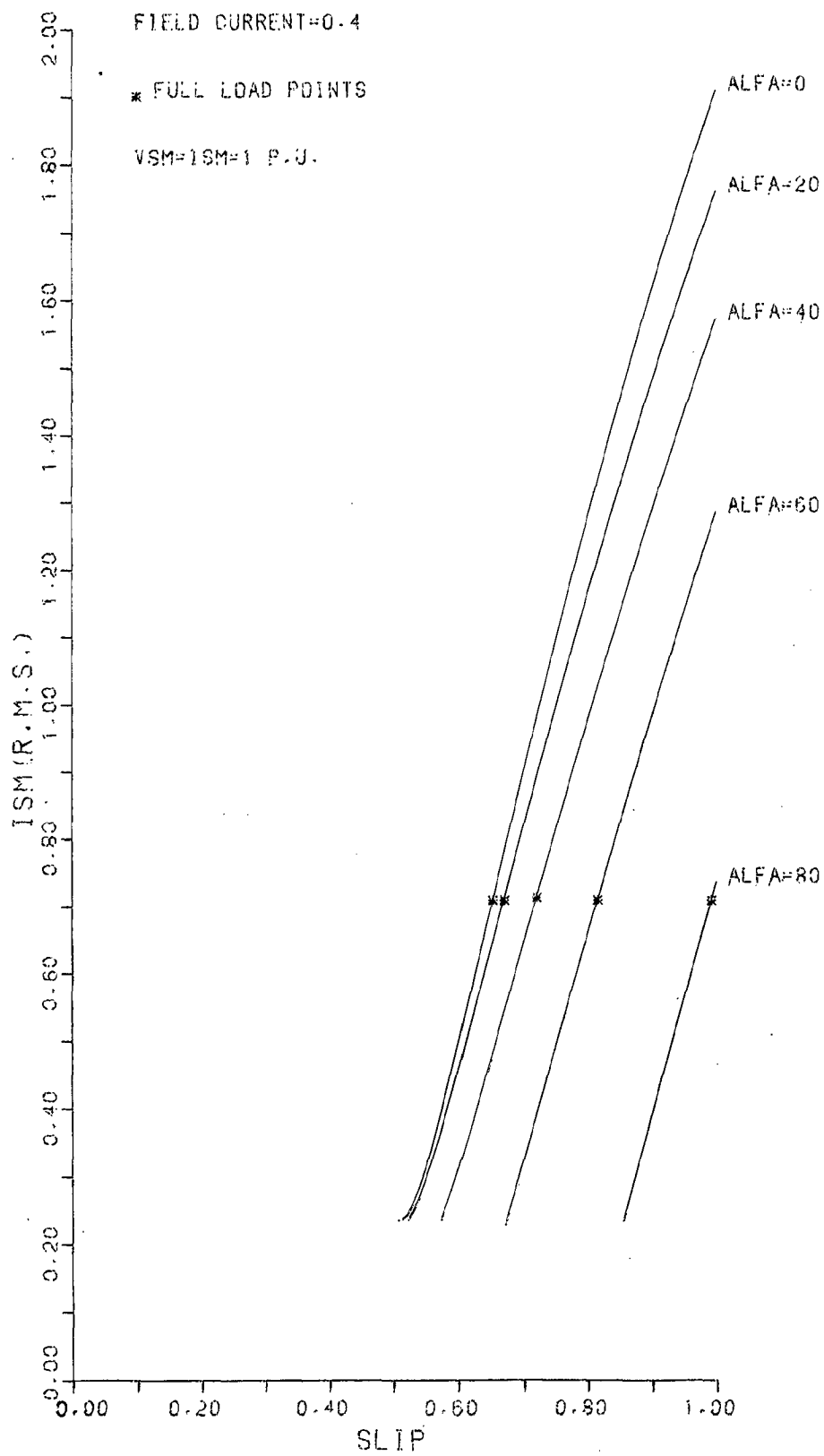FIG.3.1 : VARIATION OF IDEAL NO LOAD SLIP

FIG 3.2(a) INPUT CURRENT-SLIP CURVE

FIG:3.2(B) SUPPLY CURRENT-SLIP CURVE

the rated current of induction motor. These points should not be mistaken as co-responding to rated output power.

Since peak value of rated current is considered as 1 p.u., the r.m.s. value of rated current is 0.707 p.u. as shown in Fig. 3.2(a).

3.3.3 OUTPUT POWER - SLIP CHARACTERISTICS

Power output given by the system has been computed using equation (3.21). Fig. 3.3(a) and Fig. 3.3(b) depict the output power vs slip curve at different field current settings and different firing angle settings respectively. Both the curves show that output power is zero at no load slip and slip = 1. Maximum power output and power output at full load under field current control is fairly constant [Fig. 3.3(a)] but decreases significantly under firing angle control [Fig. 3.3(b)].

3.3.4 INPUT POWER-SLIP CHARACTERISTICS

Power input to the system is determined using equation (3.20). Fig. 3.4(a) and Fig. 3.4(b) show the input power vs slip characteristics under field current control and firing angle control respectively. Input power increases from zero as load increases and becomes constant at standstill condition [Fig. 3.4(a)] under field current control but decreases at standstill under firing angle control [Fig. 3.4(b)]. Input power at full load remains fairly constant at increased field current settings but decreases at increased firing angle settings.
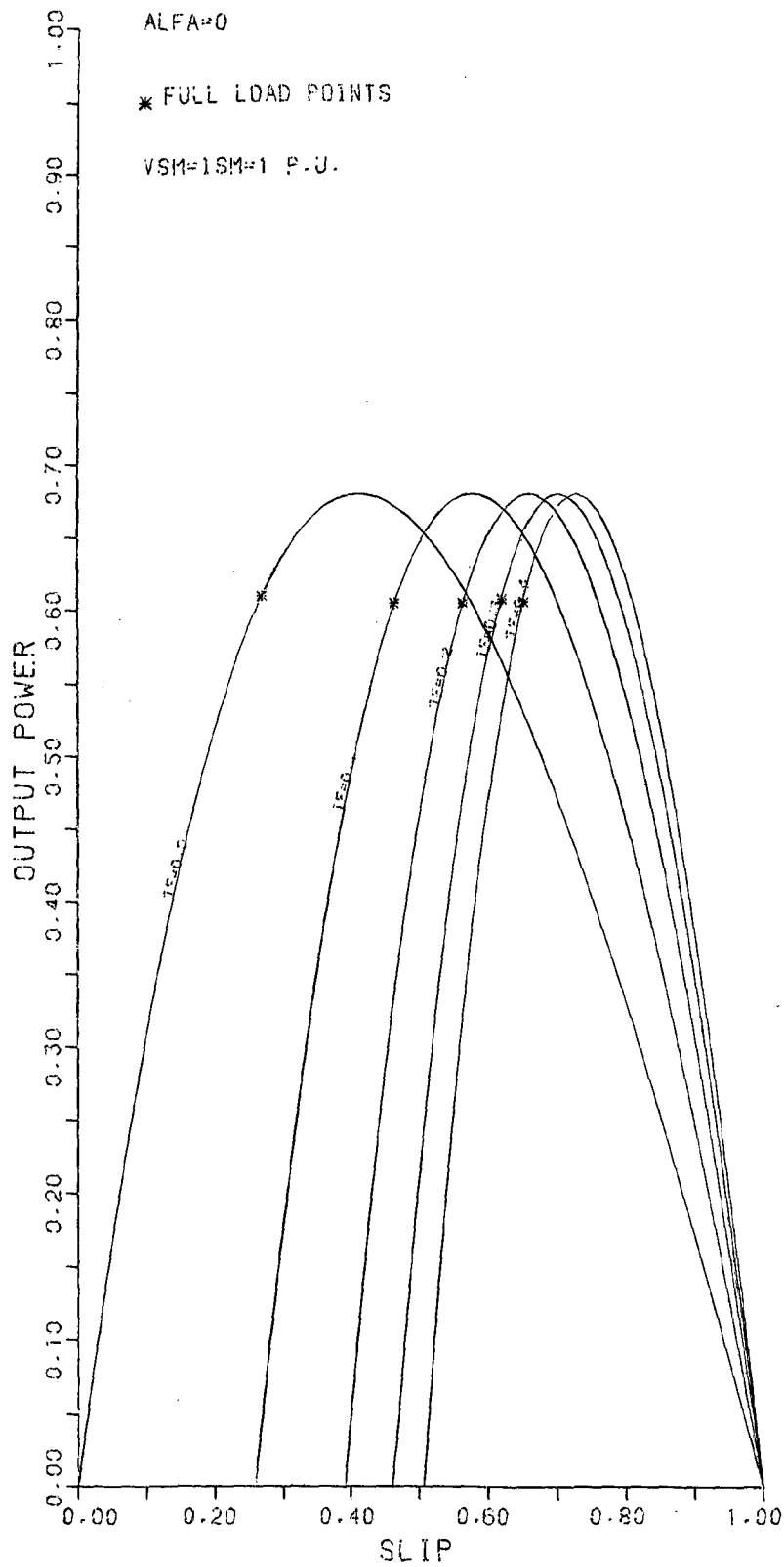
FIG: 3.3 (A) OUTPUT POWER-SLIP CURVE

FIELD CURRENT=0.4

* FULL LOAD POINTS

VSM=ISM=1 P.U.

OUTPUT POWER

SLIP

ALFA=0
ALFA=20
ALFA=40
ALFA=60
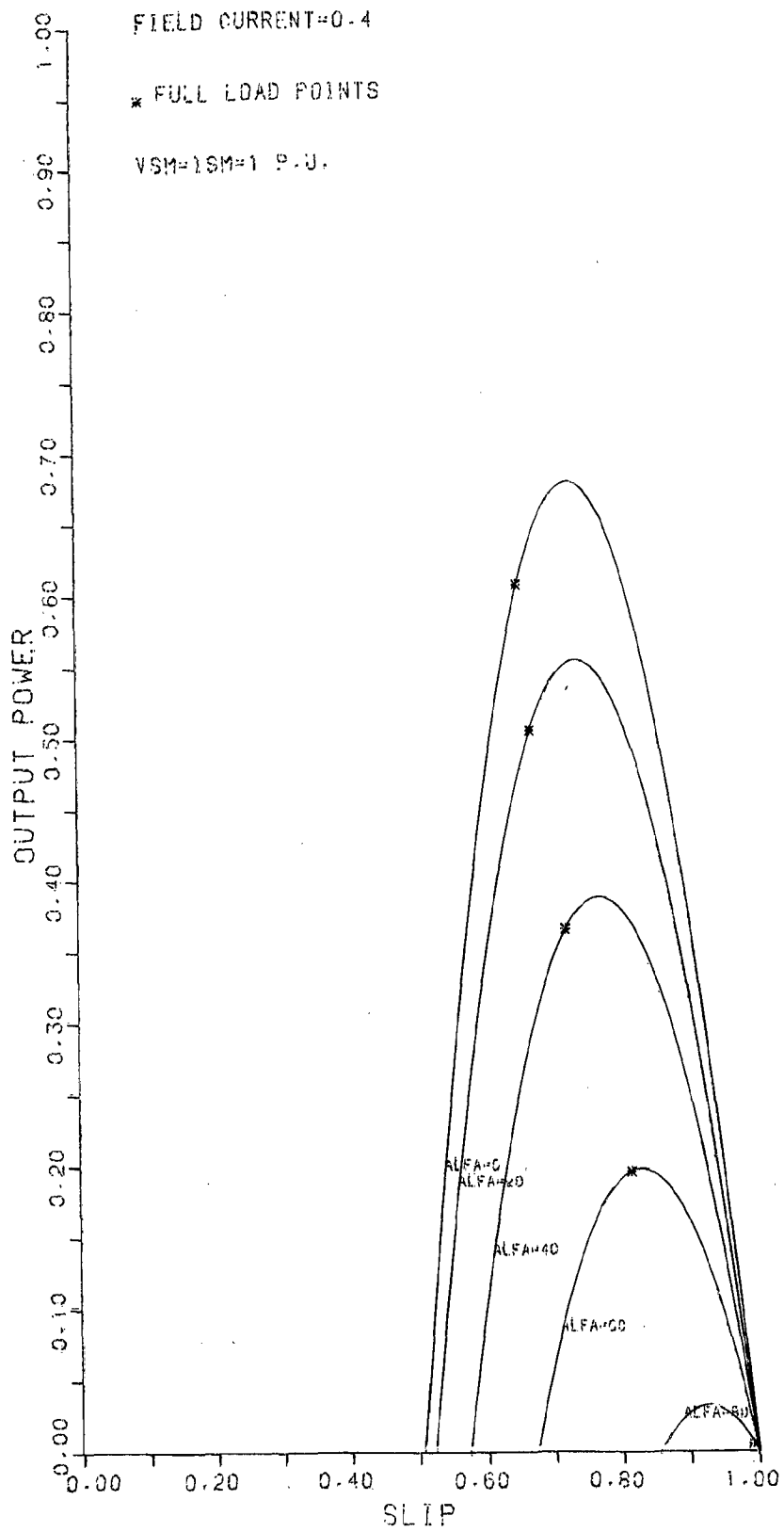ALFA=80

FIG:3.3(B) OUTPUT POWER-SLIP CURVE

ALFA=0

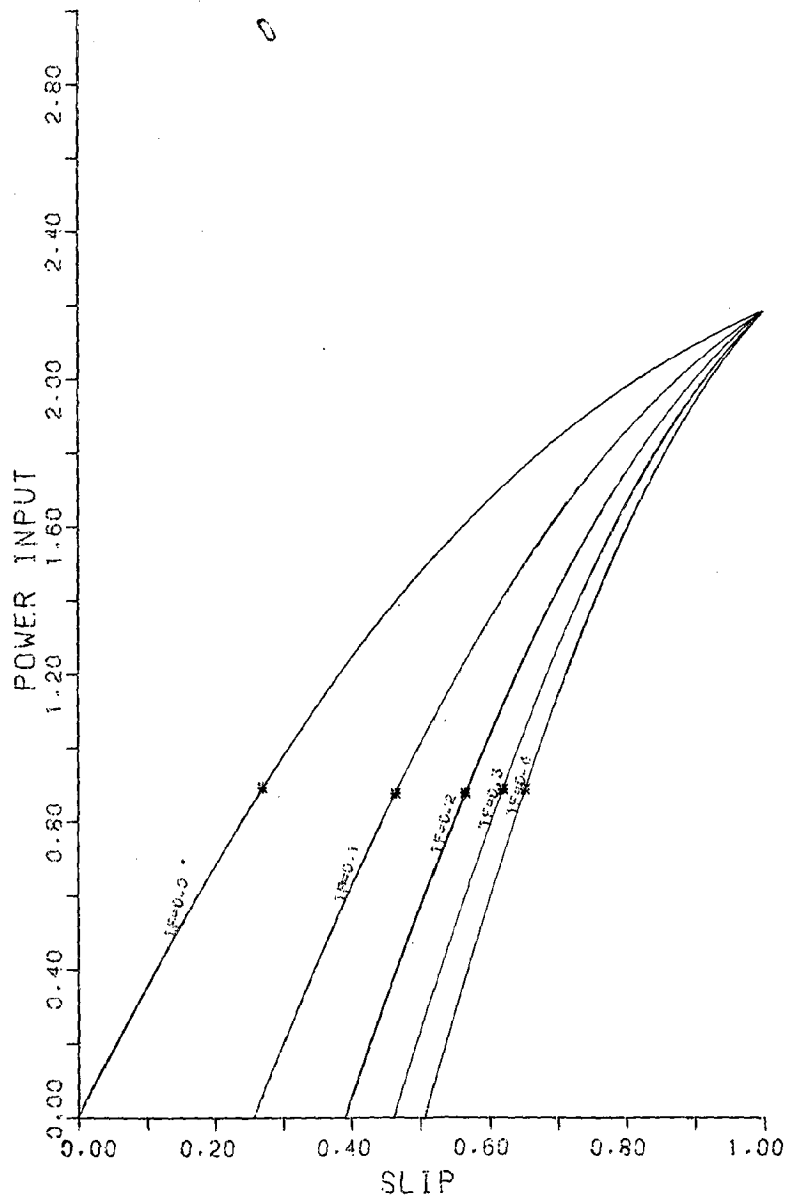* FULL LOAD POINTS

VSM=ISM=1 P.U.

FIG 3.4(A) POWER INPUT-SLIP CURVE
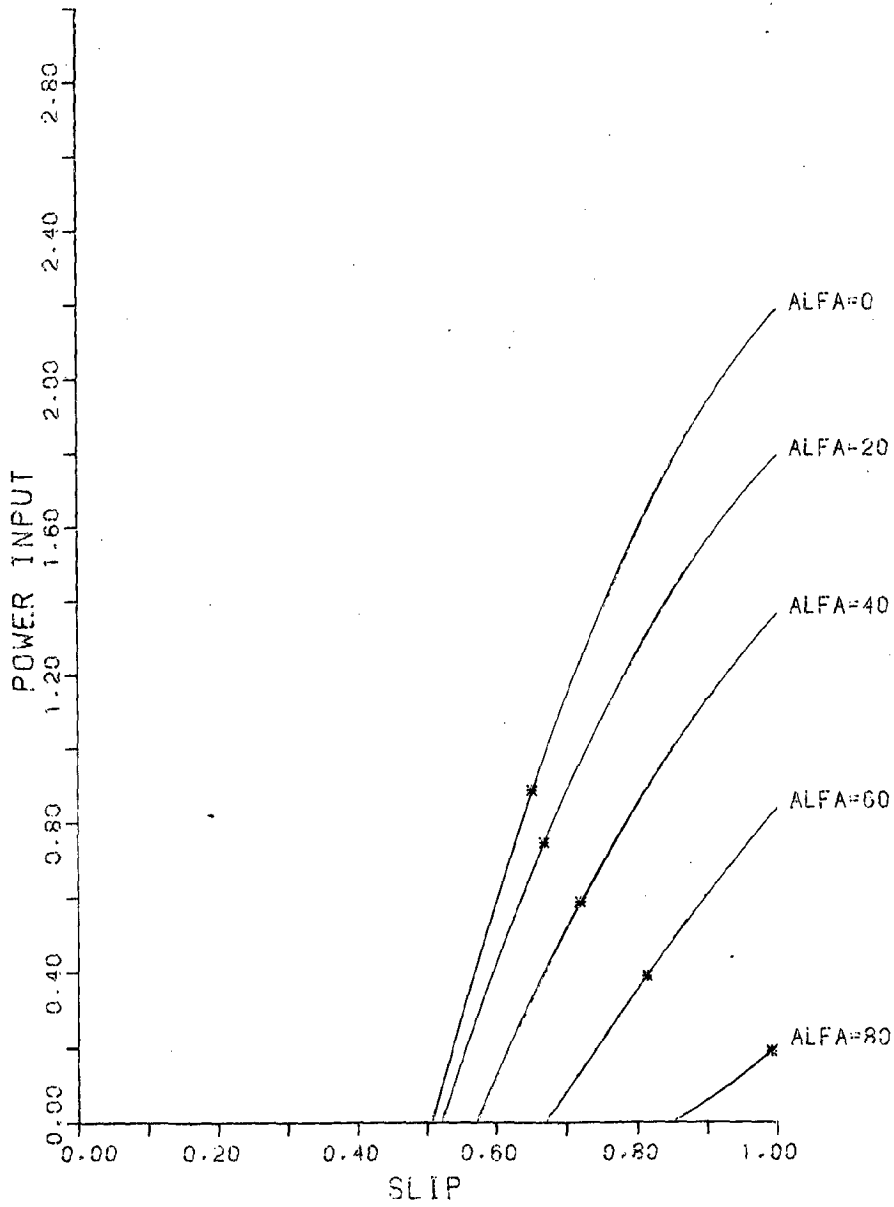
FIELD CURRENT=0.4

* FULL LOAD POINTS

VSM=ISM=1 P.U.

FIG:3.4(B) POWER INPUT-SLIP CURVE

3.3.5 TORQUE-SLIP-CHARACTERISTICS

Electromagnetic torque developed by the system is computed by equation (1.41). The torque vs slip characteristics at different field current settings and different settings of firing angle are depicted in Fig. 3.5(a) and Fig. 3.5(b) respectively. At zero field current setting, the drive offers familiar induction motor torque slip curve. Fig. 3.5(a) clearly shows that hardness of the curve improves as field current is increased resulting in improved speed regulation but remains unchanged under firing angle control. Starting torque as well as full load torque developed by the drive improves with increase in field current. This is due to the fact that d.c. motor provides additional torque, as shown later in this chapter. However the full load torque as well as starting torque fall with increase in firing angle settings.

3.3.6 POWER FACTOR-SLIP CHARACTERISTICS

Power factor vs slip characteristics for different field current settings and different firing angle settings are shown in Fig. 3.6(a) and Fig. 3.6(b) respectively. Power factor is very poor under no load condition. Fig. 3.6(a) shows that power factor is fairly constant at full load at all settings of the field current. Full load power factor, however, decreases as expected on increasing the firing angle [Fig. 3.6(b)]. This was noted earlier in equation(1.18).
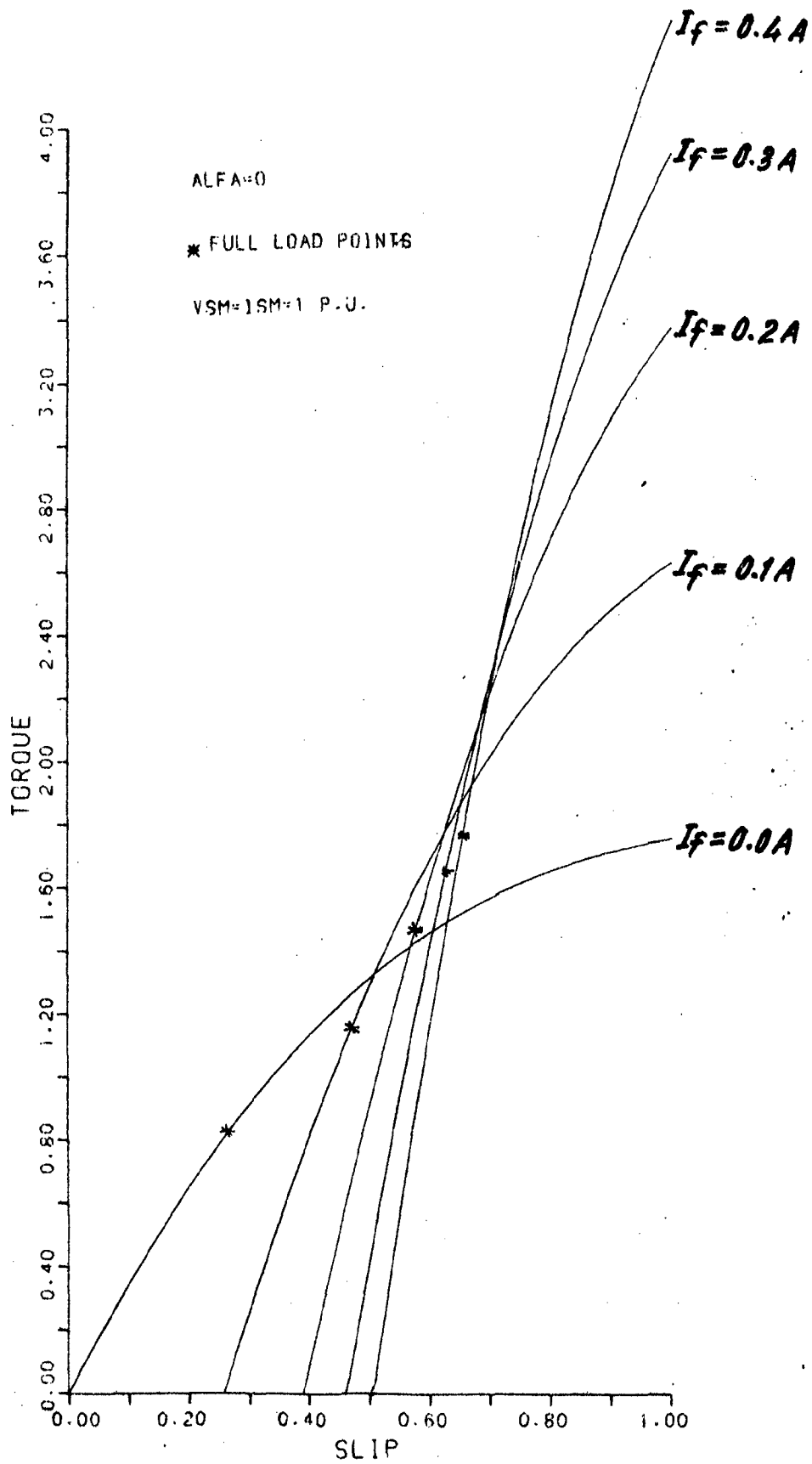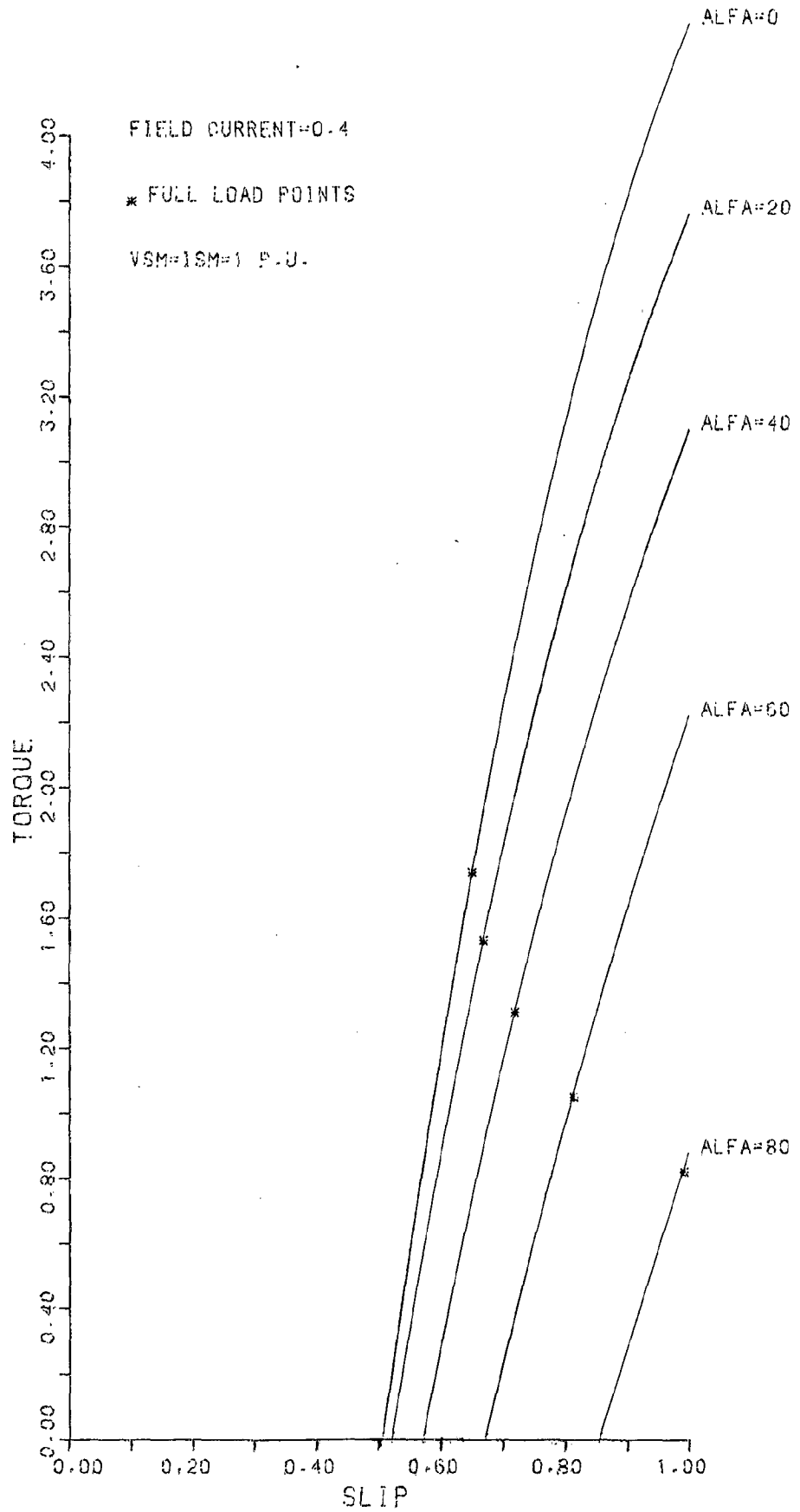
FIG:3.5(A) TORQUE-SLIP CURVE

FIG: 3.5 (B) TORQUE-SLIP CURVE
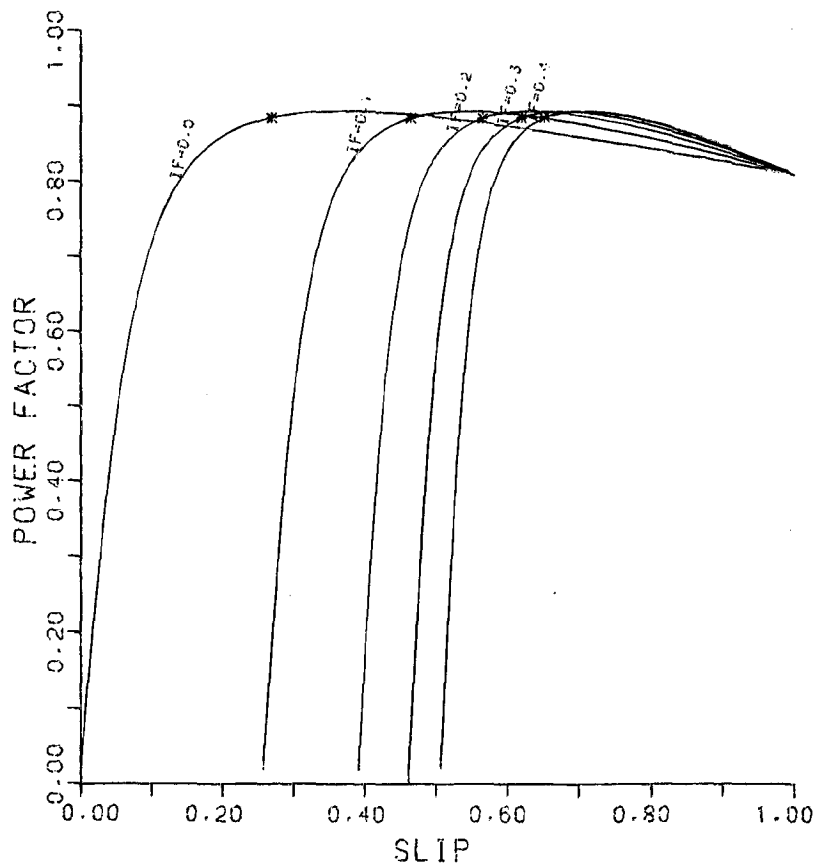
ALFA=0

* FULL LOAD POINTS

VSM=ISM=1 P.U.

FIG:3.6(A) POWER FACTOR-SLIP CURVE

FIELD CURRENT=0.4

* FULL LOAD POINTS

VSM=ISM=1 P.U.

ALFA=0

ALFA=20

ALFA=40

ALFA=60
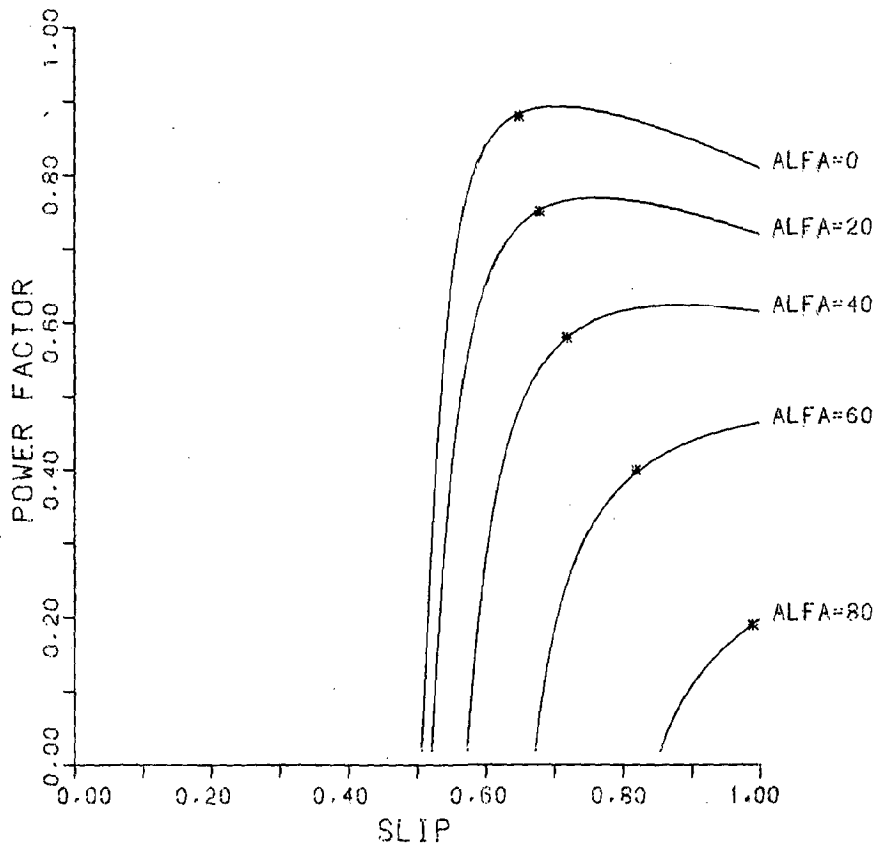
ALFA=80

POWER FACTOR

SLIP

FIG:3.6(B) POWER FACTOR-SLIP CURVE

3.3.7 EFFICIENCY SLIP-CHARACTERISTICS

Fig. 3.7(a) shows that efficiency at full load is fairly constant at different settings of the field current, however, it decreases on increasing the firing angle settings [Fig. 3.7(b)]. It is for this reason that such drive be operated with as low a value of firing angle as possible. This evidently leads to the conclusion that for the purpose of lowering drive's speed, field control be used with firing angle = zero as far as possible. Firing angle control be used only when field current control has exhausted.

3.3.8 FUNDAMENTAL ROTOR PHASE CURRENT-SLIP CHARACTERISTICS

Fig. 3.8(a) and Fig. 3.8(b) show the fundamental rotor phase current vs slip curves for field current control and firing angle control respectively. Under standstill condition, current is constant in field current control but decreases with increased firing angle settings. Full load current remains fairly constant under field current control but decreases under firing angle control.

3.3.9 ARMATURE CURRENT-SLIP CHARACTERISTICS

Armature current-slip characteristics shown in Fig. 3.9(a) and Fig. 3.9(b) under field current control and firing angle control respectively are similar to fundamental rotor phase current-slip characteristics. It is evident from equation (2.14) also that armature current and fundamental rotor phase current are proportional.
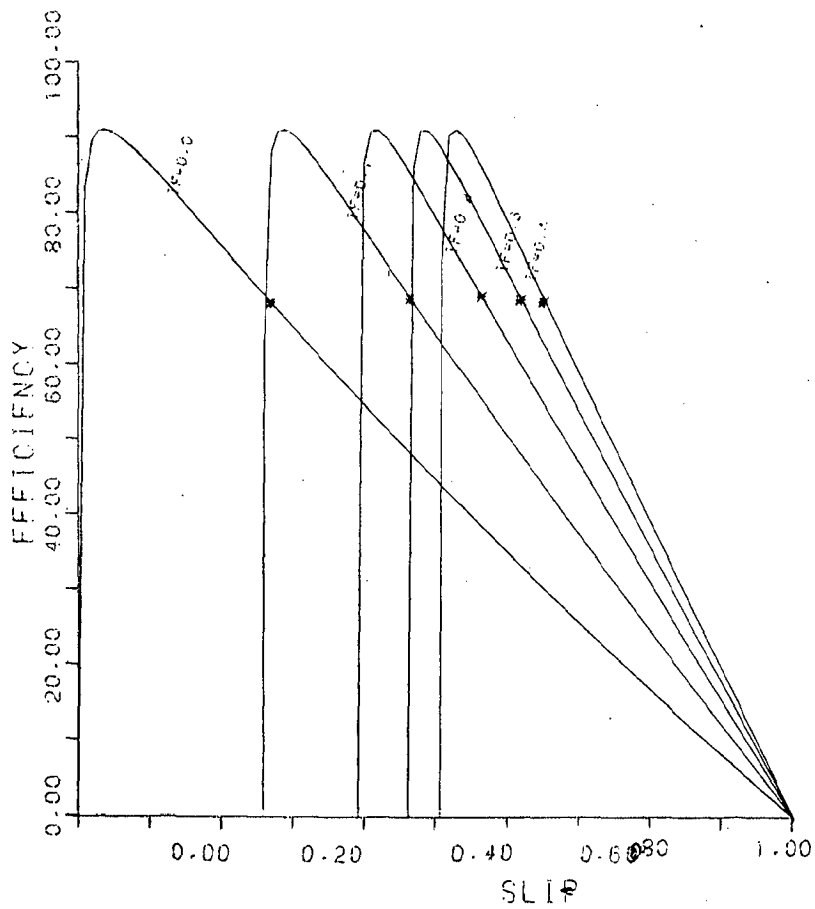
ALFA=0

* FULL LOAD POINTS

VSM=1SM=1 P.U.

FIG:3.7(A) EFFICIENCY-SLIP CURVE

FIELD CURRENT=0.4

* FULL LOAD POINTS
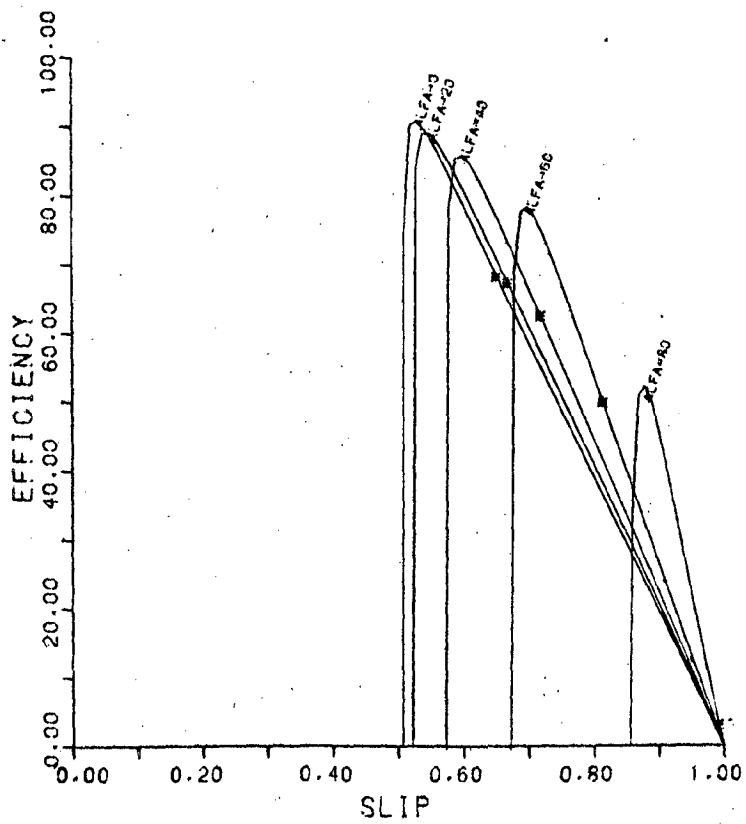
VSM=ISM=1 P.U.

FIG:3.7(B) EFFICIENCY-SLIP CURVE
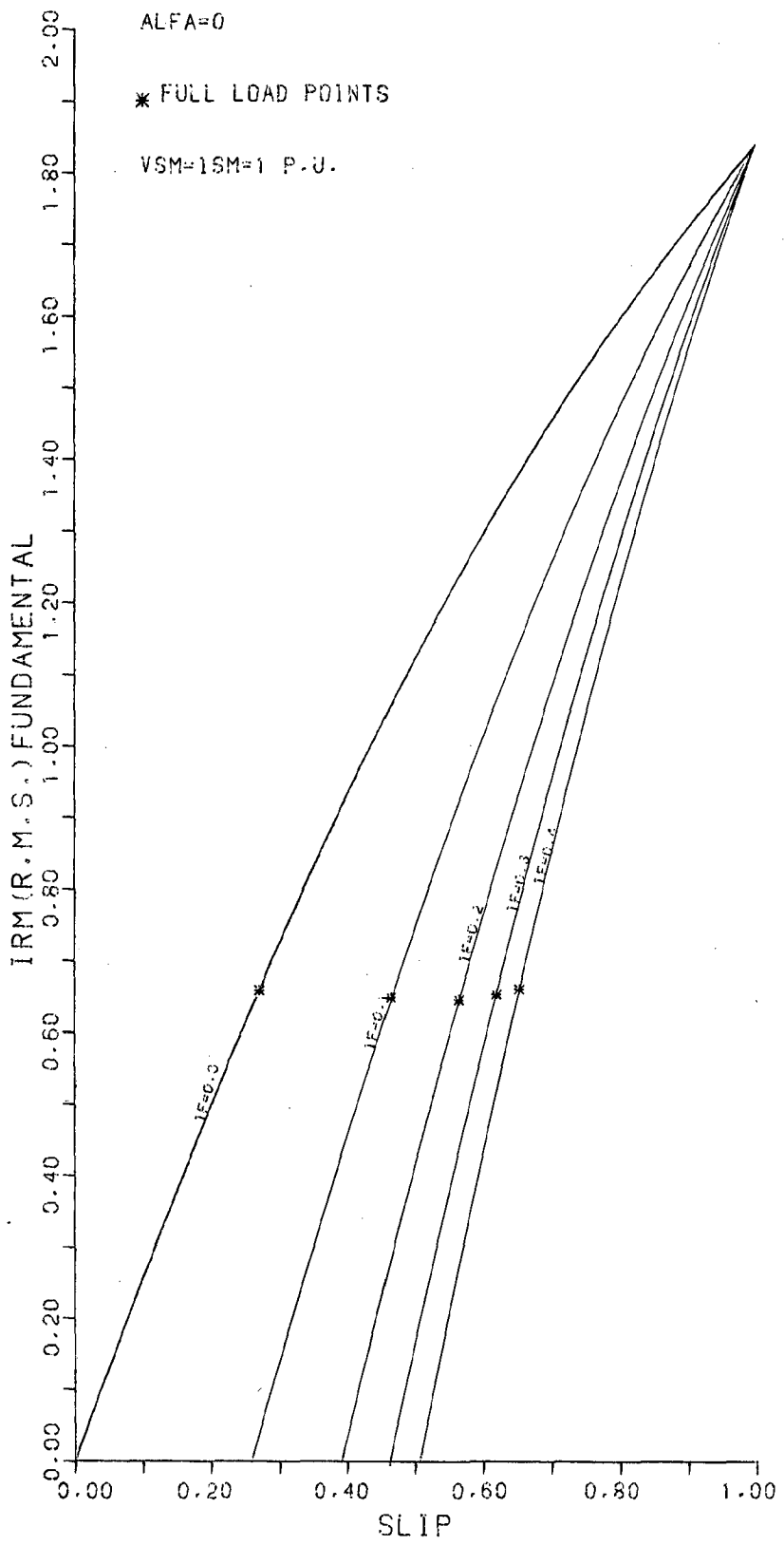
FIG:3.8(A) FUNDAMENTAL ROTOR PHASE CURRENT VS SLIP CURV
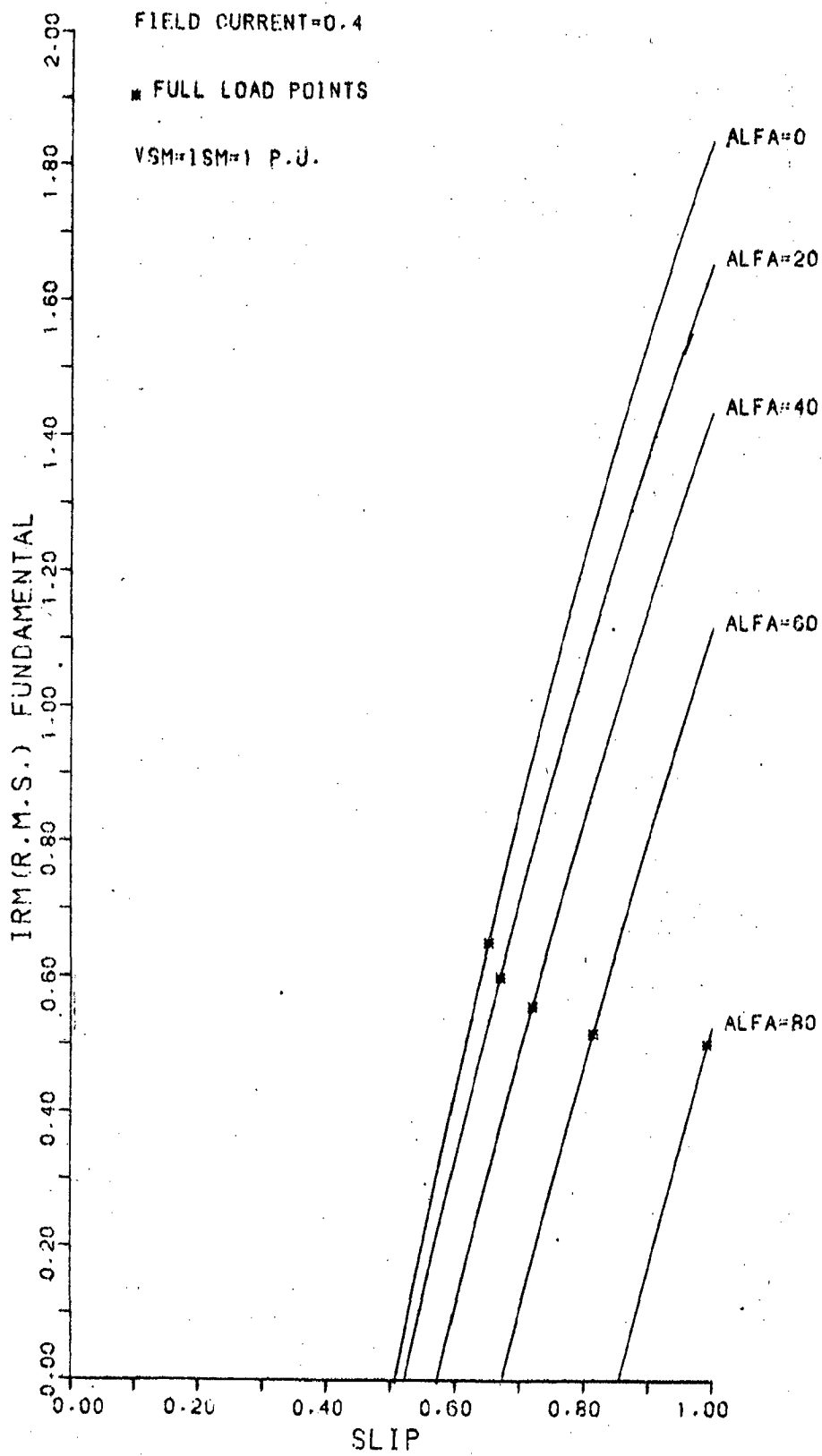
FIG:3.8(B) FUNDAMENTAL ROTOR PHASE CURRENT-SLIP CURVE
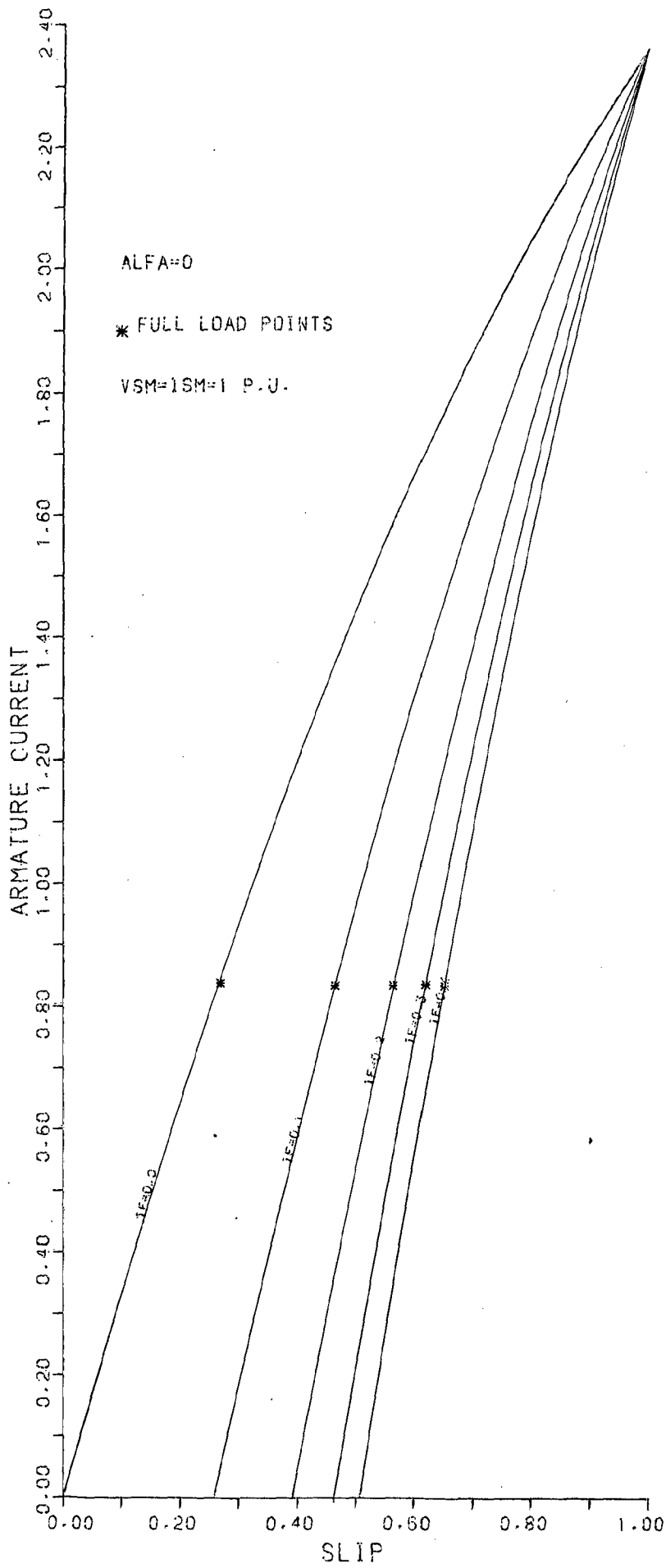
FIG 3.9(A) ARMATURE CURRENT-SLIP CURVE
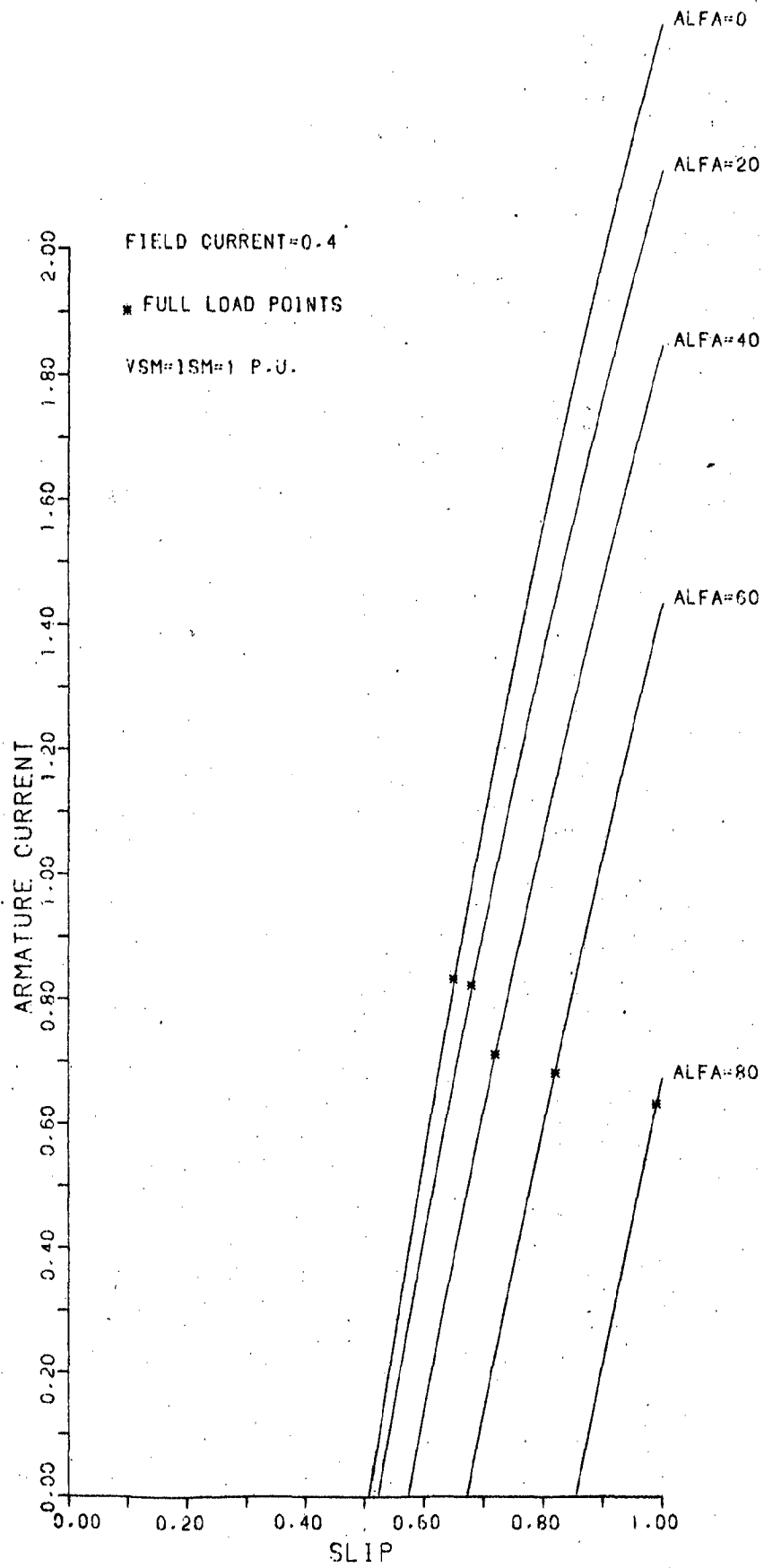
FIG 3.9(b) ARMATURE CURRENT-SLIP CURVE

3.4 FULL LOAD PERFORMANCE OF THE DRIVE

Full load performance of the drive is shown in Fig. 3.10 to Fig. 3.16, for different settings of field current and firing angle. The drive is considered to be at full load when peak value of supply current equals its rated value (1 p.u.) and the supply voltage is also equal to its rated value (1 p.u.). It is aimed to determine drive's performance under rated input VA, when speed control is exercised.

Fig. 3.10 shows the variation of p.u. supply current and p.u. fundamental rotor phase current for entire control range. Supply current is constant at 1 p.u. Fundamental rotor phase current remains fairly constant in field current control region but progressively decreases as firing angle is increased. Power input and power output are fairly constant under field current control region but decrease sharply under firing angle control region (Fig. 3.11). It is to be noted here that at $\alpha = 80^\circ$, output power is zero. This is due to the fact that drive's speed under this condition falls to zero. Fig. 3.12 shows that under field current control region, power factor remains substantially constant since power input from the mains is constant but decreases sharply under firing angle control. Stator copper losses, rotor copper losses and armature copper losses remain fairly constant in field current control since supply current, fundamental rotor phase current and hence armature current also remain fairly unchanged. This is shown in Fig. 3.13. Armature copper losses and rotor copper losses decrease under
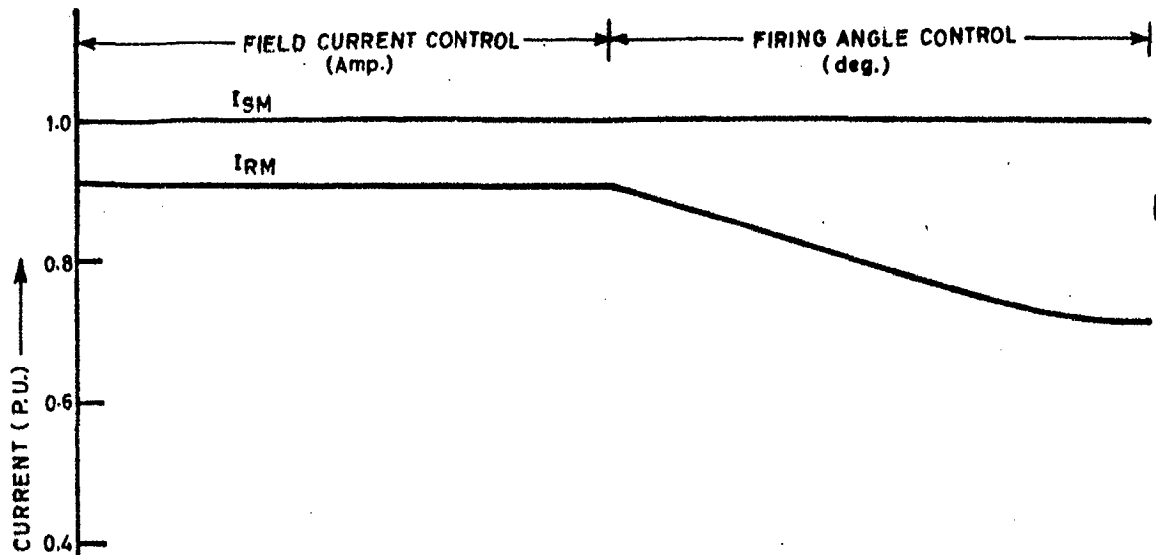
FIG.3.10
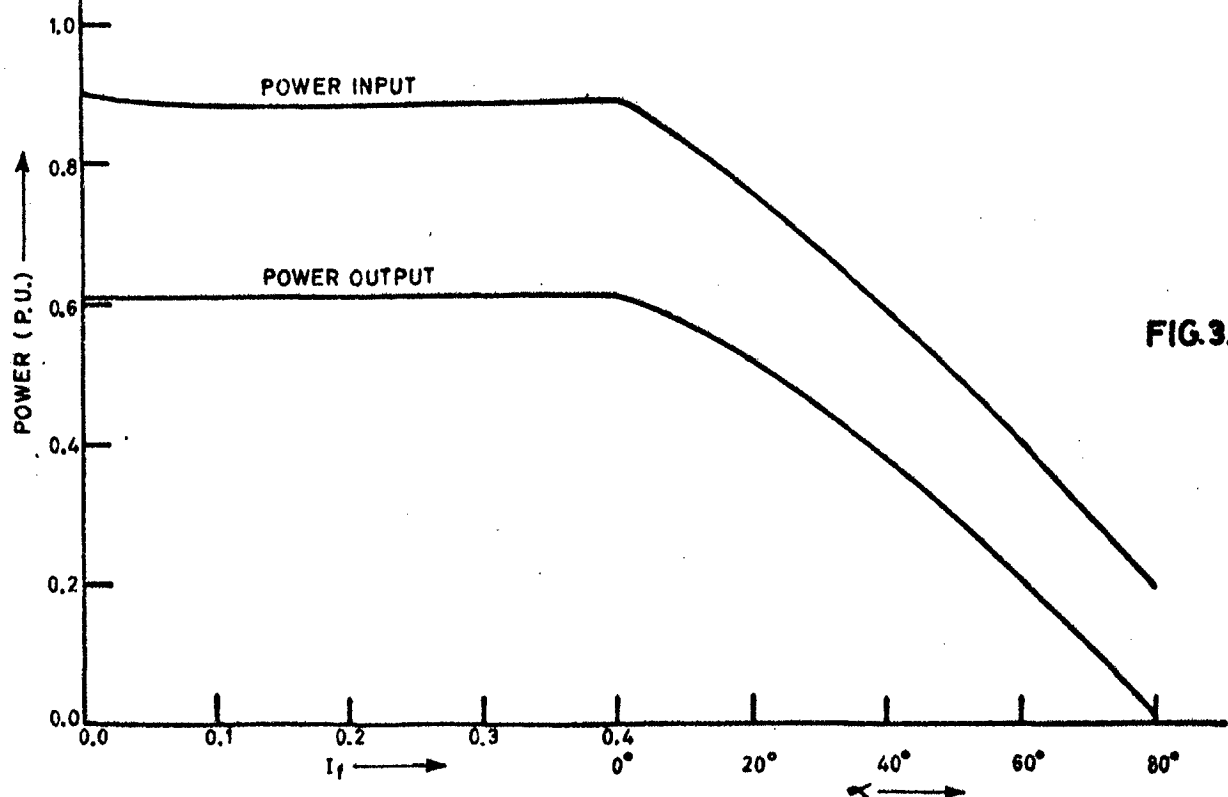
FIG.3.11

PERFORMANCE UNDER RATED VA INPUT
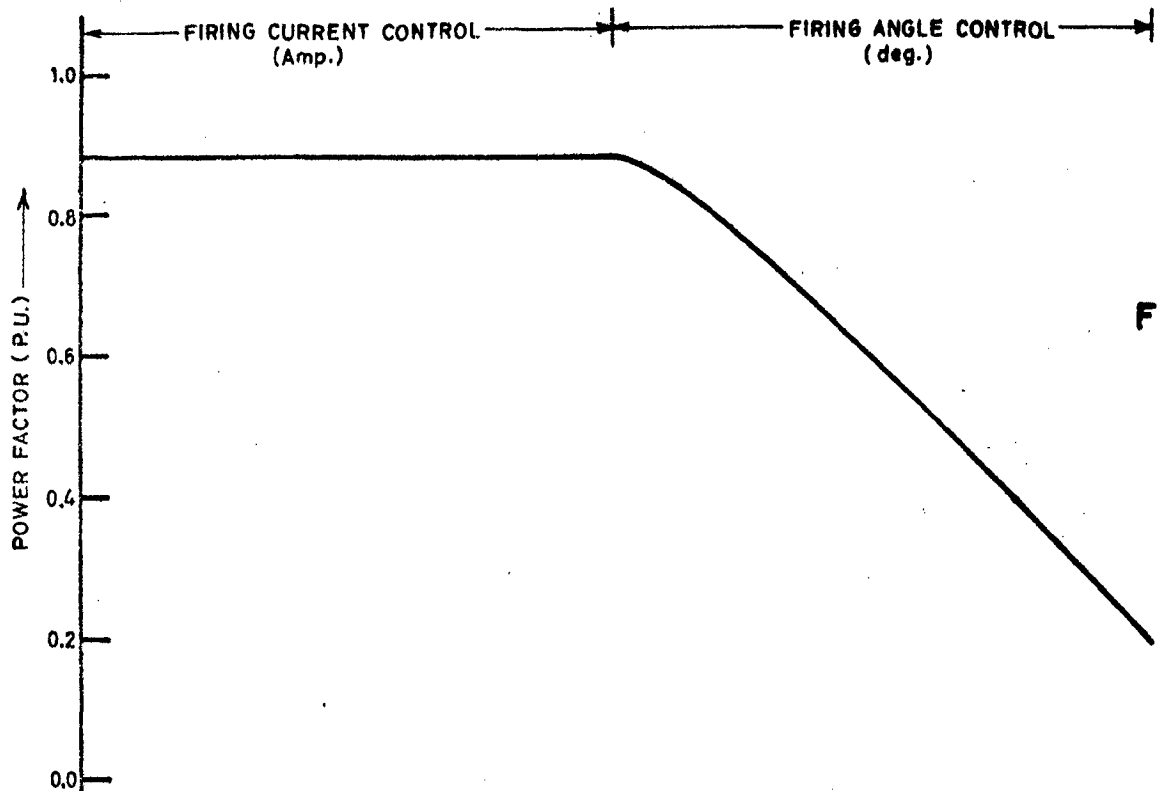
FIG.3.12
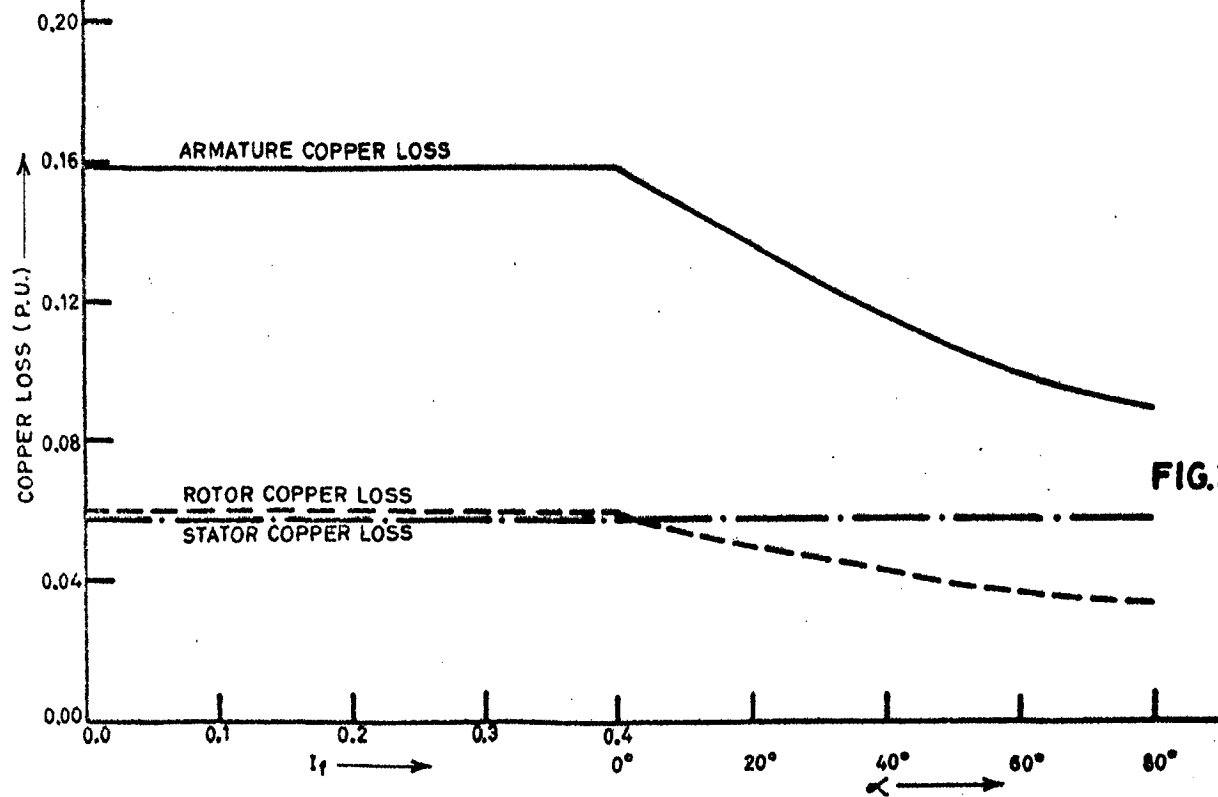
FIG.3.13

PERFORMANCE UNDER RATED VA INPUT

firing angle control but stator copper losses reamin fairly
constant.Fig. 3.14 indicates a sharp fall in efficiency of
the drive under firing angle control. However efficiency
at full load remains fairly constant under field current
control. It reveals that field current control is always
superior than firing angle control and therefore latter should
be adopted only in case of absolute necessity.

Fig. 3.15 shows that torque developed by induction
motor remain fairly constant but decreases under firing
angle control as it is proportional to air gap power which
is again proportional to power input. Torque developed by
d.c. motor increases linearly being proportional to field
current under field current control but decreases under firing
angle control as armature current decreases. Fig. 3.16 depicts
variation of full load slip in entire range. It shows that
drive comes to standstill at $\alpha = 80^{\circ}$ confirming once again
that output power is zero at $\alpha = 80^{\circ}$, under rated input VA
condition.

3.5 CONCLUSION

Expressions have been developed for predetermining
the steady state performance of a slip energy recovery drive
employing a controlled rectifier. System equations presented
predict the operating characteristics accurately. It is
observed that field current control is undoubtedly superior
than firing angle control but latter has its own merits as
mentioned below:
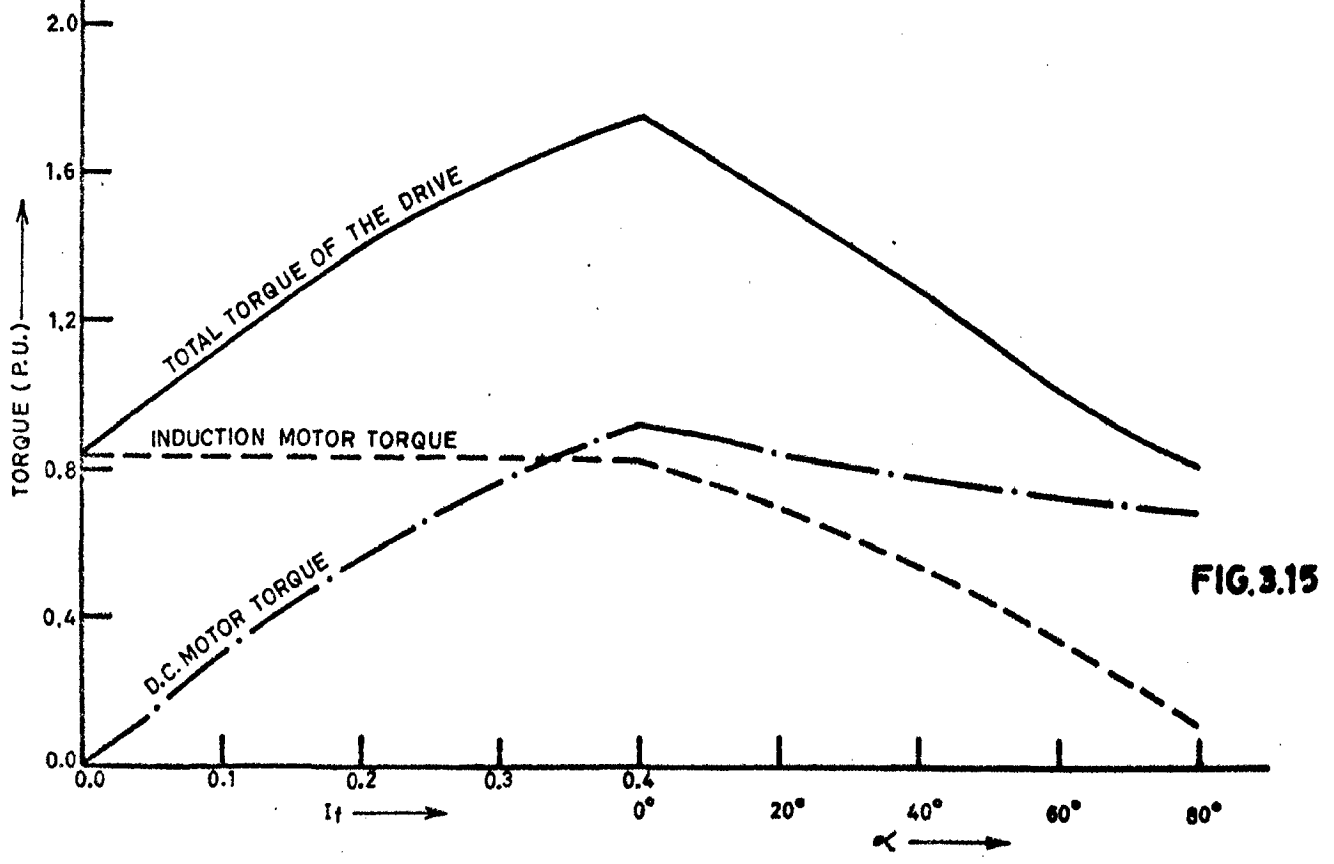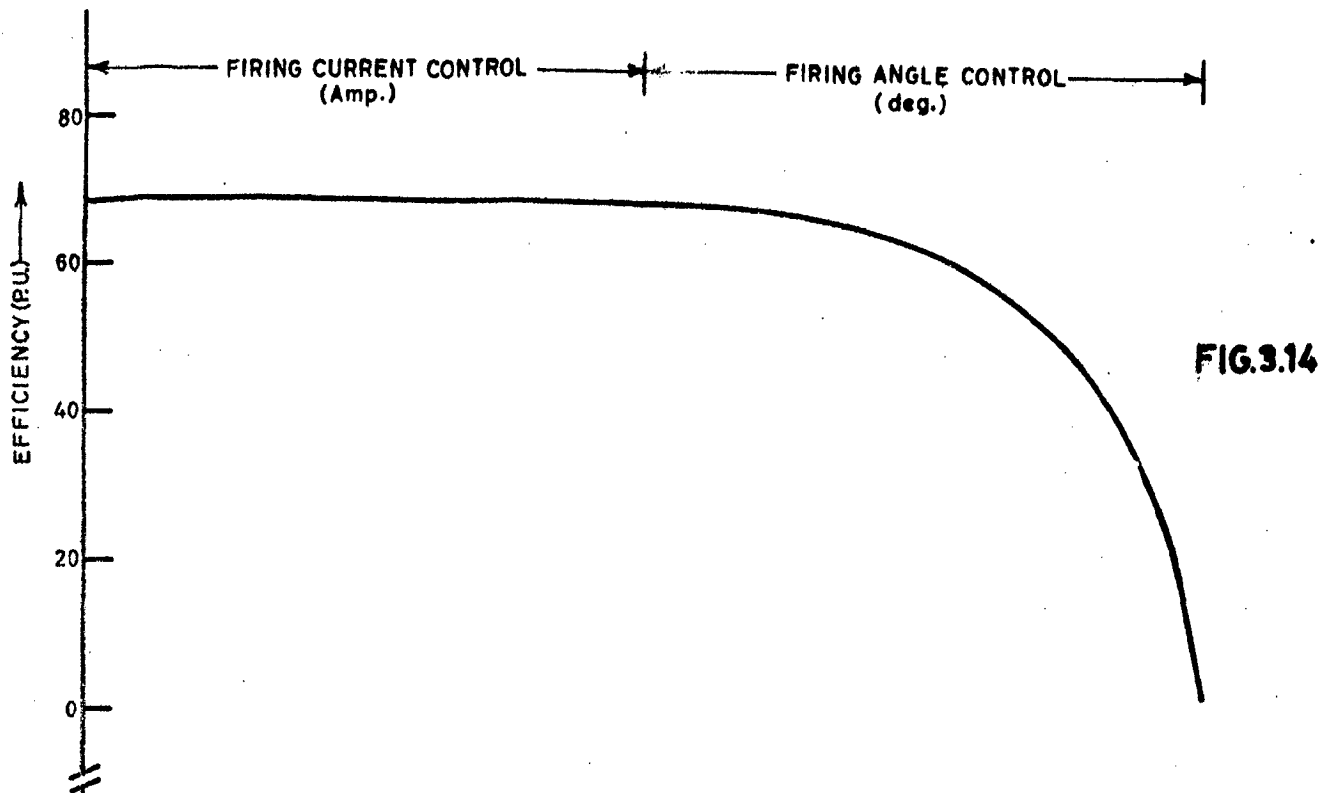
PERFORMANCE UNDER RATED VA INPUT
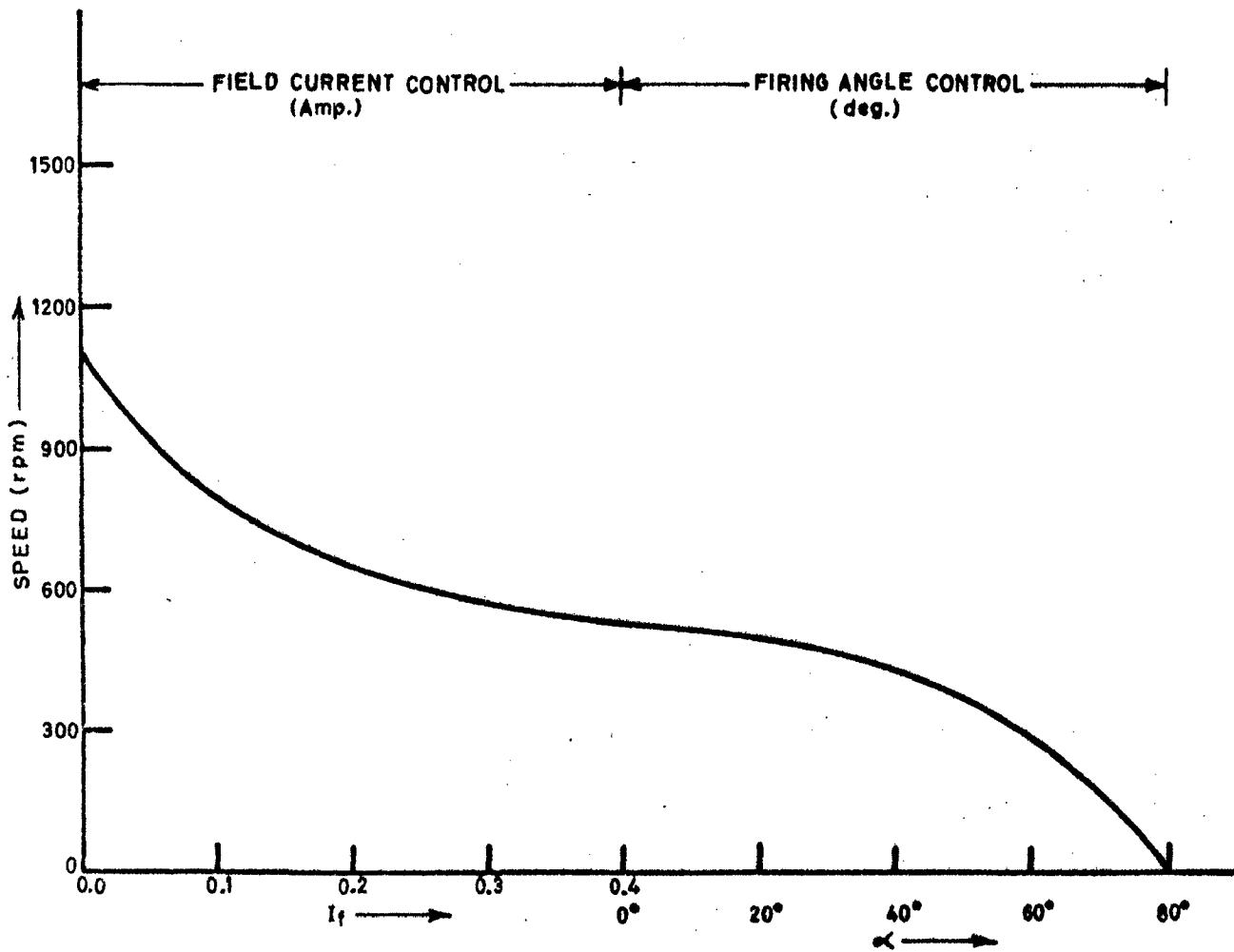
FIG. 3.16 : VARIATION OF FULL LOAD SLIP

(i)   To reduce the speed further when field current control
        has exhausted.

(ii)   The necessity of a starting device like a 3-phase
        starting rheostat connected across slip ring
        to start the drive is eliminated as the drive can be
        started at high firing angle settings.

It is further noted from the study of performance at full input ($V_{sm} = i_{sm} = 1.00$ p.u.) that firing angle control should be adopted only when it is absolutely necessary.

CHAPTER IV

STABILITY ANALYSIS

This chapter deals with the determination of the instability regions of a static slip energy recovery system. Perturbation equations are developed by linearising the dynamic equations of the system about an operating point. Using the characteristic equation of the linearized model and Routh-Hurwitz criterion, instability regions have been plotted. The effect of system parameters upon the unstable regions have been investigated.

4.1 INTRODUCTION

Performance of a drive can not be judged by its steady state behaviour alone. Induction machines which are perfectly stable on an infinite bus may become unstable with controlled thyristors in the circuit. Static slip power recovery drive may display system instability in a particular operating condition with certain combinations of firing angle of the controlled rectifier and other parameters of the drive. It is necessary to identify these combinations to ensure stable operation.

The stability analysis of a symmetrical induction machine has been carried out by Nelson, Lipo and Crause(10). Their investigation reveals that a symmetrical induction motor may become unstable at low speeds (low frequencies) even though balanced, constant amplitude, sinusoidal

voltages are applied to the stator terminals. The influence of various parameters of the system on stability has also been investigated and the following are some of their conclusions:

(i) The region of instability increases with an increase in the applied stator voltage.

(ii) An increase in the stator and rotor resistances promote system stability.

(iii) Instability region is depleted on increasing the magnetizing reactance.

(iv) A decrease in system inertia results in an increase in the region of instability.

Other researchers have also arrived at similar conclusions for the case of induction motor (11-16).

Like induction motor drive, one may expect the regions of instability in the present slip energy recovery drive as well. Apparently, although the presence of d.c. motor should promote system's stability, since it makes the drive's characteristics harder.

Non linear differential equations expressing the dynamic behaviour of system have been linearised by the method of small oscillations. The perturbation equations of the system have been developed. The characteristic equation of the linearised model is obtained from the perturbation

equations of the system. The effects of system inertia, applied voltage to the stator, stator and rotor leakage reactance, magnetizing reactance, stator and rotor resistance, filter inductance, field current and firing angle upon the stability of the system have been investigated.

4.2 APPLICATION OF SMALL DISPLACEMENT THEORY

Nonlinear equations (2.37 and 2.42) of the system are difficult to solve for a closed form solution. Therefore these equations are linearized about an operating point by the application of small displacement theory, and the important information about the system stability is obtained by investigating the resulting perturbation equations.

Derivation of perturbation equations of Ist and IIIrd equation of equation (2.37 and equation (2.42) are shown as typical cases.

4.2.1 PERTURBATION EQUATION OF Ist EQUATION OF EQUATION(2.37)

From equations (2.37), Ist equation is written as

$$V_{sm} = (R_{ss} + \frac{X_{ss}}{w_b} p) i_{ds} - F_R X_{ss} i_{qs} - \frac{X_M}{w_b} p\ i_{rm} Cos\alpha_r$$

$$+ F_R X_M i_{rm} Sin\alpha_r \qquad \ldots\ldots\ldots (4.1)$$

Under steady state, above equation reduces to

$$V_{sm} = R_{ss} i_{ds_0} - F_R X_{ss} i_{qs_0} + F_R X_M i_{rm_0} Sin\alpha_{r_0}$$

$$\ldots(4.2)$$

Now if the variables are allowed to change by a small amount about an initial operating point, then

$$V_{sm} = (R_{ss} + \frac{X_{ss}}{w_b} p)(i_{ds_0} + \Delta i_{ds}) - F_R X_{ss} (i_{qs_0} + \Delta i_{qs})$$

$$- \frac{X_M}{w_b} p (i_{rm_0} + \Delta i_{rm}) Cos(\alpha_{r_0} + \Delta \alpha_r) +$$

$$F_R X_M (i_{rm_0} + \Delta i_{rm}) Sin(\alpha_{r_0} + \Delta \alpha_r)$$

$$\dots\dots(4.3)$$

In above equation substituting $p\, i_{ds_0} = 0$,

$pi_{rm_0} = 0$ and equation (4.2), the final perturbation equation reduces to

$$0 = (R_{ss} + \frac{X_{ss}}{w_b} p) \Delta i_{ds} - F_R X_{ss} \Delta i_{qs} +$$

$$X_M i_{rm_0} (F_R Cos(F_R Cos\alpha_{r_0} + \frac{p}{w_b} Sin\alpha_{r_0}) \Delta \alpha_r$$

$$+ X_M (F_R Sin\alpha_{r_0} - \frac{p}{w_b} Cos\alpha_{r_0}) \Delta i_{rm}$$

$$\dots\dots(4.4)$$

Similarly, perturbation equation for IInd equation of equation (2.37) can be written as

$$0 = F_R X_{ss} \Delta i_{ds} + (R_{ss} + \frac{X_{ss}}{w_b} p) \Delta i_{qs} +$$

$$X_M i_{rm_0} (F_R Sin\alpha'_{r_0} - \frac{p}{w_b} Cos\alpha'_{r_0}) \Delta \alpha_r$$

$$- X_M (F_R Cos\alpha'_{r_0} + Sin\alpha'_{r_0} \frac{p}{w_b}) \Delta i_{rm} \qquad \dots\dots(4.5)$$

4.2.2 PERTURBATION EQUATION OF IIIrd EQUATION OF EQUATION(2.37)

$$K_2 \, F_R(1-s) \frac{Cos\alpha_r}{Cos\alpha} = X_M \frac{p}{w_b} i_{ds} - s \, F_R \, X_M \, i_{qs} -$$

$$(R_{eq1} + X_{eq1} \frac{p}{w_b}) \, i_{rm} \, Cos(\alpha_r - \alpha)$$

$$+ S \, F_R \, X_{rr} \, i_{rm} \, Sin(\alpha_r - \alpha)$$

Substituting $K_3 = \dfrac{K_2}{Cos\alpha}$ and $\alpha_r - \alpha = \alpha_r'$ in above equation

$$K_3 \, F_R(1-s)Cos\alpha_r = X_M \frac{p}{w_b} i_{ds} - s \, F_R \, X_m \, i_{qs} - (R_{eq1} + X_{eq1} \frac{p}{w_b}) i_{rm} Cos\alpha_r'$$

$$+ s \, F_R \, X_{rr} \, i_{rm} \, Sin\alpha_r' \quad \ldots(4.6)$$

For steady state conditions, above equation becomes,

$$K_3 \, F_R(1-s_0) \, Cos\alpha_0 = -s_0 \, F_R \, X_M \, i_{qs_0} - R_{eq1} \, i_{rm_0} \, Cos\alpha_{r_0}' +$$

$$s_0 \, F_R \, X_{rr} \, i_{rm_0} \, Sin\alpha_{r_0}' \qquad \ldots\ldots(4.7)$$

Now with small displacement of variables the resulting equation becomes,

$$K_3 \, F_R(1-s_0-\Delta s) \, Cos(\alpha_{r_0}+\Delta\alpha_r) = X_M \frac{p}{w_b} (i_{ds_0} + \Delta i_{ds}) -$$

$$(s_0 + \Delta s) \, F_R \, X_M(i_{qs_0} + \Delta i_{qs})$$

$$- (R_{eq1} + X_{eq1} \frac{p}{w_b}) (i_{rm_0} + \Delta i_{rm}) \, Cos(\alpha_{r_0}' + \Delta\alpha_r)$$

$$+ (s_0 + \Delta s) \, F_R \, X_{rr}(i_{rm_0} + \Delta i_{rm}) \, Sin(\alpha_{r_0}' + \Delta\alpha_r)$$

$$\ldots(4.8)$$

Substituting $p(i_{ds_0}) = 0$, $p(i_{rm_0}) = 0$, equation (4.7) in above equation and neglecting the product of two very small quantities, the perturbation equation is,

$$0 = \frac{X_M p}{w_b} \Delta i_{ds} - F_R X_M s_0 \Delta i_{qs} + \Delta i_{rm} [-(R_{eq1} + \frac{X_{eq1} p}{w_b}) \cos \alpha_{r_0}'$$

$$+ F_R X_{rr} s_0 \sin \alpha_{r_0}']$$

$$+ \Delta \alpha_r [K_3 F_R (1-s_0) \sin \alpha_{r_0} + (R_{eq1} + \frac{X_{eq1} p}{w_b}) i_{rm_0} \sin \alpha_{r_0}' +$$

$$+ F_R X_{rr} s_0 i_{rm_0} \cos \alpha_{r_0}']$$

$$+ \Delta s [K_3 F_R \cos \alpha_{r_0} - F_R X_M i_{qs_0} + F_R X_{rr} i_{rm_0} \sin \alpha_{r_0}']$$

$$\ldots\ldots(4.9)$$

Similarly perturbation equation for IVth equation of equation (2.37) can be written as,

$$0 = F_R X_M s_0 \Delta i_{ds} + X_M \frac{p}{w_b} \Delta i_{qs} - [F_R X_{rr} s_0 \cos \alpha_{r_0}' +$$

$$(R_{eq2} + X_{eq2} \frac{p}{w_b}) \sin \alpha_{r_0}'] i_{rm}$$

$$-[K_3 F_R (1-s_0) \cos \alpha_{r_0} - F_R X_{rr} s_0 i_{rm_0} \sin \alpha_{r_0}' +$$

$$(R_{eq2} + X_{eq2} \frac{p}{w_b}) i_{rm_0} \cos \alpha_{r_0}'] \Delta \alpha_r$$

$$+ [K_3 F_R \sin \alpha_{r_0} + F_R X_M i_{ds_0} - F_R X_{rr} i_{rm_0} \cos \alpha_{r_0}'] \Delta s$$

$$\ldots\ldots(4.10)$$

4.2.3 PERTURBATION EQUATION FOR TORQUE

Equation (2.42) is written as

$$T_L = X_M \, i_{rm}(i_{ds} \, Sin\alpha_r' - i_{qs} \, Cos\alpha_r') + K_2 \, i_{rm} + 2H \, F_R \, ps$$

$$\ldots\ldots(4.11)$$

For steady state conditions, above equation reduces to

$$T_{Lo} = X_M \, i_{rm_0}(i_{ds_0} \, Sin\alpha_{r_0}' - i_{qs_0} \, Cos\alpha_{r_0}') + K_2 \, i_{rm_0}$$

$$\ldots\ldots(4.12)$$

Now, if a small displacement is given to all the variables, the above equation becomes

$$T_{Lo} + \Delta T_L = X_M(i_{rm_0} + \Delta i_{rm}) \, [(i_{ds_0} + \Delta i_{ds}) \, Sin(\alpha_{r_0}' + \Delta\alpha_r) -$$

$$(i_{qs_0} + \Delta i_{qs}) \, Cos(\alpha_{r_0}' + \Delta\alpha_r)] + K_2(i_{rm_0} + \Delta i_{rm}) +$$

$$+ 2H \, F_R \, p \, (s_0 + \Delta s)$$

$$\ldots\ldots(4.13)$$

Substituting $p(s_0) = 0$, equation (4.12) in above equation and neglecting the product of two very small quantities, the perturbation equation becomes,

$$\Delta T_L = X_M[i_{rm_0} \, Sin\alpha_{r_0}' \, \Delta i_{ds} - i_{rm_0} \, Cos\alpha_{r_0}' \, \Delta i_{qs} + (i_{ds_0} \, Sin\alpha_{r_0}' -$$

$$i_{qs_0} \, Cos\alpha_{r_0}' + \frac{K_2}{X_M}) \, \Delta i_{rm} + i_{rm_0}(i_{ds_0} \, Cos\alpha_{r_0}' +$$

$$i_{qs_0} \, Sin\alpha_{r_0}') \, \Delta\alpha_r] + 2H \, F_R \, p \, \Delta s$$

$$\ldots\ldots(4.14)$$

4.2.4 FINAL PERTURBATION EQUATIONS

Final perturbations equations (4.4), (4.5), (4.9), (4.10) and (4.14) can be written in matrix form as,

$$
\begin{bmatrix} 0 \\ 0 \\ 0 \\ 0 \\ \Delta T_L \end{bmatrix} =
\begin{bmatrix}
Z_1 + Z_2 p & Z_3 & Z_4 + Z_5 p & Z_6 + Z_7 p & 0 \\
Z_8 & Z_9 + Z_{10} p & Z_{11} + Z_{12} p & Z_{13} + Z_{14} p & 0 \\
Z_{15} p & Z_{16} & Z_{17} + Z_{18} p & Z_{19} + Z_{20} p & Z_{21} \\
Z_{22} & Z_{23} p & Z_{24} + Z_{25} p & Z_{26} + Z_{27} p & Z_{28} \\
Z_{29} & Z_{30} & Z_{31} & Z_{32} & Z_{33} p
\end{bmatrix}
\begin{bmatrix} \Delta i_{ds} \\ \Delta i_{qs} \\ \Delta i_{rm} \\ \Delta \alpha_r \\ \Delta s \end{bmatrix}
$$

$$\dots\dots(4.15)$$

where,

$$Z_1 = R_{ss}$$

$$Z_2 = \frac{X_{ss}}{w_b}$$

$$Z_3 = - F_R X_{ss}$$

$$Z_4 = X_M F_R \sin\alpha_{r_o}'$$

$$Z_5 = - \frac{X_M}{w_b} \cos\alpha_{r_o}'$$

$$Z_6 = X_M i_{rm_o} F_R \cos\alpha_{r_o}'$$

$$Z_7 = \frac{X_M}{w_b} i_{rm_o} \sin\alpha_{r_o}'$$

$$Z_8 = F_R X_{ss}$$

$$Z_9 = R_{ss} = Z_1$$

$$Z_{10} = \frac{X_{ss}}{w_b} = Z_2$$

$$Z_{11} = - F_R X_M \cos\alpha_{r_o}'$$

$$Z_{12} = - \frac{X_M}{w_b} \sin\alpha_{r_o}'$$

$$Z_{13} = X_M i_{rm_o} F_R \sin\alpha_{r_o}'$$

$$Z_{14} = - \frac{X_M}{w_b} i_{rm_o} \cos\alpha_{r_o}'$$

$$Z_{15} = \frac{X_M}{w_b}$$

$$Z_{16} = - F_R X_M s_o$$

$$Z_{17} = F_R X_{rr} s_o \sin\alpha_{r_o}' - R_{eq_1} \cos\alpha_{r_o}'$$

$$Z_{18} = \frac{X_{eq_1}}{w_b} \cos\alpha_{r_o}'$$

$$Z_{19} = K_3 F_R (1-s_o) \sin\alpha_{r_o} + R_{eq_1} i_{rm_o} \sin\alpha_{r_o}' +$$

$$F_R X_{rr} s_o i_{rm_o} \cos\alpha_{r_o}'$$

$$Z_{20} = \frac{X_{eq_1}}{w_b} i_{rm_o} \sin\alpha_{r_o}'$$

$$Z_{21} = K_3 F_R \cos\alpha_{r_o} - F_R X_M i_{qs_o} + F_R X_{rr} i_{rm_o} \sin\alpha_{r_o}'$$

$$Z_{22} = F_R X_M s_o = - Z_{16}$$

$$Z_{23} = \frac{X_M}{w_b} = Z_{15}$$

$$Z_{24} = -F_R X_{rr} s_0 \cos\alpha_{r_0}' - R_{eq_2} \sin\alpha_{r_0}'$$

$$Z_{25} = -\frac{X_{eq_2}}{w_b} = \sin\alpha_{r_0}' = Z_{15}$$

$$Z_{26} = K_3 F_R (1-s_0) \cos\alpha_{r_0} + F_R X_{rr} s_0 i_{rm_0} \sin\alpha_{r_0}' - R_{eq_2} i_{rm_0} \cos\alpha_{r_0}'$$

$$Z_{27} = \frac{X_{eq_2}}{w_b} i_{rm_0} \cos\alpha_{r_0}'$$

$$Z_{28} = K_3 F_R \sin\alpha_{r_0} + F_R X_M i_{ds_0} - F_R X_{rr} i_{rm_0} \cos\alpha_{r_0}'$$

$$Z_{29} = X_M i_{rm_0} \sin\alpha_{r_0}'$$

$$Z_{30} = -X_M i_{rm_0} \cos\alpha_{r_0}'$$

$$Z_{31} = X_M(i_{ds_0} \sin\alpha_{r_0}' - i_{qs_0} \cos\alpha_{r_0}' + \frac{K_2}{X_M})$$

$$Z_{32} = X_M(i_{ds_0} \cos\alpha_{r_0}' + i_{qs_0} \sin\alpha_{r_0}') i_{rm_0}$$

$$Z_{33} = 2H F_R$$

4.3 CHARACTERISTIC EQUATION

It is assumed that change in load torque is negligible for small deviation in speed, therefore substituting $\Delta T_L = 0$ in equation (4..15), dynamic equations are represented as,

$$
\begin{bmatrix} 0 \\ 0 \\ 0 \\ 0 \\ 0 \end{bmatrix}
=
\begin{bmatrix}
Z_1+Z_2p & Z_3 & Z_4+Z_5p & Z_6+Z_7p & 0 \\
Z_8 & Z_9+Z_{10}p & Z_{11}+Z_{12}p & Z_{13}+Z_{14}p & 0 \\
Z_{15}p & Z_{16} & Z_{17}+Z_{18}p & Z_{19}+Z_{20}p & Z_{21} \\
Z_{22} & Z_{23}p & Z_{24}+Z_{25}p & Z_{26}+Z_{27}p & Z_{28} \\
Z_{29} & Z_{30} & Z_{31} & Z_{32} & Z_{33}p
\end{bmatrix}
\begin{bmatrix} \Delta i_{ds} \\ \Delta i_{qs} \\ \Delta i_{rm} \\ \Delta \alpha_r \\ \Delta s \end{bmatrix}
$$

$$\dots\dots(4.16)$$

Characteristic equation of the system is obtained by putting the 5 x 5 determinant formed by equation (4.16) to zero.

For simplicity five equations represented by equation (4.16) are reduced to three by eliminating any two variables.

From Ist equation of equations (4.16), Δi_{qs} may be expressed as,

$$\Delta i_{qs} = -\frac{1}{Z_3}\left[(Z_1+Z_2p)\Delta i_{ds} + (Z_4+Z_5p)\Delta i_{rm} + (Z_6+Z_7p)\Delta \alpha_r\right]$$

$$\dots\dots(4.17)$$

From IIIrd equation of equations (4.16), Δs may be expressed as,

$$\Delta s = -\frac{1}{Z_{21}}\left[Z_{15}p\,\Delta i_{ds} + Z_{16}\,\Delta i_{qs} + (Z_{17}+Z_{18}p)\Delta i_{rm} + \right.$$
$$\left. (Z_{19}+Z_{20}p)\Delta \alpha_r\right]$$

$$\dots\dots\dots(4.18)$$

Substituting for i_{qs} in equation (4.18) from equation (4.17)

$$
\Delta s = \left[\frac{z_1}{z_3} \frac{z_{16}}{z_{21}} + \left\{ \frac{z_2}{z_3} \frac{z_{16}}{z_{21}} - \frac{z_{15}}{z_{21}} \right\} p \right] \Delta i_{ds} + \left[\left\{ \frac{z_{16}}{z_3} \frac{z_4}{z_{21}} - \frac{z_{17}}{z_{21}} \right\} \right.
$$

$$
\left. + \left\{ \frac{z_{16}}{z_{21}} \frac{z_5}{z_3} - \frac{z_{18}}{z_{21}} \right\} p \right] \Delta i_{rm} + \left[\left\{ \frac{z_{16}}{z_{21}} \frac{z_6}{z_3} - \frac{z_{19}}{z_{21}} \right\} \right.
$$

$$
\left. + \left\{ \frac{z_{16}}{z_{21}} \frac{z_7}{z_3} - \frac{z_{20}}{z_{21}} \right\} p \right] \Delta \alpha_r
$$

$$\dots\dots(4.19)$$

Now, substituting for Δi_{qs} and Δs from equation (4.17) and equation (4.19) in the remaining second, fourth and fifth equations of equations (4.16), the solution is expressed as,

$$C_{11} \Delta i_{ds} + C_{12} \Delta i_{rm} + C_{13} \Delta \alpha_r = 0$$

$$C_{21} \Delta i_{ds} + C_{22} \Delta i_{rm} + C_{23} \Delta \alpha_r = 0$$

$$C_{31} \Delta i_{ds} + C_{32} \Delta i_{rm} + C_{33} \Delta \alpha_r = 0$$

$$\dots\dots\dots\dots(4.20)$$

where

$$C_{11} = z_{34} p^2 + z_{35} p + z_{36}$$

$$C_{12} = z_{37} p^2 + z_{38} p + z_{39}$$

$$C_{13} = z_{40} p^2 + z_{41} p + z_{42}$$

$$C_{21} = z_{43} p^2 + z_{44} p + z_{45}$$

$$C_{22} = z_{46} p^2 + z_{47} p + z_{48}$$

$$C_{23} = Z_{49} \, p^2 + Z_{50}p + Z_{51}$$

$$C_{31} = Z_{52} \, p^2 + Z_{53}p + Z_{54}$$

$$C_{32} = Z_{55} \, p^2 + Z_{56}p + Z_{57}$$

$$C_{33} = Z_{58} \, p^2 + Z_{59}p + Z_{60}$$

$$Z_{34} = \frac{Z_2 \, Z_{10}}{Z_8 \, Z_3}$$

$$Z_{35} = \frac{1}{Z_8 \, Z_3}(Z_{10} \, Z_1 + Z_2 \, Z_9)$$

$$Z_{36} = -1 + \frac{Z_1 \, Z_9}{Z_8 \, Z_3}$$

$$Z_{37} = \frac{Z_{10} \, Z_5}{Z_8 \, Z_3}$$

$$Z_{38} = \frac{1}{Z_8 \, Z_3}(Z_9 \, Z_5 + Z_{10} \, Z_4) - \frac{Z_{12}}{Z_8}$$

$$Z_{39} = \frac{Z_9 \, Z_4}{Z_8 \, Z_3} - \frac{Z_{11}}{Z_8}$$

$$Z_{40} = \frac{Z_{10} \, Z_7}{Z_8 \, Z_3}$$

$$Z_{41} = \frac{1}{Z_8 \, Z_3}(Z_9 \, Z_7 + Z_{10} \, Z_6) - \frac{Z_{14}}{Z_8}$$

$$Z_{42} = \frac{Z_9 \, Z_6}{Z_8 \, Z_3} - \frac{Z_{13}}{Z_8}$$

$$Z_{43} = -\frac{Z_{23}}{Z_3} \, Z_2$$

$$Z_{44} = -\frac{Z_{23}}{Z_3} \, Z_1 + Z_{28}\left(\frac{Z_{16} \, Z_2}{Z_3 \, Z_{21}} - \frac{Z_{15}}{Z_{21}}\right)$$

$$Z_{45} = Z_{22} + Z_{28} \left(\frac{Z_{16}}{Z_3} \frac{Z_1}{Z_{21}} \right)$$

$$Z_{46} = - \frac{Z_{23}}{Z_3} Z_5$$

$$Z_{47} = - \frac{Z_{23}}{Z_3} Z_4 + Z_{25} + Z_{28} \left(\frac{Z_{16}}{Z_3} \frac{Z_5}{Z_{21}} - \frac{Z_{18}}{Z_{21}} \right)$$

$$Z_{48} = Z_{24} + Z_{28} \left(\frac{Z_{16}}{Z_3} \frac{Z_4}{Z_{21}} - \frac{Z_{17}}{Z_{21}} \right)$$

$$Z_{49} = - \frac{Z_{23}}{Z_3} Z_7$$

$$Z_{50} = - \frac{Z_{23}}{Z_3} Z_6 + Z_{27} + Z_{28} \left(\frac{Z_{16}}{Z_3} \frac{Z_7}{Z_{21}} - \frac{Z_{20}}{Z_{21}} \right)$$

$$Z_{51} = Z_{26} + Z_{28} \left(\frac{Z_{16}}{Z_3} \frac{Z_6}{Z_{21}} - \frac{Z_{19}}{Z_{21}} \right)$$

$$Z_{52} = Z_{33} \left(\frac{Z_{16}}{Z_3} \frac{Z_2}{Z_{21}} - \frac{Z_{15}}{Z_{21}} \right)$$

$$Z_{53} = - \frac{Z_{30}}{Z_3} \frac{Z_2}{Z_3} + Z_{33} \frac{Z_1}{Z_3} \frac{Z_{16}}{Z_{21}}$$

$$Z_{54} = Z_{29} - \frac{Z_{30}}{Z_3} \frac{Z_1}{Z_3}$$

$$Z_{55} = Z_{33} \left(\frac{Z_{16}}{Z_3} \frac{Z_5}{Z_{21}} - \frac{Z_{18}}{Z_{21}} \right)$$

$$Z_{56} = - \frac{Z_{30}}{Z_3} Z_5 + Z_{33} \left(\frac{Z_{16}}{Z_3} \frac{Z_4}{Z_{21}} - \frac{Z_{17}}{Z_{21}} \right)$$

$$Z_{57} = - \frac{Z_{30}}{Z_3} Z_4 + Z_{31}$$

$$Z_{58} = Z_{33} \left(\frac{Z_{16}}{Z_3} \frac{Z_7}{Z_{21}} - \frac{Z_{20}}{Z_{21}} \right)$$

$$Z_{59} = - \frac{Z_{30}}{Z_3} Z_7 + Z_{33} \left(\frac{Z_{16}}{Z_3} \frac{Z_6}{Z_{21}} - \frac{Z_{19}}{Z_{21}} \right)$$

$$Z_{60} = - \frac{Z_{30}}{Z_3} Z_6 + Z_{32}$$

Characteristic equation of the system can be obtained by equating the 3×3 determinant formed by coefficient of equation (4.20) to zero.

$$\begin{vmatrix} c_{11} & c_{12} & c_{13} \\ c_{21} & c_{22} & c_{23} \\ c_{31} & c_{32} & c_{33} \end{vmatrix} = 0$$

$$\dots\dots\dots\dots(4.21)$$

Simplifying equation (4.21), it becomes a sixth order equation but the coefficient of sixth power term is found to be always zero. It is not unexpected as 5×5 determinant of equation (4.16) clearly indicates that the order of the characteristic equation must be five. Thus the characteristic equation may be expressed as,

$$D_5 p^5 + D_4 p^4 + D_3 p^3 + D_2 p^2 + D_1 p + D_0 = 0$$

$$\dots\dots\dots(4.22)$$

where various coefficients, D_5 to D_0, are expressed as,

$$D_5 = (z_{34}\, z_{46}\, z_{59} + z_{34}\, z_{47}\, z_{58} + z_{35}\, z_{46}\, z_{58})$$

$$- (z_{34}\, z_{55}\, z_{50} + z_{34}\, z_{56}\, z_{49} + z_{35}\, z_{55}\, z_{49})$$

$$- (z_{37}\, z_{43}\, z_{59} + z_{37}\, z_{44}\, z_{58} + z_{38}\, z_{43}\, z_{58})$$

$$+ (z_{37}\, z_{52}\, z_{50} + z_{37}\, z_{53}\, z_{49} + z_{38}\, z_{52}\, z_{49})$$

$$+ (z_{40}\, z_{43}\, z_{56} + z_{40}\, z_{44}\, z_{55} + z_{41}\, z_{43}\, z_{55})$$

$$- (z_{40}\, z_{52}\, z_{47} + z_{40}\, z_{53}\, z_{46} + z_{41}\, z_{52}\, z_{46})$$

$$D_4 = (z_{34}\, z_{46}\, z_{60} + z_{34}\, z_{47}\, z_{59} + z_{34}\, z_{48}\, z_{58} +$$

$$z_{35}\, z_{46}\, z_{59} + z_{35}\, z_{47}\, z_{58} + z_{36}\, z_{46}\, z_{58})$$

$$- (z_{34}\, z_{55}\, z_{51} + z_{34}\, z_{56}\, z_{50} + z_{34}\, z_{57}\, z_{49}$$

$$+ z_{35}\, z_{55}\, z_{50} + z_{35}\, z_{56}\, z_{49} + z_{36}\, z_{55}\, z_{9})$$

$$-(z_{37}\, z_{43}\, z_{60} + z_{37}\, z_{44}\, z_{59} + z_{37}\, z_{45}\, z_{58} + z_{38}\, z_{43}\, z_{59}$$

$$+ z_{38}\, z_{44}\, z_{58} + z_{39}\, z_{43}\, z_{58})$$

$$+(z_{37}\, z_{52}\, z_{51} + z_{37}\, z_{53}\, z_{50} + z_{37}\, z_{54}\, z_{49} + z_{38}\, z_{52}\, z_{50}$$

$$+ z_{38}\, z_{53}\, z_{49} + z_{39}\, z_{52}\, z_{49})$$

$$+(z_{40}\, z_{43}\, z_{57} + z_{40}\, z_{44}\, z_{56} + z_{40}\, z_{45}\, z_{55} + z_{41}\, z_{43}\, z_{56}$$

$$+ z_{41}\, z_{44}\, z_{55} + z_{42}\, z_{43}\, z_{55})$$

$$- (z_{40}\, z_{52}\, z_{48} + z_{40}\, z_{53}\, z_{47} + z_{40}\, z_{54}\, z_{46} + z_{41}\, z_{52}\, z_{47}$$

$$+ z_{41}\, z_{53}\, z_{46} + z_{42}\, z_{52}\, z_{46})$$

$$D_3 = (z_{34}\, z_{47}\, z_{60} + z_{34}\, z_{48}\, z_{59} + z_{35}\, z_{46}\, z_{60} + z_{35}\, z_{47}\, z_{59}$$

$$+ z_{35}\, z_{48}\, z_{58} + z_{36}\, z_{46}\, z_{59} + z_{36}\, z_{47}\, z_{58})$$

$$- (z_{34}\, z_{56}\, z_{51} + z_{34}\, z_{57}\, z_{50} + z_{35}\, z_{55}\, z_{51} + z_{35}\, z_{56}\, z_{50}$$

$$+ z_{35}\, z_{57}\, z_{49} + z_{36}\, z_{55}\, z_{50} + z_{36}\, z_{56}\, z_{49})$$

$$- (z_{37}\, z_{44}\, z_{60} + z_{37}\, z_{45}\, z_{59} + z_{38}\, z_{43}\, z_{60} + z_{38}\, z_{44}\, z_{59}$$

$$+ z_{38}\, z_{45}\, z_{58} + z_{39}\, z_{43}\, z_{59} + z_{39}\, z_{44}\, z_{58})$$

$$+ (z_{37}\, z_{53}\, z_{51} + z_{37}\, z_{54}\, z_{50} + z_{38}\, z_{52}\, z_{51} + z_{38}\, z_{53}\, z_{50}$$

$$+ z_{38}\, z_{54}\, z_{49} + z_{39}\, z_{52}\, z_{50} + z_{39}\, z_{53}\, z_{49})$$

$$+ (z_{40}\, z_{44}\, z_{57} + z_{40}\, z_{45}\, z_{56} + z_{41}\, z_{43}\, z_{57} + z_{41}\, z_{44}\, z_{56}$$

$$+ z_{41}\, z_{45}\, z_{55} + z_{42}\, z_{43}\, z_{56} + z_{42}\, z_{44}\, z_{55})$$

$$- (z_{40}\, z_{53}\, z_{48} + z_{40}\, z_{54}\, z_{47} + z_{41}\, z_{52}\, z_{48} + z_{41}\, z_{53}\, z_{47}$$

$$+ z_{41}\, z_{54}\, z_{46} + z_{42}\, z_{52}\, z_{47} + z_{42}\, z_{53}\, z_{46})$$

$$D_2 = (z_{34}\, z_{48}\, z_{60} + z_{35}\, z_{47}\, z_{60} + z_{35}\, z_{48}\, z_{59}$$

$$+ z_{36}\, z_{46}\, z_{60} + z_{36}\, z_{47}\, z_{59} + z_{36}\, z_{48}\, z_{58})$$

$$- (z_{34}\, z_{57}\, z_{51} + z_{35}\, z_{56}\, z_{51} + z_{35}\, z_{57}\, z_{50}$$

$$+ z_{36}\, z_{55}\, z_{51} + z_{36}\, z_{56}\, z_{50} + z_{36}\, z_{57}\, z_{49})$$

$$- (z_{37}\, z_{45}\, z_{60} + z_{38}\, z_{44}\, z_{60} + z_{38}\, z_{45}\, z_{59}$$

$$+ z_{39}\, z_{43}\, z_{60} + z_{39}\, z_{44}\, z_{59} + z_{39}\, z_{45}\, z_{58})$$

$$+ (z_{37}\, z_{54}\, z_{51} + z_{38}\, z_{53}\, z_{51} + z_{38}\, z_{54}\, z_{50}$$

$$+ z_{39}\, z_{52}\, z_{51} + z_{39}\, z_{53}\, z_{50} + z_{39}\, z_{54}\, z_{49})$$

$$+ (z_{40}\, z_{45}\, z_{57} + z_{41}\, z_{44}\, z_{57} + z_{41}\, z_{45}\, z_{56}$$

$$+ z_{42}\, z_{43}\, z_{57} + z_{42}\, z_{44}\, z_{56} + z_{42}\, z_{45}\, z_{55})$$

$$- (z_{40}\, z_{54}\, z_{48} + z_{41}\, z_{53}\, z_{48} + z_{41}\, z_{54}\, z_{47})$$

$$+ z_{42}\, z_{52}\, z_{48} + z_{42}\, z_{53}\, z_{47} + z_{42}\, z_{54}\, z_{46})$$

$$D_1 = (z_{35}\, z_{48}\, z_{60} + z_{36}\, z_{47}\, z_{60} + z_{36}\, z_{48}\, z_{59})$$

$$- (z_{35}\, z_{57}\, z_{51} + z_{36}\, z_{56}\, z_{51} + z_{36}\, z_{57}\, z_{50})$$

$$- (z_{38}\, z_{45}\, z_{60} + z_{39}\, z_{44}\, z_{60} + z_{39}\, z_{45}\, z_{59})$$

$$+ (z_{38}\, z_{54}\, z_{51} + z_{39}\, z_{53}\, z_{51} + z_{39}\, z_{54}\, z_{50})$$

$$+ (z_{41}\, z_{45}\, z_{57} + z_{42}\, z_{44}\, z_{57} + z_{42}\, z_{45}\, z_{56})$$

$$- (z_{41}\, z_{54}\, z_{48} + z_{42}\, z_{53}\, z_{48} + z_{42}\, z_{54}\, z_{47})$$

$$D_o = Z_{36} Z_{48} Z_{60} + Z_{36} Z_{57} Z_{51} + Z_{39} Z_{45} Z_{60}$$

$$+ Z_{39} Z_{54} Z_{51} + Z_{42} Z_{45} Z_{57} - Z_{42} Z_{54} Z_{48}$$

Equation (4.22) may be normalised to minimize the variation between the minimum and maximum value of the coefficients.

Dividing equation (4.22) by D_5

$$p^5 + \frac{D_4}{D_5} p^4 + \frac{D_3}{D_5} p^3 + \frac{D_2}{D_5} p^2 + \frac{D_1}{D_5} p + \frac{D_o}{D_5} = 0$$

$$\dots\dots\dots\dots(4.23)$$

Let $\frac{D_o}{D_5} = y^5$, where y is a constant, equation (4.23) becomes,

$$p^5 + \frac{D_4}{D_5} p^4 + \frac{D_3}{D_5} p^3 + \frac{D_2}{D_5} p^2 + \frac{D_1}{D_5} p + y^5 = 0$$

$$\dots\dots\dots\dots(4.24)$$

Dividing by y^5 and defining another differnetial operator $q = \frac{p}{y}$ equation (4.24) becomes,

$$q^5 + \frac{D_4}{D_5 y} q^4 + \frac{D_3}{D_5 y^2} q^3 + \frac{D_2}{D_5 y^3} q^2 + \frac{D_1}{D_5 y^4} q + 1 = 0$$

$$\dots\dots\dots(4.25)$$

The various Z terms appearing in the characteristic equation (4.25) are functions of the Z's (Z_1 to Z_{33}) appearing in perturbation equation (4.16), which in turn are expressed in terms of drive parameters, the steady state currents i_{ds_o}, i_{qs_o}, i_{rm_o} and α_{r_o} corresponding to steady state operating slip s_o at a given d.c. motor field current I_f and given firing angle α of the controlled rectifier.

4.4 STABILITY STUDIES

Numerical values of various coefficients of characteristic equation (4.25) can be determined and therefore stability test can now be applied. These coefficients are arranged in Routh array. Stability of the system is investigated by determining change of sign of the elements appearing in first column of Routh array (22)

The computer program is FORTRAN language for the stability analysis is so written that the logic involved can determine directly whether the system is stable or not for given system parameters. Flow chart and listing of the program used, are given in Appendix 4.

Present drive has an induction motor as its main motor. It is well known that induction motor offers stable operation when supplied from a 3 phase source of rated voltage and of rated frequency. However, it may show region of instability when supply frequency is considerably reduced. The present drive has a controlled rectifier and a d.c. motor directly coupled to the induction motor. These components should logically influence the stability behaviour of the drive. In order to systematically establish the contribution of d.c. motor and the controlled rectifier in influencing the stability of the induction motor, present study takes up first the case of induction motor alone, establish its stability behaviour The effect of other components is gradually introduced next and change in stability behaviour is noted.

Stability behaviour of induction motor has been reported by several researchers (9-13) in torque-frequency ratio plane. The same representation is used here although it may be noted that the slip energy recovery drive, considered here, operates from a rated voltage rated frequency source and hence frequency ratio is always unity for the drive. The variable "frequency ratio" is introduced only to facilitate the study of stability behaviour of induction motor alone.

In variable speed induction motor fed from a variable frequency source the amplitude of the applied voltage is typically decreased as frequency decreases in order to avoid saturation of the machine. However, if the voltage is decreased in proportion to the frequency, the breakdown torque is depleted significantly at low frequencies since an increased percentage of the applied voltage is dropped across the stator resistance as frequency is reduced. In this study, as a single means of i_R compensation the voltage required to produce rated flux linkage at rated load ($T_L = 1.0$ p.u.) and rated speed ($F_R = 1.0$) has been predetermined. When system is operating from a variable frequency source, the terminal voltage has been adjusted so that for any frequency,

$$V_{sm} = V_K + F_R V_m$$

$$\dots\dots\dots(4.26)$$

where $V_K = 0.025$ and $V_m = 1.0$ p.u.

From equation (4.26), it is evident that the constant factor V_K serves to compensate for the stator i_R drop at very low frequencies.

Regions of instability can be determined in torque-frequency ratio plane for the induction motor. A particular value of frequency ratio and motor parameters give a point on the instability contour if slip is varied from no load slip to unity in small intervals, say .01. This process is again repeated after giving a very small increment to frequency ratio. Thus a number of points are determined on the instability contour. Finally all these points are joined together to demarcate the regions of instability in torque-frequency ratio plane. The effect of changing the various parameters on the instability region are then investigated

4.5 STABILITY RESULTS OF INDUCTION MOTOR

The per unit parameters of the induction motor are given in Appendix II. It is observed that this motor shows absolute stability at all frequencies, when fed from a variable frequency supply. The motor does not depict instability even if one of its parameters is varied by ± 20 percent However motor becomes unstable, if its inertia constant is taken as low as .05 sec and its rotor resistance in p.u. as 0.015 . The unstable region under these parameters is depicted by the area enclosed by curve II of Fig. 4.1. It may be noted that instability occurs in frequency ratio range of 0.5 to 0.74.
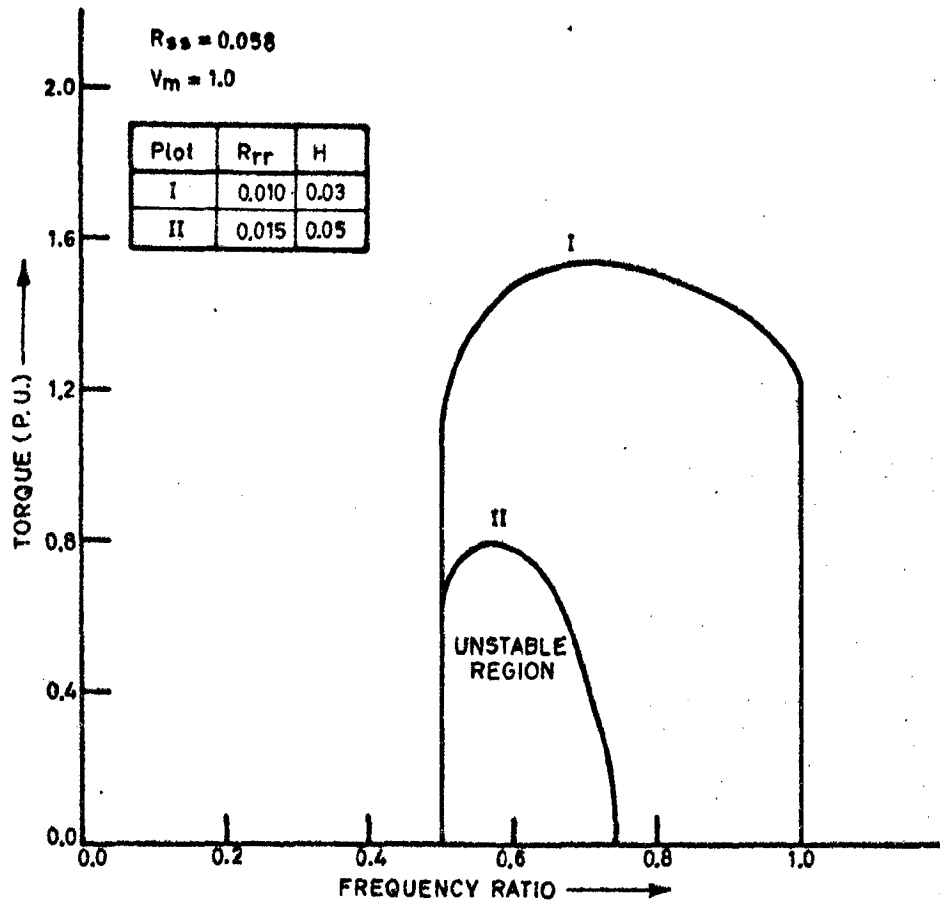
FIG.4.1: INSTABILITY REGION FOR INDUCTION MOTOR

In the present drive the supply to induction motor is of constant voltage and constant frequency, both fixed at rated values. Thus frequency ratio is always unity. In order to see the effect of additional components of the drive on stability behaviour of the induction motor at unity frequency ratio, it is necessary to first note the behaviour of induction motor alone at unity freq. ratio. This is done by further reducing the values of R_{rr} andH to .01 and .03, respectively. The resulting stability contour is shown by curve (I) of Fig. 4.1. It may be noted that under these parameters, a large unstable region is present and the motor is unstable even at unity frequency ratio up to a load torque of 1.2 p.u. Considering this as our base curve, the effect of varying other parameters may now be studied.

The values of parameters and the quantities varied in each case are given in table 4.1

Figure	Inertia Constant H	Applied Voltage V_m	Stator Resistance R_{ss}	Rotor Resistance R_{rr}
4.2	Varied	1.0	0.058	0.010
4.3	0.03	Varied	0.058	0.010
4.4	0.03	1.0	Varied	0.010
4.5	0.03	1.0	0.058	Varied

Table 4.1 Per Unit parameters of induction motor

4.5.1 EFFECT OF INERTIA CONSTANT

Regions of instability for H = 0.03, 0.04 and 0.05 second are shown in Fig. 4.2. It is observed that H = 0.03 second produces the largest area of instability as compared to other two value of Inertia Constant. Stability contours also show that the stability is improved with increased inertia contant.

4.5.2 EFFECT OF APPLIED VOLTAGE

Regions of instability for V_m = 0.9, 1.0 and 1.1 are shown in Fig. 4.3. For V_m = 0.9 instability region present is smallest. This indicates that the region of instability increases with an increase in terminal voltage.

4.5.3 EFFECT OF STATOR RESISTANCE

The contours shown in Fig. 4.4 depict the effect of stator resistance on the instability region. Regions of instability are shown for R_{ss} = 0.45, 0.050 and 0.058. It is noted that region of instability increases on decreasing the stator resistance.

4.5.4 EFFECT OF ROTOR RESISTANCE

Variation in the region of instability due to change in rotor resistance is shown in Fig. 4.5. Contours for R_{rr} = 0.008, 0.010 and 0.012 are shown. It reveals that increasing rotor resistance tends to stabilize the machine.
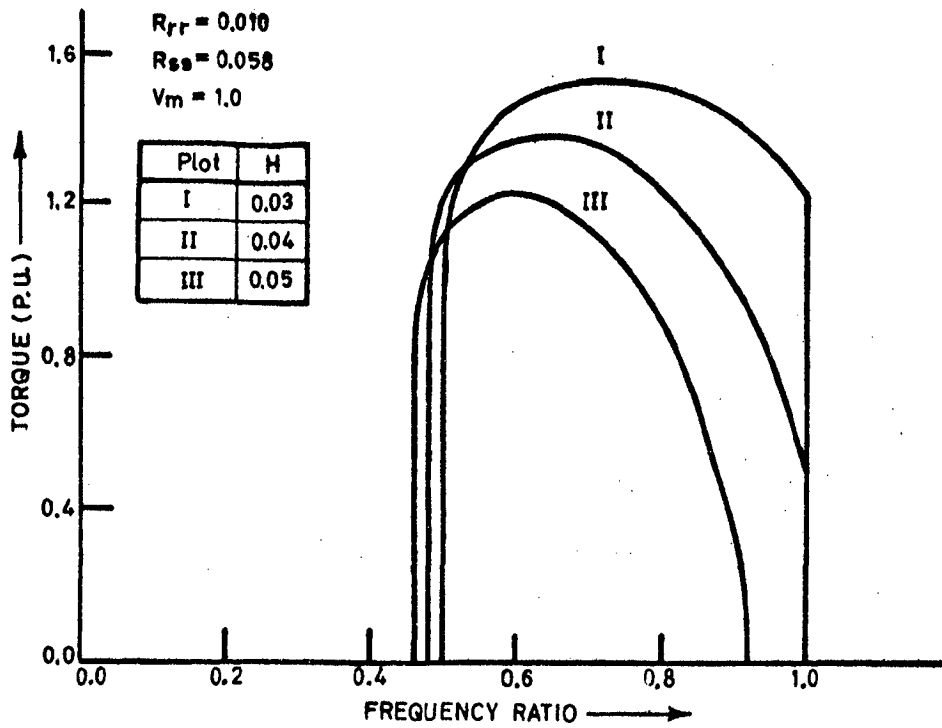
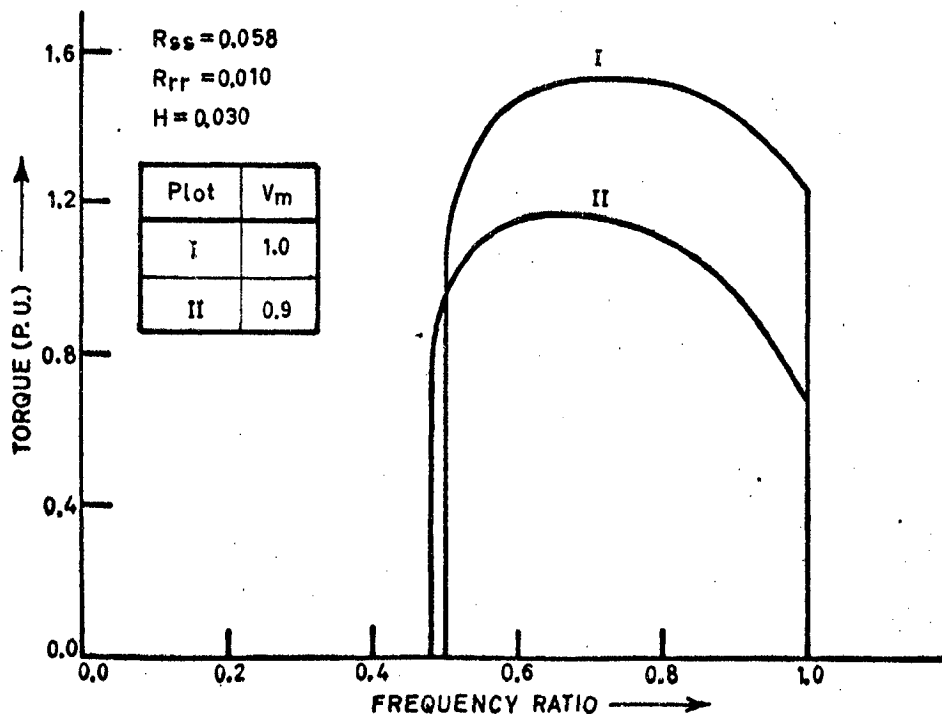FIG.4.2: REGIONS OF INSTABILITY FOR INCREASE IN INERTIA CONSTANT

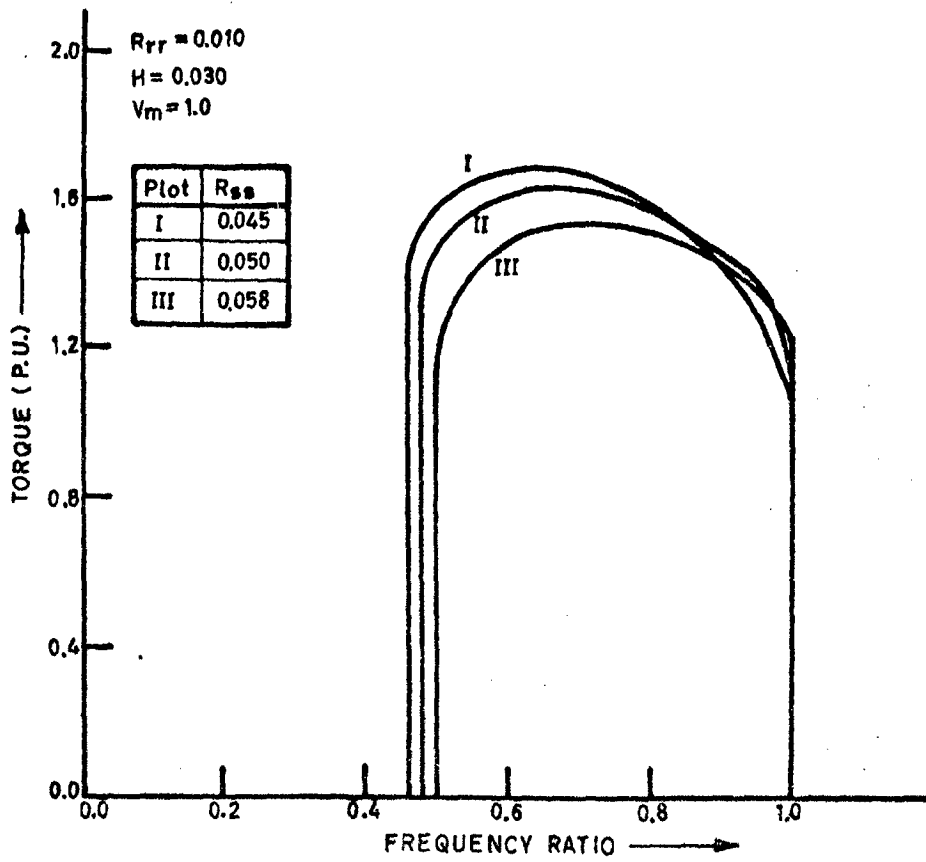FIG.4.3: REGIONS OF INSTABILITY FOR DIFFERENT VALUES OF APPLIED STATOR VOLTAGE

FIG.4.4: REGIONS OF INSTABILITY FOR DIFFERENT
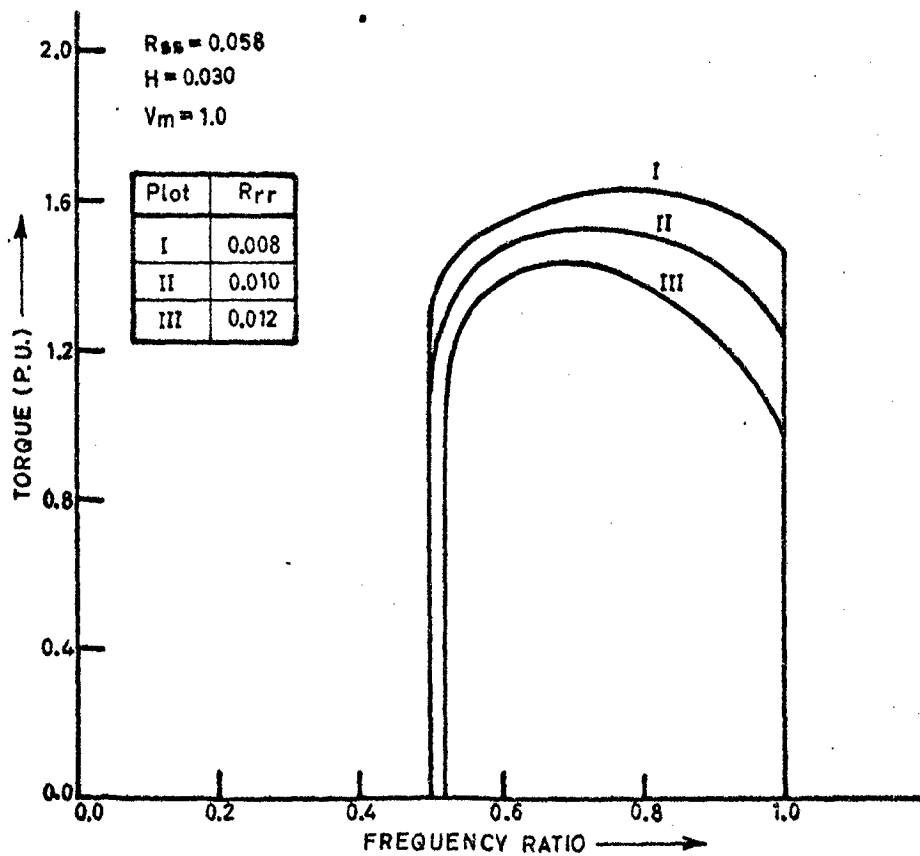VALUES OF STATOR RESISTANCE

FIG.4.5: REGIONS OF INSTABILITY FOR CHANGES
IN ROTOR RESISTANCE

The induction motor parameters in present case
are such that it does not become unstable even at low frequencies. However by considering reduced values of rotor
resistance and inertia constant, it has been possible to
find instability contours on parametric variation. The
conclusions drawn tally with those reported by Nelson Lipo
Krause (10), although some parameters have been greatly
reduced to observe unstable region. This approach will now
be extended to study the effect of other components of the
drive.

4.6 STABILITY RESULTS OF THE COMPLETE DRIVE

4.6.1 EFFECT OF D.C. LINK RESISTANCE AND REACTANCE

Stability of the drive is now investigated. In the
process, the first step chosen is to see the influence of
D.C. link resistance (R) and reactance (X) on the stability
behaviour of induction motor at unity frequency ratio, already
obtained in the form of curve (I) of Fig. 4.1. The values
of field current and firing angle are kept as 0.0 amp and 0°
respectively, so that their effect is eliminated while studying
the effect of R and X. The results are shown in Fig. 4.6.

It is observed that the unstable region decreases
as values of R and X are increased. It is noted that motor
becomes stable at unity frequency ratio when R and X are
.007 and .05 respectively. Therefore, to investigate the
stability behaviour of drive at unity frequency ratio as
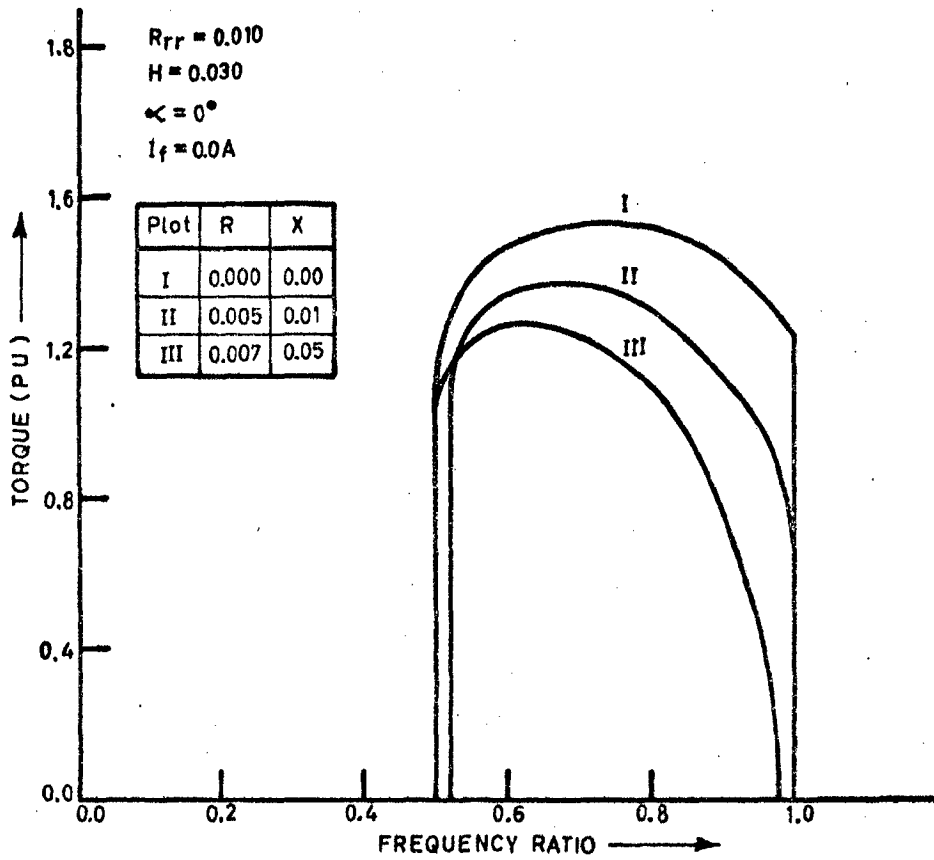
FIG.4.6: INSTABLITY REGIONS OF SLIP-ENERGY
-RECOVERY DRIVE

mentioned in section 4.5, values of R and X are chosen as
.005 and .01 respectively, for further study.

4.6.2 EFFECT OF FIELD CURRENT

The effect of field current on stability of the
drive is now studied. For this purpose, the firing angle is
set at 0° and the effect of increasing field current is noted
on stability curve (I) of Fig. 4.6. The values of field
current chosen are 0.05 and 0.1 amp and the results are shown
in Fig. 4.7(a).

It is noted that area enclosed by the stability
curve goes on increasing as field current is increased.
Fig. 4.7(b) shows the unstable region at unity frequency
ratio when field current is increased from 0 to 0.4A with
other parameters of the drive remaining unchanged. The level
of torque beyond which the drive will work under stable
condition increases with increase in field current. The
nature of this curve is found to be similar to the one
reported by Venkatesan (16) for a similar drive with
uncontrolled rectifier.

4.6.3 EFFECT OF FIRING ANGLE OF CONTROLLABLE RECTIFIER

In order to study the effect of firing angle,
the field current of the d.c. motor is set at zero and
firing angle setting is increased. Fig. 4.8(a) shows the
results for $\alpha = 0^\circ$, 20° and 40°. It is noted that as
firing angle increases, the unstable region goes on reducing.

R = 0.005
X = 0.010
Rss = 0.058
Rrr = 0.010
H = 0.030
$\propto$ = 0°

Plot	I_f
I	0.10
II	·0.05
III	0.00
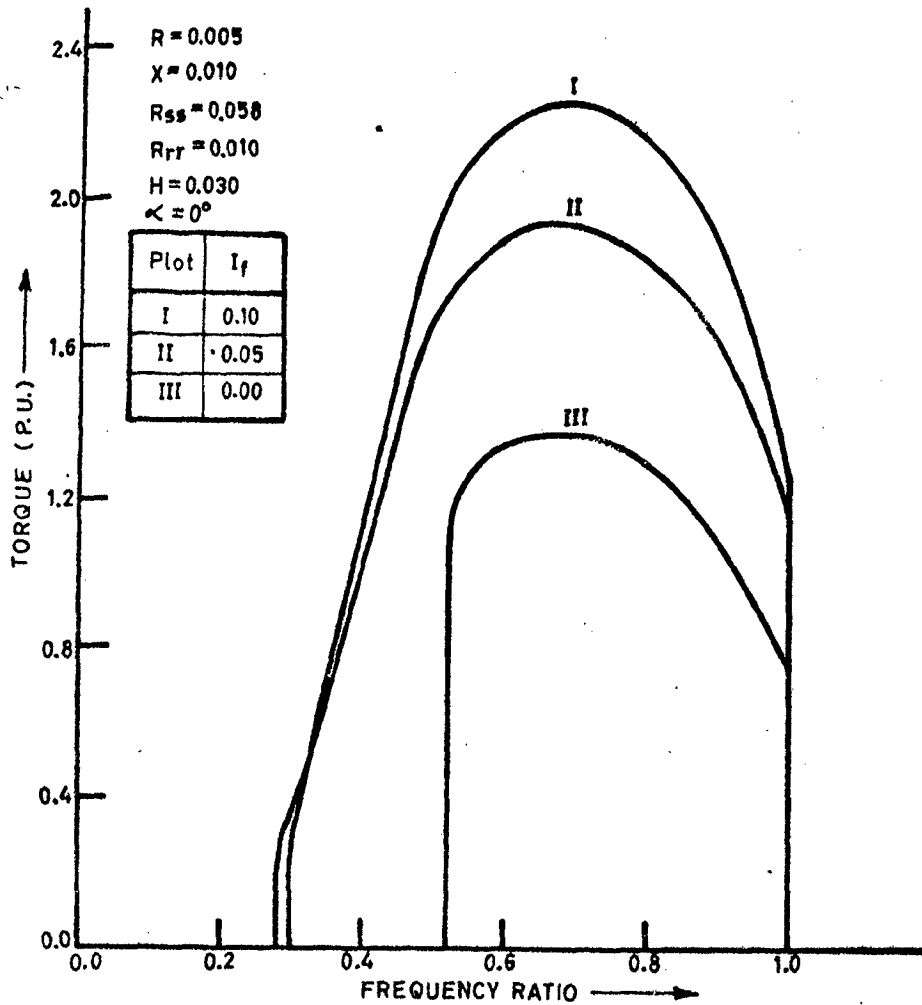
FIG.4.7(a): REGIONS OF INSTABILITY FOR
INCREASE IN FIELD CURRENT

Rss = 0.058, Rrr = 0.01, R = 0.005, X = 0.01, H = 0.03,
F_R = 1.0, $\propto$ = 0°

STABLE

UNSTABLE

FIG.4.7(b): EFFECT OF FIELD CURRENT AT
UNITY FREQUENCY RATIO
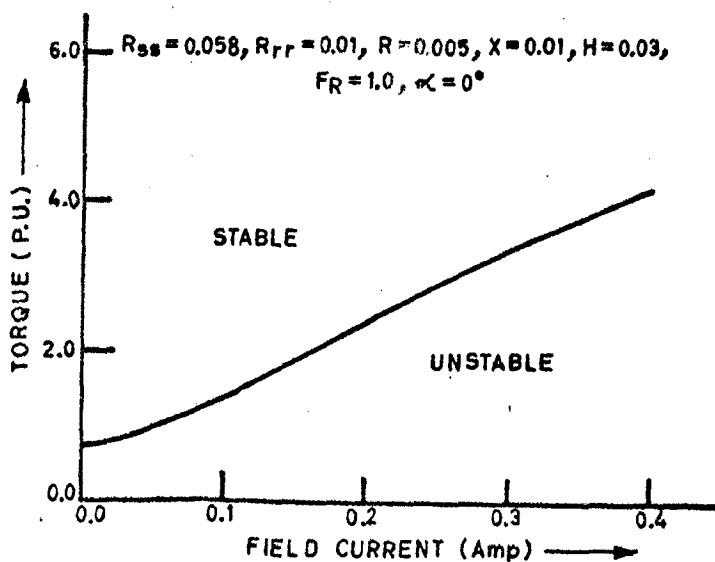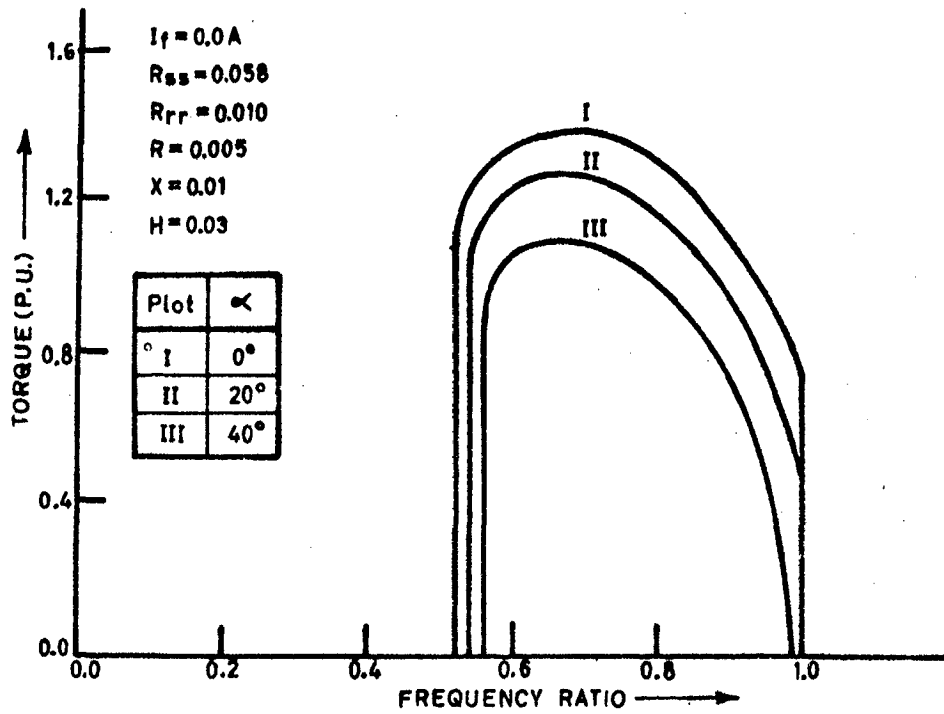
FIG.4.8(a): REGIONS OF INSTABILITY FOR
INCREASE IN FIRING ANGLE
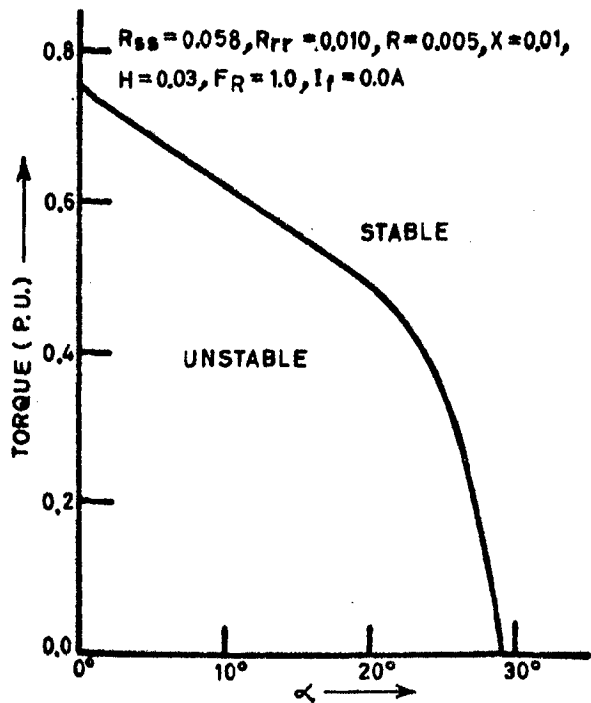
FIG.4.8(b): EFFECT OF FIRING
ANGLE AT UNITY
FREQUENCY RATIO

Fig. 4.8(b) shows the unstable region when frequency ratio is unity. The unstable region is seen to be limited in this case for operation with $\alpha = 0°$ to $28°$.

4.7 CONCLUSION

From stability point of view, the drive is found to be highly stable. A variation of $\pm$ 20 percent in its parameters too does not bring instability in the entire operating range of the drive. However if some parameters are exceptionally reduced, unstable regions appear. With these low values of some parameters, the effect of other parameters on stability is studied and following conclusions are drawn:

(i)   Increasing stator resistance improves stability.

(ii)   Increasing rotor resistance improves stability.

(iii)   Increasing inertia constant improves stability.

(iv)   Increasing applied voltage deteriorates stability.

(v)   Increasing d.c. link resistance and reactance improve stability.

(vi)   As field current setting is increased from zero to maximum value, the minimum torque for stable operation goes on increasing.

(vii)   In firing angle control, unstable region is limited in the present drive upto $28°$. This suggests that operation at higher firing angle is more stable.

CHAPTER V

CONCLUSIONS

The aim of this dissertation has been to study the steady state and stability behaviour of a constant power type slip energy recovery system employing a controlled rectifier in rotor circuit of induction motor. A rigorous mathematical model has been developed based on coupled circuit approach. The model has been used to investigate the steady state and stability behaviour of the system.

Expressions have been developed for determining the steady state performance of the system. Full load performance of the system has been investigated which reveals that field current control is superior than firing angle control and latter be adopted when it is absolutely necessary.

Stability analysis has been carried out using the linearised equations around an operating point. It is observed that the drive is highly stable. A variation of $\pm$ 20% in its parameters fails to produce instability in the entire operating range of the drive. However if some parameters are reduced exceptionally, unstable region appears. With these low values of some parameters, the effects of system inertia, stator resistance, rotor resistance, applied voltage, d.c. link resistance and reactance, field current and firing angle of controlled rectifier on stability have

been investigated and following conclusions are drawn:

(i)   Increasing stator resistance improves stability.

(ii)   Increasing rotor resistance improves stability.

(iii)   Increasing inertia constant improves stability.

(iv)   Increasing applied voltage deteriorates stability.

(v)   Increasing d.c. link resistance and reactance improve stability.

(vi)   Minimum torque for stable condition increases on increasing field current settings.

(vii)   Instability region decreases on increasing the firing angle.

BIBLIOGRAPHY

1. Bland, R.J., Hancock, N.N., White head, R.W., Considerations concerning a modified Kramer system, proc. IEE, Vol. 110, No.12, pp. 2228-32, Dec. 1963.

2. Kazuno, H., 'A wide range speed control of an induction motor with static scherbius and Kramer systems, Electrical Engineering Japan (U.S.A.) Vol. 89, No.2, pp. 10-19, Feb. 1969.

3. Shepherd, W., Stanway, J., Slip power recovery in an induction motor by the use of a thyristor inverter, IEEE, Trans. on Industry and General Applications, Vol. IGA-5, No.1, pp. 74-82, Jan.-Feb. 1969.

4. Lavi, A., Polge, R.J., 'Induction motor speed control with static inverter in the rotor, IEEE, Trans. on Power Apparatus and Systems, Vol. PAS-85, No.1, pp. 76-84, Jan. 1966.

5. Mittle, V.N., 'Steady state and transient analysis of a static slip energy recovery drive, Ph.D. thesis, University of Roorkee, July 1978.

6. Hori, T., Hiro, Y., 'The characteristics of an induction motor controlled by scherbius system, Seventh Annual meeting of the IEEE Industry Application Society, pp. 775-82, 1972.

7.   Gupta, S.P., Verma, V.K., 'Chopper controlled slip energy recovery drive steady-state performance', International Conference on Electrical Machines 1984, Lausanne, Switzerland.

8.   Venkatesan, K., Gupta, S.P., 'Chopper controlled Kramer drive', Journal of the institution of engineers (India) Vol. 60, pt EL3, pp. 102-107, Dec. 1979.

9.   Lipo, A., Krause, P.C., 'Stability analysis of a rectifier - inverter induction motor drive', IEEE Trans. on Power Apparatus and Systems, Vol. PAS-88, No.1, pp. 55-56, Jan. 1969.

10.   Nelson, R.H., Lipo, T.A., Krause, P.C., 'Stability analysis of a symmetrical induction machine', IEEE. Trans. on Power Apparatus and Systems, Vol. PAS-88, No.11, pp. 1710-17, Nov. 1969.

11.   Nanda, J., Narender Singh, 'Routh Hurwitz technique for determination of instability regions for a variable frequency induction motor drive', Journal, IE(I), Part EL-4, Vol.55, pp. 180-83, April, 1975.

12.   Murthy, K.K., Satpathi, H., 'Evaluation of stability limits of induction motors on parametric plane', IEEE. Trans. Automatic Control (U.S.A.), Vol. AC-15, No.1, pp. 149-52, Feb. 1970.

13. Lach, K.D., 'A study of the effect of variable frequency operation on induction motor stability,' IEEE. Trans. on Industrial Electronics and Control Instrumentation, Vol. IECI-15, No.1, pp. 43-47, Nov. 1968.

14. Mittle, V.N., Venkatesan, K., Gupta, S.C., 'Determination of instability region for a static slip power recovery drive,' Journal of institution of engineers (India) Vol.59, EL-2, pp. 59-63, Oct. 1978.

15. Gupta, S.P., Verma, V.K., 'Chopper controlled slip energy recovery drive - dynamic performance,' International Conference on Electrical Machines 1984, Lausanne, Switzerland.

16. Venkatesan, K., 'Steady state and stability analysis of a modified Kramer drive,' Journal of the institution of engineers (India), Vol.59, pt. EL-4, pp. 234-238, Feb. 1979.

17. Krause, P.C., Thomas, C.H., 'Simulation of symmetrical induction machinery,' IEEE Trans. Vol. PAS-84, No.11, pp. 1038, Nov. 1965.

18. Fitzerald, A.E., Kingsley, C., 'Electrical machinery' (Book) Megraw Hill New York, 1952.

19. Ramamoorthy, M., 'An introduction to thyristors and their applications' (Book), East - West press, New Delhi - Madras, 1972.

20. Murphy, J.M.D., 'Thyristor control of A.C. motors' (Book), Pergamon Press, 1973, Oxford, England.

21. Pelly, B.R., 'Thyristor phase controlled converters and cycloconverters', (Book), Wiley-Interscience, New York, London - Sydney, Toronto 1971.

22. Benjamin, C. Kuo, 'Automatic Control systems', (Book), Prentice - Hall of India Pvt. Ltd., New Delhi, India 1970.

APPENDIX 1

SPECIFICATION OF INDUCTION MOTOR AND BASE VALUES

1.   Detailed specification of induction motor - P.S.G.

Industrial Institute Coimbatore

INDUCTION MOTOR

Made in India

MACH NO. 40876   Frame   MS5W

Volts   230/400 V,   PH 3,   CY 50,   CON Δ/Y

KW   3.75   H.P. 5,   R.P.M.   1440

Amps   7.5   Rotor volts 140, Rotor amps. 22

Rating CONT, Class of Insulation A

2.   Base values for various quantities

Unit current = Peak value of rated current = 10.6 A

Unit voltage = Peak value of phase rated voltage = 325 V

Unit impedance = $\dfrac{\text{Unit voltage}}{\text{Unit current}}$ = 30.66 ohms

Unit power = rated apparent power = $\dfrac{3}{2}$ x 230 $\sqrt{2}$ x 7.5 $\sqrt{2}$

$$= 5.175 \text{ KW}$$

Unit frequency = Rated frequency = 50 Hz

Unit electrical angular speed = $2\pi f_b$ = 100π radians/sec.

Unit mechanical speed = πf_b = 50π radians/sec

Unit torque = $\dfrac{\text{Unit power}}{\text{Unit mechanical speed}}$ = $\dfrac{5.175 \times 10^3}{50\pi}$

$$= 39.23 \text{ N-m}$$

APPENDIX 2

PARAMETERS OF DRIVE

1. ACTUAL PARAMETER VALUES

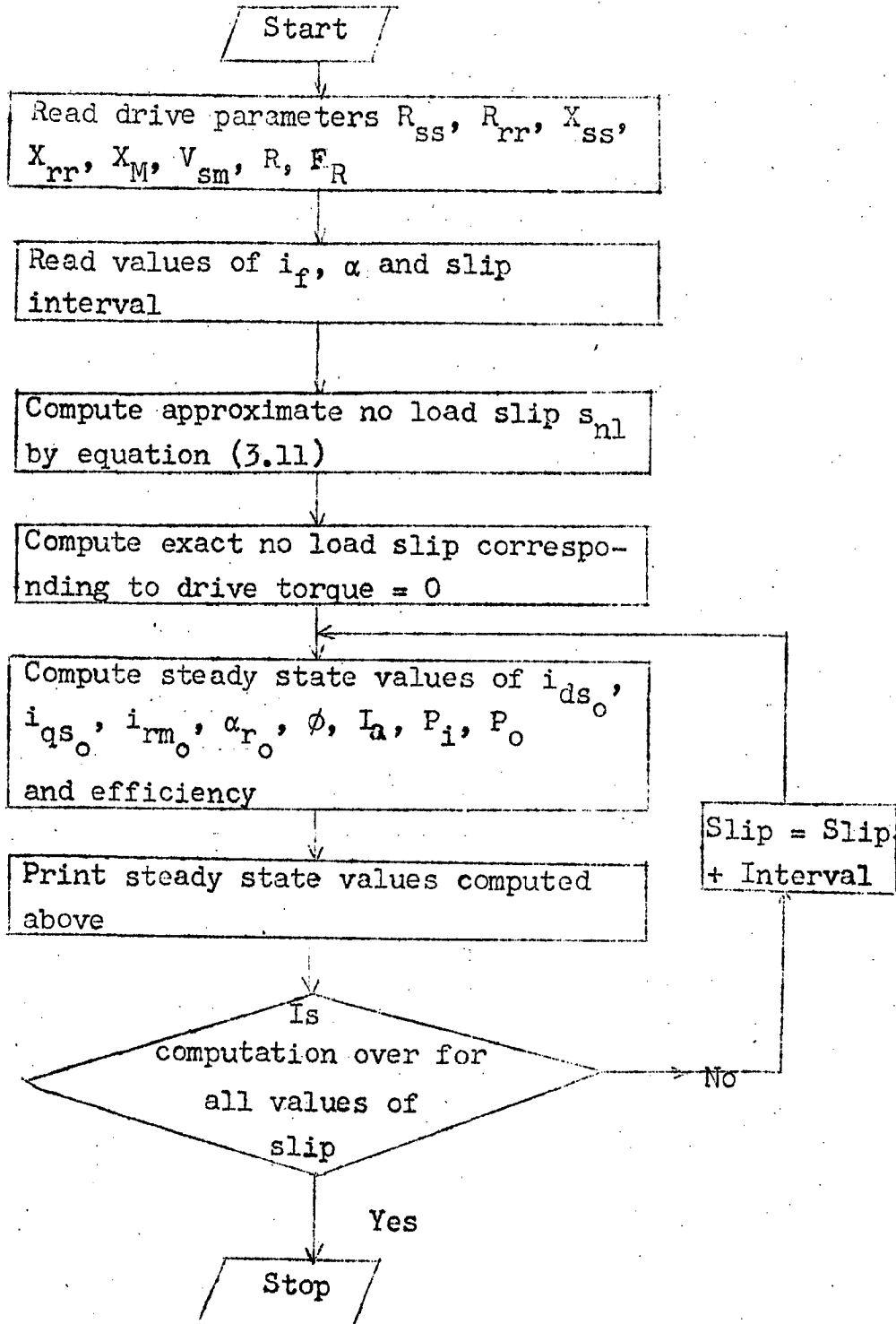The values of measured parameters of the three phase induction motor are as follows:

X_{ss} = 92.1 ohms R_{ss} = 1.8 ohms

X_{rr} = 11.3 ohms R_{rr} = 0.28 ohms

X_{12} = 31.0 ohms   a = 2.85 ohms

X_{rr}' = 92.1 ohms R_{rr}' = 2.21 ohms

X_M = X_{12}' = 88.57 ohms   R = 1.3 ohms

R' = 10.56 ohms

X = 24.8 ohms

X' = 201.4 ohms

2. PER-UNIT VALUES OF PARAMETERS

Parameters when expressed in per-unit form are

X_{ss} = 3.0, X_{rr}' = 3.0, X_M = 2.9

R_{ss} = 0.058, R_{rr}' = 0.072,   R = 0.344,

X = 6.57

K_f = 3.5 Volts/(rad/sec)/field ampere

H = 1.4 sec

APPENDIX 3

```
     ┌─────────┐
    /  Start   /
   └─────────┘
        │
        ▼
```

Read drive parameters R_{ss}, R_{rr}, X_{ss}, X_{rr}, X_M, V_{sm}, R, F_R

Read values of i_f, α and slip interval

Compute approximate no load slip s_{nl} by equation (3.11)

Compute exact no load slip corresponding to drive torque = 0

Compute steady state values of i_{ds_o}, i_{qs_o}, i_{rm_o}, α_{r_o}, ϕ, I_a, P_i, P_o and efficiency

Print steady state values computed above

Slip = Slip + Interval

Is computation over for all values of slip

No

Yes

Stop

Flow chart for steady state calculations

```
$    PROGRAM FOR STEADY STATE PERFORMANCE OF A SLIP ENERGY RECOVERY DRIVE
$    ALL PARAMETERS ARE FED IN PER UNIT
$    THIS PROGRAM DIRECTLY GIVES TORQUE,SUPPLY CURRENT,FUNDAMENTAL
$    ROTOR PHASE CURRENT,POWER FACTOR,POWER INPUT POWER OUTPUT
$    DC LINK CURRENT AND EFFICIENCY OF THE DRIVE AT STEADY
$    STATE FOR A GIVEN VALUE OF SLIP,FIELD CURRENT AND ALFA
     DIMENSION KF(5).        ROTATIONAL VOLTAGE COEFFICIENT
     COMPLEX Y,C,D,E,F
     REAL IFD,K2,IRM,ISM,IDS,IQS,IDR,IQR,KF,IA
     N=100! N=100 TO GIVE AN INCREMENT OF .01 TO THE SLIP
     KF(1)=4.05;KF(2)=3.75;KF(3)=3.35;KF(4)=3.
     XM=2.9
     RSS=.058
     L2=4!   MAX LIMIT OF FIELD CURRENT
     XSS=3.
     XRR=3.
     VSM=1.
     RRR=.072
     R=.344
     FR=1.
     PY=3.1415926
     DO 100J=0,80,20! VARIATION OF FIRING ANGLE
     ALFA=J*PY/180.! FIRING ANGLE IN RADIANS
     DO 10K=L1,L2!   VARIATION OF FIELD CURRENT
     I1=0;I2=0
     IF(K.EQ.L2)L1=L2
     IFD=K/10.
     K2=0.8287401*KF(K)*IFD
     SNL=K2*FR/(K2*FR+VSM*COS(ALFA))
$    APPROX NO LOAD SLIP IS CALCULATED
     PRINT1,J,IFD,SNL
     TYPE1,J,IFD,SNL
     DO 10I=1,N!      VARIATION OF SLIP
     AI=I
18   S=AI/N
$    SLIP IS VARIED AT A REGULAR INTERVAL DEPENDING UPON N
     SS=S
     IF(SNL.GT.S)GOTO10
     IF(I1.GE.1)GOTO16
$    EXACT NO LOAD SLIP IS OBTAINED BY SENSING TORQUE
     LL=SNL*10000
     LM=LL+150
     I1=1
16   DO2 IL=LL,LM
```

```
045            IF(I2.EQ.1)GOTO17
046            S=L/10000.
047            IF(S.EQ.0.)S=0.01
048      $     STEADY STATE SOLUTION EQUATIONS DEVELOPED ARE FED
049      17    Z1=(VSM*S*FR*XM)/SQRT(RSS*RSS+FR*FR*XSS*XSS)
050            Z2=(S*FR*FR*XM*XM)/(RSS*RSS+FR*FR*XSS*XSS)
051            Z3=K2*FR*(1.-S)/COS(ALFA)
052            Z4=RRR*COS(ALFA)+PY*PY*R/(18.*COS(ALFA))+S*FR*XRR*SIN(ALFA)
053           1+Z2*(RSS*COS(ALFA)-FR*XSS*SIN(ALFA))
054            Z5=RRR*SIN(ALFA)-S*FR*XRR*COS(ALFA)+
055           1Z2*(FR*XSS*COS(ALFA)+RSS*SIN(ALFA))
056            Z6=Z4*Z4+Z5*Z5
057            Z7=2.*Z3*Z4
058            Z8=Z3*Z3-Z1*Z1
059            IRM=(-Z7+SQRT(Z7*Z7-4.*Z6*Z8))/(2.*Z6)
060            ALFR=PY/2.-ATAN(FR*XSS/RSS)-ATAN((-IRM*Z5)/(Z3+IRM*Z4))
061            B=ALFR-ALFA
062            C=CMPLX(COS(ALFA),-SIN(ALFA))
063            D=CMPLX(COS(ALFR),SIN(ALFR))
064            E=CMPLX(0.,S*FR*XM)
065            F=CMPLX(RRR,S*FR*XRR)
066      $     PHASOR ISM IS CALCULATED
067            Y=((K2*FR*(1.-S)/COS(ALFA))+IRM*(PY*PY*R/(18.*COS(ALFA))
068           1+F*C))*D/E
069            ISM=CABS(Y)
070            P=ISM/1.4142!    RMS VALUE OF ISM
071            PHI=ATAN(AIMAG(Y)/REAL(Y))
072            IDS=ISM*COS(PHI)
073            IQS=ISM*SIN(PHI)
074            IDR=IRM*COS(B)
075            IQR=IRM*SIN(B)
076            TORQIM=XM*(IDS*IQR-IQS*IDR)
077            TORQDC=K2*IRM
078            TORQ=TORQIM+TORQDC
079            IF(TORQ.LT.0)GOTO20
080            IF(TORQ.LT.0.001)GOTO15
081      20    CONTINUE
082      15    LL=LM
083            I2=1
084            PF=IDS/ISM
085            IA=.9069*IRM!    ARMATURE CURRENT
086            PI=VSM*IDS
087            PO=TORQ*(1.-S)*FR
088            SL=(IDS*IDS+IQS*IQS)*RSS
```

```
089          RL=(IDR*IDR+IQR*IQR)*RRR
090          AL=PY*PY*R*(IDR*IDR+IQR*IQR)/18.
091          EFF=PO*100./PI
092          ALFD=ALFR*180./PY!      ALFR IN DEGREES
093          Q=IRM/1.4142!   IRM IN RMS
094          PRINT2,S,Q,ALFD,P,IDS,IQS,IDR,IQR,PF,PI,PO,SL,RL,AL,TORQ,EFF,IA
095          TYPE2,S,Q,ALFD,P,IDS,IQS,IDR,IQR,PF,PI,PO,SL,RL,AL,TORQ,EFF,IA
096          IF(S.LT.SS)GOTO18
097    10    CONTINUE
098    2     FORMAT(16F8.3,F5.2)
099    1     FORMAT(//,4X,'FIRING ANGLE=',I3,' DEGREE'10X,'FIELD CURR
00          1ENT=',F6.2,10X,'NO LOAD SLIP=',F8.4,/,
01          1' SLIP    IRM    ALFR     ISM    IDS',5X,
02          1'IQS    IDR    IQR    POWER   POWER   POWER',7X,
03          1'COPPER LOSSES',7X,'TORQUE   EFF   IA',/,10X,'(RMS)    D
04          1EGREE   (RMS)',
05          135X,'FACTOR  INPUT   OUTPUT  STATOR  ROTOR  ARMATURE',//)
06          STOP
07          END
```

APPENDIX 4
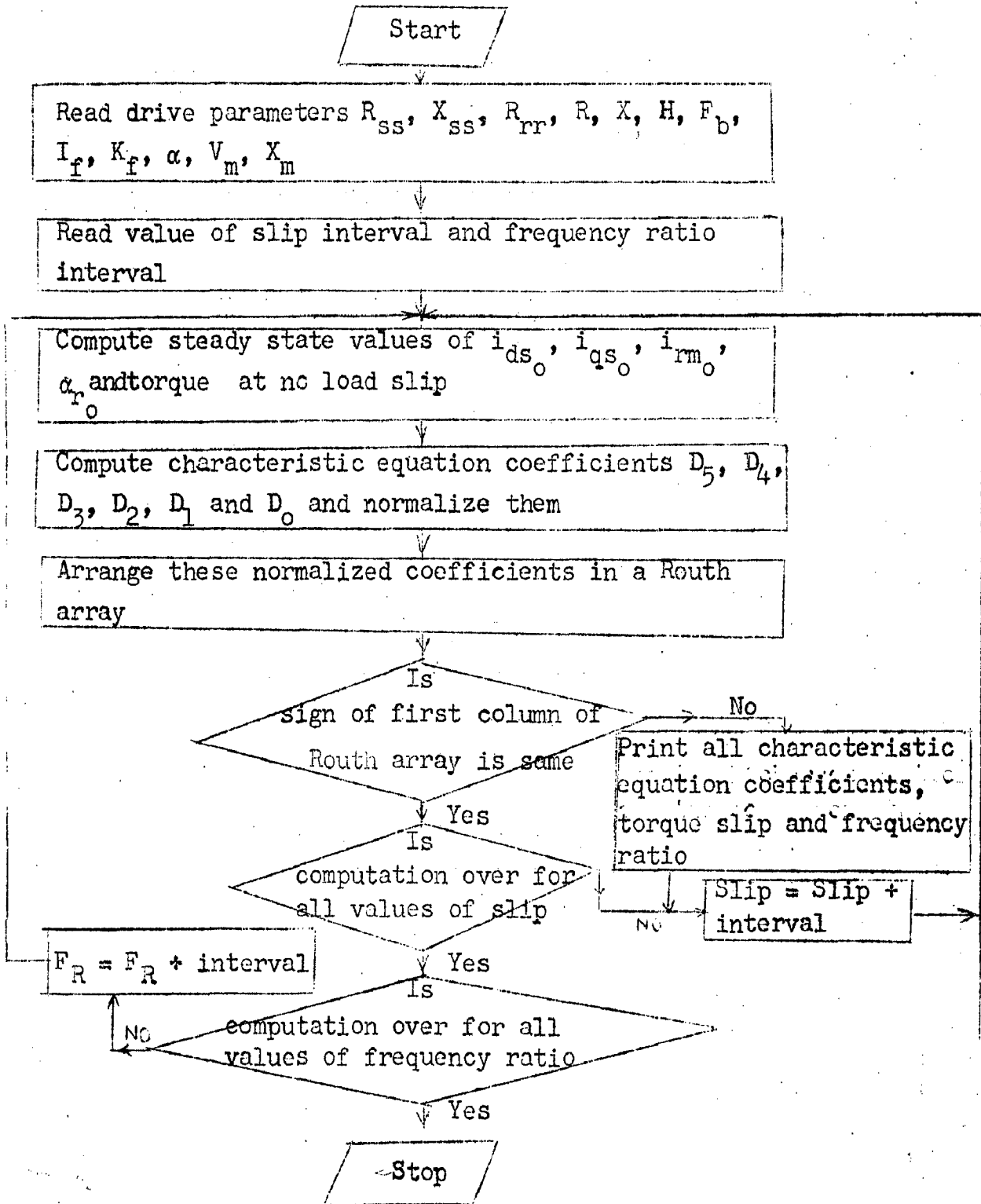
Flow chart for stability analysis of the drive

```
          + .. ..T.3( .  )=. *.S..*S.( ... .))
           = . ..( ... )=. ..X .*C..S( .P )+
           .( .. ..C .( ... )+...S*S.( ...P ))
             .= .. + ..
         7= . . .
       . = . . - .T .
       . =(- ..,...( .. .-.. .*. .S*. .))/(2.*..)
     ... = ./ ...  ( ... /..S.)-A.. ((-.P .* .S)/(..+.X * .))
   .= .. .- .
7     C=. .X((C..S( .. .),-.L (ALFA))
.     U=. .X(C. S(A.. ),.. .(ALFR))
.     .=C..X( ..,.*..*.X.)
      .. .X(. ..,.*C..*.X..)
..    V=((.. *FR*(1.-..))/((..( .LFR))+IFR*(PY*FY*R/(18.*COS(ALFR))
..     .+...))*0/.
..     . =C./S(Y)
       F..= .. (.) ..(Y)/..(Y))
..     ..S=I.R.*COS(P..)
..     .. .=.. *SI.(P..)
.7     I..=I..*COS(..)
..     I.. =.. *.. (..)
..     ...=P.5
.       .=.0
..     .R=..3.
..     ...=..2.
.       ...=...
..     ...=.01.
..     ...=.1R.
..     ... =X..*(IF..*IC..-I...*I..)+..*.R.
.7     IF(...L.. .)G.T.
7.,  S  ... TATTY RESULTS OF ..IV..
..     P.C.=P.F+PY*PY*I.*COS(ALFR)/(1P.*COS(ALFR)*C.S(P))
..     ...=...+PY*PY*P*SI.(ALFR)/(18.*COS(ALFR)*SI.(3))
.      X..1=XA.+PY*PY*X*COS(ALFR)/(1..*COS(ALFR)*C.S(3))
.      X.02=X...+PY*PY*X*SI.(ALFR)/(1..*COS(ALFR)*SI.(5))
.      F.=..2/C.S(ALFA)
.      Z.=...
.      Z.=X../..G.
.      Y.=-..*XSS
.      Z.=..*.SI.()
.7     ..=-.*C.S()/..G.
.      .=...*..*C.S()
.      .Z=...*SI.()/...
```

$Z = $

$Z = $

$Z = $

$Z = - \quad ( )$

$Z = - \quad I( )/$

$Z = - \quad * Z \quad ( )$

$Z = - \quad * \cos( )/$

$Z = X / $

$Z16 = - F \quad Y \quad$

$Z17 = F \quad * Y \quad * ( ) - \quad 1 * \cos( )$

$Z1 = - \quad * C \quad ( )/ \quad GB$

$Z1 = \quad * (1 - S) * \quad (\alpha + E) + \quad 01 * I \quad * SI(\beta) + \quad * XRR * S \quad $

$* \quad ( )$

$Z = Y \quad + I \quad * SI(\beta)/ \quad G$

$Z = \quad * \cos(\alpha + E) - F \quad * X \quad * I0S + FR * XRR * IR \quad * SI(\beta)$

$Z = - Z1$

$Z = Z1$

$Z24 = - \quad * X \quad * S * \cos( ) - \quad 2 * SI(\beta)$

$Z25 = - \quad * S \quad ( )/ \quad GB$

$Z26 = - \quad * (1 - S) * \cos(+I + E) + FR * XRR * S * IR \quad * SI(\beta) - R \quad 2 *$

$(IR \quad * \cos( )$

$Z 7 = - \quad * 2 * \quad * \cos( )/ \quad GB$

$Z2 = \quad 3 * \quad * SI \quad (\alpha + E) + \quad * X \quad * I0S - FR * XRR * IR \quad * \cos(e)$

$Z = Y \quad * \quad * SI( )$

$Z3 = - Y \quad * \cos( )$

$Z31 = - X \quad * I0S * \cos( ) + X \quad * I0S * SI(\beta) + \quad 2$

$Z \quad = Y \quad * \quad * (I0S * SI( ) + I0S * \cos( ))$

$Z 3 = Z \quad * S$

$Z \quad = Z \quad * \quad / (Z \quad * Z3)$

$Z \quad 5 = (Z \quad + Z + Z \quad * Z)/ (Z \quad * Z3)$

$Z \quad = Z \quad + Z \quad / (\quad + Z) - \quad $

$Z \quad 7 = Z \quad + Z \quad / (Z3 * \quad)$

$Z \quad = (Z5 * Z \quad + Z1 \quad * Z \quad)/ (Z3 * Z8) - Z1 \quad / Z8$

$Z \quad = Z \quad * Z \quad / (Z3 * Z \quad) - Z \quad / Z \quad $

$Z \quad = Z \quad + Z7/ (Z3 * Z9)$

$Z \quad = (Z9 * Z7 + Z1 \quad * Z \quad)/ (Z3 * Z9) - Z1 \quad / Z \quad $

$Z \quad 2 = Z \quad * Z \quad / (Z \quad * Z3) - Z13/ Z \quad $

$Z \quad 3 = - Z2 \quad * Z2/ Z3$

$Z \quad = - Z \quad * Z \quad / Z \quad + Z \quad * (Z1 \quad * Z \quad / (Z3 * Z21) - Z1 \quad / Z21)$

$Z \quad = Z \quad * (Z1 \quad * Z \quad / (Z \quad * Z \quad)) + Z \quad $

$Z \quad = - Z \quad * Z \quad / Z3$

$Z \quad 7 = - \quad * Z \quad / Z3 + Z \quad + Z \quad * (Z \quad * Z5/ (Z3 * Z2 \quad) - Z1 \quad / Z2 \quad)$

$Z \quad = \quad + Z \quad * (Z1 \quad * \quad / (Z3 * Z21) - Z17/ Z21)$

$Z \quad = - \quad Z7/ Z3$